Master's thesis

NTNU
Norwegian University of Science and Technology
Faculty of Information Technology and Electrical Engineering
Department of Engineering Cybernetics

Gitle Seim Brekke

Leg Design and Control for Jumping Quadrupeds

Master's thesis in Industrial Cybernetics
Supervisor: Prof. Dr. Kostas Alexis
Co-supervisor: Phd. Jørgen Anker Olsen
June 2022

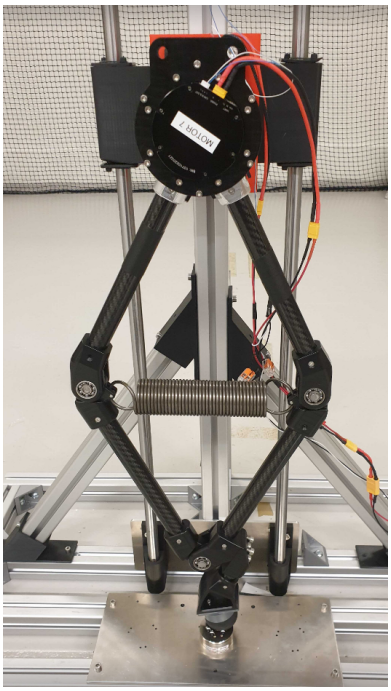

NTNU
Norwegian University of
Science and Technology

Gitle Seim Brekke

Leg Design and Control for Jumping Quadrupeds

Master's thesis in Industrial Cybernetics
Supervisor: Prof. Dr. Kostas Alexis
Co-supervisor: Phd. Jørgen Anker Olsen
June 2022

Norwegian University of Science and Technology
Faculty of Information Technology and Electrical Engineering
Department of Engineering Cybernetics

NTNU
Norwegian University of
Science and Technology

Preface

This thesis is submitted as the final master's project for the master's degree at the Department of Engineering Cybernetics, at the Norwegian University of Science and Technology. The thesis tackles the problem of designing a legged design for quadrupedal robots, capable of performing feats such as jumping and locomotion.

This project proved to be a most challenging task, and it would not be achieved without the help of numerous people. I would like to thank the workshop at the Department of Engineering Cybernetics. Their help in the manufacturing of all mechanical parts, and consult for the practicality and usage of numerous manufacturing and assembling challenges. I am also hugely grateful for the help of my Co-supervisor Jørgen Anker Olsen, whose continuous help during this project and the project thesis the year prior have been essential for making the final results, and the completion of the thesis as a whole. I would also thank Prof. Dr. Kostas Alexis for making this thesis possible. And for allowing me to work on this challenging and interesting project.

Lastly, I would like to thank all my family and friends for their continued support during this project that has helped to make it happen.

Abstract

The development of legged robotics has over the years received increasingly more focus. This is a result of the rapid growth in interest from robotic developers. The demand for a safe, dexterous, and efficient robotic system that can complete complex tasks has been a driving force in this evolution. The relevance of such robotic systems is dependent on their capabilities to operate in increasingly challenging environments and to be able to traverse rugged and uneven terrain.

This thesis will focus on the design, control system, and exploration abilities of a quadruped-legged robotic system. The development of different means of locomotion has been a focal point for the development of quadrupedal designs. Different gaits of static and dynamical nature have been developed for different tasks. The robot will be designed with a focus on locomotion abilities. By incorporating different gaits these can be utilized for different tasks.

Dynamical jumping as a form of locomotion will have a heavy influence on the final mechanical design choices. The ability to change gaits between dynamical jumping and a more standard quadrupedal walking gait will be essential for the versatility and flexibility of the capabilities of the design. Earlier studies have shown that the most efficient way for these kinds of robots to move is in a combination of roving, hoping, and walking.

However, this has proven to be a major challenge. The individual movements can be solved separately, and several systems have good solutions for individual locomotion tasks. Incorporating multiple gaits and locomotion means will give the design a greater means for reversibility in different terrains. To address this, research has been conducted on control systems for increased complex movements and locomotion. The greatest challenge may the combination of different types of movements into continuous, fluid movements.

The other great challenge is the control and efficiency of the jumping mechanism of the robot. A prioritized area will be on making the changes between different movements become fluid and without stopping in between.

The robotic design was manufactured and tested to categorize its physical abilities and determine the impacts and forces to which it will be exposed. Simulations was done to test the system's different capabilities. A physical test was done to observe how the system will respond to real-world tests in a controlled environment.

Sammendrag

Utviklingen av roboter med bein har opp gjennom årene fått stadig mer fokus. Dette som et resultat av den raskt økende interessen fra robotutviklere. En drivkraft for denne utviklingen, har vært kravet om trygge, anvendelige og effektive robotsystemer som kan fullføre komplekse oppgaver. Relevansen til slike robotsystemer er avhengige av en rekke faktorer, som blant annet deres evne til å operere i stadig mer utfordrende miljøer, samt deres evne til å kunne krysse jevnt og ujevnt terreng.

Denne oppgaven vil fokusere på design, kontrollsystem og utforskningsevner til et firebeint robotsystem. Utviklingen av forskjellige bevegelsesmidler har vært et fokuspunkt for utviklingen av firebeindesign, og ulike gangarter av statisk og dynamisk karakter er utviklet for ulike oppgaver.

Roboten vil bli designet med stort fokus på bevegelsesevner. Ved å inkorporere forskjellige gangarter kan den utnytte disse til forskjellige oppgaver. Dynamisk hopping som en form for bevegelse vil ha stor innflytelse på de endelige mekaniske designvalgene. Evnen til å endre gangart mellom dynamisk hopping og en mer standard firbent gange vil være avgjørende for allsidigheten og fleksibiliteten til designets evner.

Tidligere studier har vist at den mest effektive måten å bevege seg på for denne typen roboter, er en kombinasjon av kjøring, gåing og hopping.

Dette har imidlertid vist seg å være en stor utfordring. De enkelte bevegelsene kan løses separat, og flere systemer har gode løsninger for individuelle bevegelsesoppgaver. Å inkludere flere gangarter og bevegelsesmidler vil gi designet bedre egenskaper for framkommelighet i forskjellige terreng. For å løse dette har det blitt forsket på kontrollsystemer for mer komplekse bevegelser og bevegelse. En av de største utfordringene med dette kan være å kombinere de ulike bevegelsestypene til kontinuerlige og flytende bevegelser.

Den andre store utfordringen er kontrollen og effektiviteten til hoppmekanismen til roboten. Fokus vil være å få endringene mellom ulike bevegelser til å bli flytende.

Robotdesignet vil bli produsert og testet for å kategorisere dens fysiske evner og bestemme påvirkningene og kreftene den blir utsatt for. Simuleringer vil bli gjort for å teste systemets ulike muligheter. En fysisk test vil bli utført for å observere hvordan systemet vil reagere på virkelige tester i et kontrollert miljø.

Abbreviations

CAN-BUS: Control Area Network BUS

CAN: Controller area network

COF: Spring coefficient

COM: Center of mass

COMP: Component

DOF: Degrees of freedom

DS: Displacement

ESC: Electronic speed controller

FOC: Field oriented control

FBD: Free body diagram

POM: Polyoxymethylene

ROS: Robot operating system

SF: Safety factor

VMS: Von Misses Stress

Contents

Figures

Tables

Chapter 1

Introduction

1.1 Background and motivation

Dynamic and mobile robots have in recent years seen an increasing complexity and competence in their ability able to perform different and complex tasks. In the last years, robots have had a rising presence in multiple fields such as; industry, exploration, military, and civilian applications. While the advance in robotics has been exponential over the last decades, several problems remain unsolved, and many systems have limitations and challenges. A primary focal point for robotic development has for a long time been locomotion and autonomy. The development of such systems can be used to replace humans for many hazardous tasks. To achieve this goal, however, there must be developed robots that can traverse and explore difficult and changeling terrain effectively.

One of the most exploited means of locomotion until recent years has been wheeled and belt-based locomotion. Robotic systems of this nature have been used as they are very stable and their complexity is often lower compared to other systems. They have for a long time been utilized in several fields, however, even due to their stability they have several limitations and drawbacks. These limitations are evident in their inability to be applied in rugged and uneven terrain. They face locomotion problems in challenging environments where elevated terrain, stairs, loose ground, or steep inclines are present. Because of these drawbacks, the introduction of other robotic systems with different locomotion properties is necessary.

To overcome these problems legged robotics provide an alternative. There have already been many different-legged robots developed over the years. An example of this is the ANYmal [1]. It has proved the capabilities of legged designs, currently being used in several industrial settings. The design has also been used by the Cerberus team that has won the DARPA subterranean challenge [2].

The evolution of legged robotic systems will also make it possible to overcome the challenges faced in other areas such as subterranean space exploring. Space exploration has been conducted with many types of technologies over the years. The most standard method has been observations with satellites, while the usage of drones and robotics has become more and more relevant. The Mars rovers are one such system that uses wheeled locomotion.

The motivation for this project is to research the different technologies and designs that are utilized today in robotic exploration. Using this already acquired knowledge will give a

better understanding of the challenges and limitations of the different solutions. For extraterrestrial exploration, especially in caves on Mars [3], there has been in recent times more and more effort to work identify the different challenges and problems that will arise in such an extreme environment. An example of this is the Multi-robot Mapping of Lava Tubes [4]. Where the focus is to find a solution to the problem of mapping lava tubes where the presence of fine sand in the martian tubes causes problems. Due to the sand, the odometry measurements in the autonomous robots are highly prone to errors.

The advancements in the robotic field that have been developed for exploration in subterrain areas have had huge improvements over the last year, while the main focus has been on exploration path planning [5] and surveillance. With the advances in the mobility and locomotion properties of these systems, there can be even greater opportunities for robotic explorations.

1.2 Objectives

The objectives of this thesis will be to explore different robotic design possibilities capable of jumping and dynamical jumping locomotion. By studying existing technologies and designs, a new quadruped-legged robotic design will be suggested. Multiple potential designs will be made and discussed to identify their different specifications, abilities, and limitations. A final design will be chosen for continued work and testing.

The suggested design will be divided into individual components. All these components will be optimized and undergo FEM analysis before the final design will be manufactured. These components will be analyzed and have important aspects that will affect the entire design identified. By using these requirements future components can be optimized even further.

The design will be made to be modular in nature, making it possible to change its properties depending on the wanted capabilities. Simulations scripts that will assist in this process will be developed. The design will be tested in a simulation environment to evaluate its physical capabilities, further optimizing the parameters of the leg design.

Physical tests will be done to properly test the final design. This will include the assembly and construction of all mechanical parts and their fittings. As well as test to test the design's capabilities and reaction to real-world applications.

1.3 Thesis structure

Chapter 1: Introduction

This chapter will consist of an introduction of the thesis, the motivation, and background for the task, an overview of the different topics, and all the chapters in the thesis.

Chapter 2: Robotic literature review

This chapter will consist of a literature review of different robotic designs quadruped-legged robotic systems, and jumping robotic systems. As well as important factors and technologies for the different designs.

Chapter 3: Robotic designs

This chapter will focus on the different challenges of designing a robotic system capable of jumping and having jumping locomotion. This section will contain different proposed designs of the jumping robots. It will also focus on the different components and requirements of the final design will consist of.

Chapter 4: Final design

This chapter will focus on the different components and design of the suggested final design. All of the parts will be presented as well as their respective designs and applications to the full design. All of the parts will have their individual requirements identified for the current and future iterations.

Chapter 5: Simulation

In this chapter, it will be discussed all the different simulations of the design. Such as FEM, workspace, Simulink Multibodies, and force design estimations. The simulation part will be a study to see the potential in the system when it comes to its jumping capabilities.

Chapter 6: Modelling

This chapter will be focused on the modeling of the robotic designs. The forward- and backward-kinematics. Which will be computed and used to mathematically calculate the workspace of the end-effector of the robotic design.

Chapter 7: Physical testing

This chapter will focus on the physical testing done on the design. Several tests will be done to test how the manufactured design will react to different real-world applications. Such as experimental testing of the workspace, passive jumping test, and drop test of the robotic design.

Chapter 8: Conclusion

This chapter will be a summary of the thesis, it will consist of a conclusion and discuss the results that have been made of all of the parts covered in the thesis.

Chapter 2

Literature review

2.1 Robotic designs

This section will contain a literature review of quadruped-legged robots, jumping robots, and robotic systems in general. The literature review will serve as a basis for the design process. Different solutions, designs, and challenges can be identified and consulted when developing the suggested design.

The research in robotics has been heavily focused on different designs that enable different approaches to locomotion. Some examples of robotic systems with different locomotion capabilities are the MIT Cheetah [6], Boston Dynamics Atlas [7], the bio-inspired Scorpion [8] and the ANYmal robot[1]. There has been conducted thorough research to identify how different design configurations will affect the locomotion capabilities of different designs.

2.1.1 Quadruped Legged Robots

In the last decades, the primary choices for mobile robots used in exploration, space, industry, and research have been rovers, drones, and legged robots. Rovers have been one of the most utilized, as these designs have few problems with the challenges legged robotics often face. Balance, gait dynamics, and tracking of leg movement are not present in these as they utilize belts or wheels as locomotion means.

However, there are limitations to the wheeled and belt designs. The main challenge of the roving robots is their movement in challenging terrain. When faced with uneven or rugged terrain these types of robots may not have the capabilities necessary to traverse these challenges. This is however where legged robots have the advantage, as they are not limited to belts or wheels. Utilizing this dexterity, legged designs can provide the ability to overcome obstacles that are impossible for their roving counterparts.

ANYmal

One example of a robot that has excellent maneuverability due to its legged system is the ANYmal [1]. A robot made by the ANYbotics company [9], a robotics company that makes

Autonomous robots for industrial inspection. An area of operation where maneuverability is a crucial factor for success.

Figure 2.1: ANYmal robot from ANYbotics [1].

The ANYmal robot has excellent maneuverability in difficult terrain. And has been shown to handle elements such as uneven grounds, rugged terrain as well as elevated surfaces, and even stairs. These are some challenges that wheeled robotic systems would never be able to overcome, that legged robot systems can.

While the reason for the robot's advantages over the wheeled and rover-based system is clear in that it has four usable limbs that can move in all directions. However, for the ANYmal the joint on the knee can also be operated on separately. This gives it, in addition to its already 3-DOF for each leg, an enormous locomotion ability when it comes to overcoming difficult terrain.

Besides the ANYmal robot, another focus of the literature review has been on the robot SpaceBok. A robot that will be explained in detail later on. Other than these, multiple different quadruped robots have been made and produced over the years. Some examples are the Spot [10] from Boston Dynamics. Which also has proved to have great traversability in varied and challenging terrain. In addition to displaying impressive choreography utilizing its high-speed actuators [11]. The MIT's Cheetah [12]. A student project at MIT that has 3-DOF for each leg. Combined with its fast-acting actuators have been shown to have an impressive range of movement [6]. The Scorpion [8] is a Bio-inspired eighth-legged robot. Designed to overcome very steep and uneven terrain. While the HyQ [13] is a more traditional quadruped-legged robot with four legs. With movements that are hydraulically and electrically actuated based. All of these have been inspirations when the final design for the robot in the project will

be made. To see what they did, and to see how it can be utilized to create the most efficient design in the project.

There have been over the years many different approaches to creating robots with increased capabilities of extraterrestrial exploration. Many of these are legged to be able to overcome different challenges. The Spaceclimber [14] has a six-legged design, and was made for extraterrestrial surface exploration in unstructured and steep terrain.

One of the more different takes on the robotic extraterrestrial exploration scene is the ATHLETE [15] from NASA. In contradiction to most other systems, it has both wheels attached to its legs. This gives it the possibility of roving in environments that allows it, to the wheel using its legs in more challenging terrain. Since it has six legs with wheels at each one it also means it can drive in an omnidirectional fashion and is not constricted with a "front-end". Another example of this kind of configuration is sprawling spider-like robots, an example is the TITAN-XIII [16].

2.1.2 Hoping Robots

Hoping robots have been over the last years been designed as alternatives to more traditional robots, such as rovers and walking robots. Often the reason for the designs of jumping robots has been to traverse and overcome terrain that may be impossible for other types of robots.

There are many types and approaches to the concept of jumping robots. And even the concept of generating power to hop has been a case of study [17]. With the purpose to find the most efficient way of generating power to jump in as small and compact form as possible.

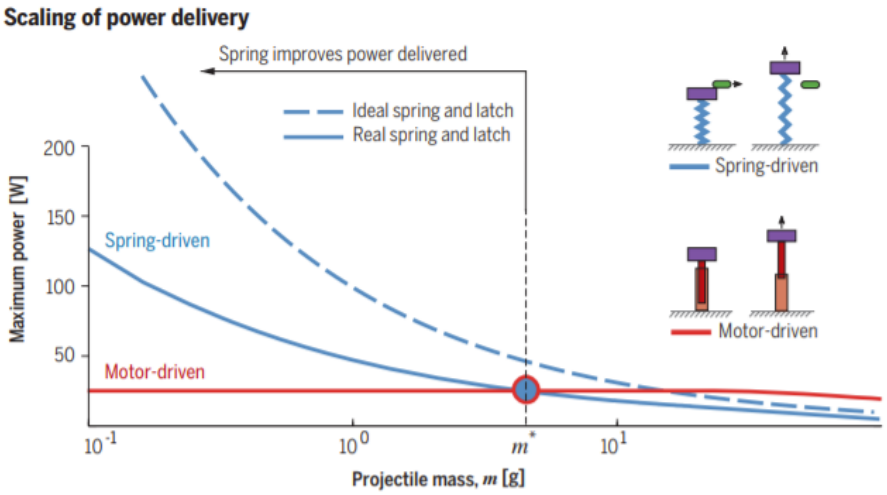

Figure 2.2: Scaling of power delivery in springs and motors [17].

As it can be seen from Figure 2.2 the power delivery is quite potent with springs. Witch is something to consider when the design and building process will eventually start.

The jumping robotics scene has many different takes on the problem. The Sand Flea from Boston Dynamics is an example of this. While operating normally as an RC car when driving normally, it has the ability to jump 9m up into the air. The Sand Flea jumping mechanism is

driven by CO2. Meaning that it has a limited amount of jumps before its reserves depletes. Another take on the jumping dynamics is the Salto [18] jumping robot. This is a robot that is capable of jumping continuously using its leg as a propellant. Much like a pogo-stick. By shifting the weight and using its fans to stabilize it can make around in a quite controlled fashion.

Another system can be based on a hybrid spring system [19], with a exceeded jump height of 30m.

As mentioned there are multiple forms of jumping robots. They can be characterized into two main groups based on their ability to have continuous jumping. The ones with a propellant, utilize this to create a force to jump. Like the sand flee that utilized CO2 to lunch levers out and throw itself upwards. Many other systems than CO2 exist. Pneumatic hydraulics can be used in the same way. While these systems often will result in the largest jumps and the greatest single results. They demand a stable basis for their jump and a calculated path for the lunch and landing. While these problems all have solutions the biggest problem is the propellant needed. Due to the need for canisters, tanks, and hydraulic systems. They can be heavy and have limited usage since their jumps are limited to a given amount of charges before they must recharge or refuel.

One of the subsequent challenges of creating a jumping movement is to be able to land. The landing of the robots is an important and difficult challenge that is necessary to solve to be able to create robotic systems able of dynamic gaits. As well as being able to utilize jumping as a valid form of movement, landing is crucial.

There are many different methods of controlling the in-air movement and landing of robots. SpaceBok [20] utilizes a flywheel that will create a torque counteracting the forces in the air during jumps. While this is a proven method, it can not react to fast-changing movement, and it will add quite an amount of weight as well. They have in later versions of the robot, made a version with a greater focus on exactly this problem in mind. Making a system capable of landing on its feet from an initial position by utilizing its legs [21].

Another solution for control and stabilization is the Salto [18] robot as mentioned earlier. Which utilizes two thrusters and a tail for reorientation as its means for stabilization.

2.1.3 SpaceBok

One of the main sources of inspiration for this project was SpaceBok [20]. This is a project that was made at ETH in Zurich [22]. Their paper explains the motivation and reasoning for their design choices. As well as the study's into the different motions their robot was able to perform. An in-depth litterateur study of their paper and results will greatly help identify different problems and challenges that exist. As well as how they overcame and adapted to these obstacles.

Motivation

Their motivation for building the SpaceBok was to make a quadrupedal robot possible for investigating celestial bodies. Their argumentation was that up until now there has solely been wheeled locomotion used for mobile exploration of celestial bodies. While these systems have been constantly improved, their applicability in uneven and steep terrain limits their mobility.

Legged robots provide an interesting alternative to the more classical rover design for space exploration. Their own studies and motivation are many of the same robots discussed in the previous section.

SpaceBok is a quadrupedal robot with two actuated degrees of freedom (DOF) per leg. These movements are the Hip flexion/extension and the knee flexion/extension. Their reasoning for the lack of abduction/adduction was that it was omitted to reduce the weight of the system.

Leg design

The leg design as can be seen in Figure 2.3 consists of two hollowed tubes (l_1) with springs inside. These legs are then connected to the drivetrain. At the bottom of the leg configuration there is a carbon spring for impact absorption.

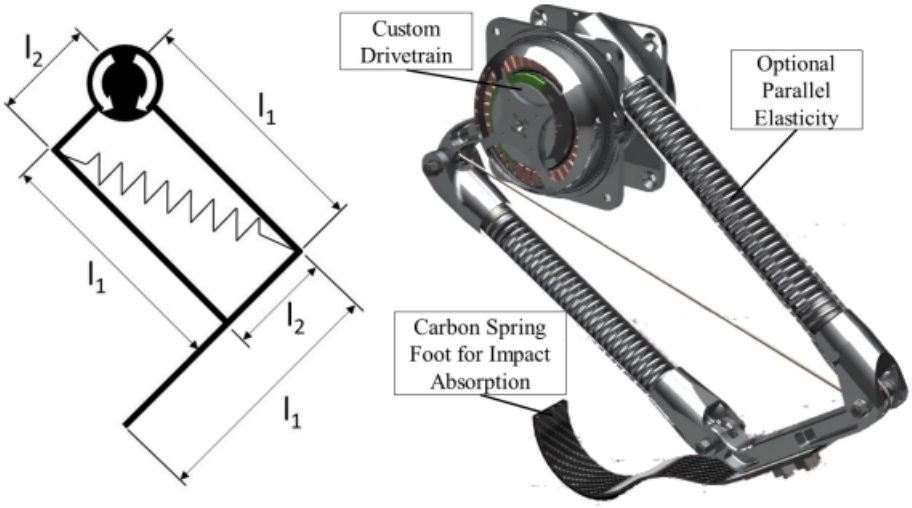

Figure 2.3: Leg design and internal mechanics of SpaceBok [20].

The drivetrain is a custom one built by the group. It consists of a T-motor model U8-KV85 [23] as well as a custom planetary gear. By utilizing this configuration they have been able to construct a high transmission drivetrain with a ratio of $1 : 9,55$ and an output of $39,5Nm$ at $30A$. The high torque motor in combination with custom-designed single-stage planetary gearboxes. In their design, the planetary gearbox is placed within the stator frame, which reduces hip-width.

Controls

The onboard control framework uses the Robot Operating System (ROS). It consists of a state estimator, ha high-level controller, and a low-level controller. The state estimator receives motor and encoder data from the low-level controller through shared memory, and IMU through ROS messages respectively to estimate the robot's state relative to a locally attached frame.

Information is processed by the high-level controller with high-level user inputs that compute the desired torque for each actuated joint. The low-level controller communicates with the eight motor controllers through an EtherCAT network.

If the robot is operated in simulation mode, the high-level controller and the state estimator exchange data directly with the simulation environment through shared memory without an additional low-level controller in the loop (for simulation). Gazebo "*GAZEBO Robot simulation*" [24] have been used for the simulation. Landes [25]

Cost of Transportation

One of the most important aspects of locomotion is to make it as effective as possible in low gravity environments. To be able to consider different types of gait and their different efficiencies. The result of this has been a study on different types of gaits that have been tested up to a cost of transportation function [26] (COT). Where They have for now implemented three different types of gaits, these being:

1. Pronking Gait
2. Dynamical Walking Gait
3. Trot Gait

The Contributions to the total work W_{tot} consist of the purely mechanical work from the actuators to move the COM of the robot. W_{com}, internal work of the system, W_{int} (electrical energy for computation, electrical heat losses, internal friction losses, etc), and the work done on the environment E_{env} (overcoming slippage, deformation of soil, etc). With P, mean mechanical power, m_r the mass of the robot, and v_{mean} as mean forward velocity.

$$COT = \frac{(W_{com} + E_{env})}{m_r g_i * d}) = \frac{P_{mech,mean}}{m_r g_i * v_{mean}} \tag{2.1}$$

$$P_{mech,mean} = \sum_{i=1}^{N} \frac{1}{S_i} \sum_{j=1}^{S_i} max(0, \tau_i \omega_i) \tag{2.2}$$

Pronking Gait

The most interesting gait is the pronking gait. This is the dynamical jumping locomotion. The pronking gait has two phases, that is the flight phase when it is in the air, and the stance phase when it is on the ground.

During stance, they utilize the virtual model controller. This controller calculates its desired virtual forces and torques that act on the center of gravity. In these calculations they only consider 2D movement, meaning x denotes the movement direction straightforward and z the movement upwards. The equations below it are shown how they calculate the virtual forces in the x direction f_x and in the z direction f_z. The virtual torques m are found by using the

orientation error e_o. All of these gives them the total virtual wrench:

$$f_x = k_{p,x,f}(v_x^* - v_x) \tag{2.3}$$
$$f_z = k_{p,z,f}(r_z^* - r_z) \tag{2.4}$$
$$m = k_p^o * e_o - k_d^o * \omega \tag{2.5}$$

In their calculations the orientation error is provided by an IMU, and given in the form of quaternions p. In the equation for orientation error they utilizes the boxminus [27] operator.

$$e_o = p^* \boxminus p = log(p^* \bigotimes p^{-}1) \tag{2.6}$$

Walking Gaits

In addition to the pronking gait, there have been implemented a walking trot and a dynamic walk. The difference between these is the way swing and stance leg has to be treated differently. Depending on what gait is used.

In the single leg motion they utilize controller of the form

$$\tau_{i,j} = k_p * (\phi_{i,j}^* - \phi_{i,j}) + k_d * (\dot{\phi}_{i,j}^* - \dot{\phi}_{i,j}) \tag{2.7}$$

Where the gains are represented by k_p and k_d while joint angles and velocities are represented by. $\phi_{i,j}$ and $\dot{\phi}_{i,j}$, desired values expressed as $\phi_{i,j}^*$ and $\dot{\phi}_{i,j}^*$. To track torso motion, they utilize same virtual motion controller as with the pronking gait, but the desired position and velocity are tracked in both horizontal and vertical direction.

$$f_x = k_{p,x,f}(v_x^* - v_x + k_{d,x,f}(v_x^* - v_x) \tag{2.8}$$
$$f_z = k_{p,z,f}(r_z^* - r_z) + k_{d,z,f} * v_z + m * g \tag{2.9}$$
$$m = k_p^o * e_o - k_d^o * \omega \tag{2.10}$$

2.2 Serial Elastic actuators

The general goal for robotics interfaces between actuators and loads has been to make them as stiff as they can be [28]. The principle to support this is that stiffness improves precision, stability as well as bandwidth in the position control. Increased stiffness has been shown to raise the resonant frequency of motor inertia and interface compliance, and lower needed corrections for load variations [29].

While stiff load-actuator interfaces have many desired properties for robotics design they have drawbacks that make them less suitable for certain designs. One of the more severe ones for this design is the reflected inertia and high back-drive from the friction of the gears, which can cause damage to the system and environment. These drawbacks can be so severe that the only feasible usage for a direct drive is industrial robots [30]. While in mobile robotics systems like hopping robots, these drive trains can cause problems.

The basic composition of a series elastic actuator is to induce elasticity between the load and the actuator. In Figure 2.4 a block diagram of the basis of the serial elastic actuator is shown.

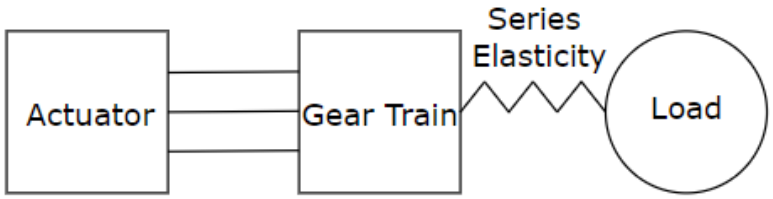

Figure 2.4: Visualisation of Series Elastic Actuators.

For the design of jumping robotics serial elastic actuation is naturally generated through the usage of more spring and dampening focused design [31]. Due to the incorporation of dampening elements in the designs presented in this thesis. Most of the suggested designs presented in this thesis can be categorized as serial elastic actuated systems.

Chapter 3

Design

The main focus of the project will be to make the quadrupedal-legged design discussed in the introduction. The design will be made to be able to produce an effective jumping movement. In addition to this, it is desired that the jumping motion can be repeated, with the basis of utilizing jumping as a method of locomotion in a pronking gait. In addition to the pronking gait, the robot also must be capable of more traditional dynamical and static gaits.

One of the crucial aspects to enable this is to make the design as lightweight as possible. A result of this is that all parts and components will be made with weight reduction as one of the most important design aspects.

An overall design review will be done of the full robotic system, and requirements for the entire robot will be stated. These requirements will be used to identify the individual requirements and aspects of components.

3.1 Requirements

Before the design phase could begin there had to be made some requirements that would govern how the choices of the design would be made. Many of the requirements are stated with a focus on weight and its ability to traverse and orient itself in challenging environments.

Requirements for the robotic design	
Jumping	Means of jumping and jumping locomotion
Locomotion	Means of locomotion besides jumping
Mass	Preferably less than 20[kg]
Payload	Have the capability to carry a payload
Size	Preferably not bigger then 500[mm] at the hip
Orientation	Have means of orientation mid air
Self adjustment	Means of self adjustment after fall

Table 3.1: Requirements for full quadrupedal robotic design.

3.2 Leg design

The final design would be chosen from several different conceptual design suggestions. When deciding the finalized basic design configuration, multiple factors such as complexity, usability, sturdiness, and potential weight would be taken into consideration. The design most fitting the different requirements would be chosen after analyzing and discussing its compatibility with the wanted qualities. Other designs were discarded for several reasons, some proved too inefficient for jumping motion, some proved to be impossible to implement a continuous jumping motion, while some required extensive design or manufacturing that would be beyond the scope of the intended project. These designs and reasoning for either discarding or further development will be discussed.

3.2.1 HOP 1

The first design was constructed to be a quadruped sprawling configuration and would have a finished design based on spider structure, instead of the more traditional quadruped-legged designs. In the early design process, this design looked quite promising. The sprawling design gave it excellent mobility and balance [32]. As well as having the potential of being completely omnidirectional and not reliant on directional-based joints. The main problem with this design proved to be the implementation of a jumping motion. To create a jumping movement a design of hydraulics was suggested. The inner mechanics as shown in Figure 3.1a would be made up of a spring that will be compressed. This compressed spring will then act as the incentive for the jumping motion.

However, this design needs two motors for the actuation of the leg. Just as the case with the other designs made, later on, one actuator would be used to control the hip movement, and one for the knee movement. The challenge proved to be the implementation of a third actuator to enable the compression. A possible solution to this was to implement an hydraulic system inside the leg. A cross-section is shown in the Figure 3.1b. The hydraulic would compress the spring and then release it to make the system jump. There proved to be several problems with this system. The jumping mechanism would be quite complex. Hydraulics meant that it would need an external source of either liquid or pneumatic pressure to drive the hydraulics. This would have required a supply, which again would mean that the system would have a limit to how many jumps it could do. The added components would also mean an increase in mass which is not desirable.

Due to the more tedious jumping mechanism, as well as it would have a limit on the number of jumps it could do. This system would not be suitable to achieve the type of dynamic jumping motion that is sought after. With all the considerations and drawbacks of this system with respect to the requirements that had been made for the wanted design, the HOP1 was discarded.

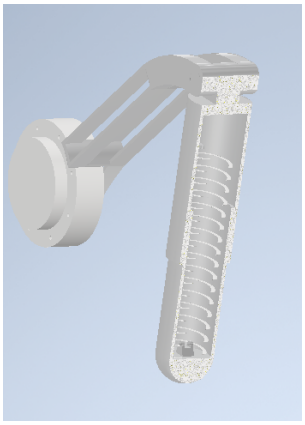

(a) Internal mechanism of HOP1.

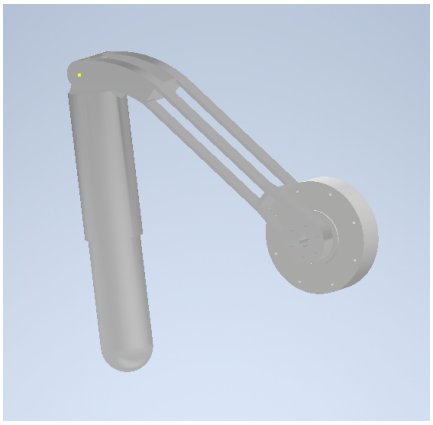

(b) Leg design of HOP1.

Figure 3.1: Conceptual leg design of HOP1.

Evaluation criteria for design	**HOP 1.0**
Potential Jumping Capabilities	High potential due to forces that can be made by hydraulic or pneumatic systems
Jumping Locomotion	Jumping locomotion would be limited due to the need of resources
Locomotion	Locomotion for sprawling designs have been proven to be quite dexterous
Mass	Potential high due to resources and hydraulic/pneumatic components
Complexity	Potential high due to hydraulic/pneumatic systems, connections and tubing
Machining/manufacturing	Potential high due to hydraulic/pneumatic systems, connections and tubing

Table 3.2: Evaluation results for the HOP1 design based on the criteria.

3.2.2 HOP 2

The second design was a more standard quadruped-legged design with an actuated knee and hip joint, this is similar to the system used in example Boston Dynamics SPOT [10] and MIT's Mini Cheetah [12]. For the jumping dynamics, the knee joint motor would extend the spring located on the ridge of the thigh on the leg design as can be seen in Figure 3.2. The extended spring would contract and create potential energy in the system. When the actuated knee was released it would create an explosive force to make the system jump. There were however several problems with this. The small leverage arm to which the spring is connected would result in a small displacement of the spring. When comparing the leverage arms of either side of the joint, the difference in energy needed from a high-torque motor was not cost-efficient or possible to get the necessary moment to displace the spring enough to get a sufficient jumping

force.

When comparing the difference in the energy needed to create a moment high enough to extend the spring to a length that would create the necessary force to create a substantial jump. And the energy needed for a high-torque motor to enable the extension of the spring was neither cost-efficient nor plausible.

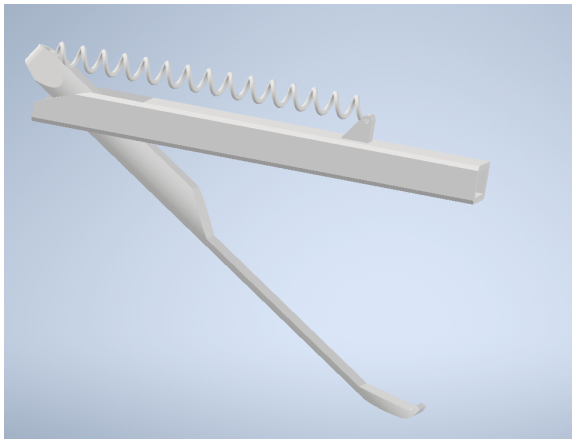

Figure 3.2: Conceptual leg design of HOP2.

Evaluations criteria of leg design	**HOP 2.0**
Potential Jumping Capabilities	Dependent on the force in spring, early tests showed limited potential due to small displacement
Jumping Locomotion	Spring would potentially have given capabilities of continuous jumping locomotion
Locomotion	Similar to normal quadrupeds, low energy efficiency due to tension of spring on knee joint
Mass	Few parts, potential low mass
Complexity	Low complexity, due to few and simple parts
Machining/manufacturing	Easy manufacturing, due to few and simple parts

Table 3.3: Evaluation results for the HOP2 design based on the criteria.

3.2.3 HOP 3

The third design is more similar to HOP2 and the standard quadruped robot configuration discussed earlier. This design is composed of two legs connected to the knee joint. These legs are then controlled by two actuators which would be placed on the hip.

While the basic layout for the design was the same as the previous one shown, there are some notable differences. The jumping mechanism was suggested to be performed by the part between the legs, the one in blue in Figure 3. This part would be some sort of composite that would bend and tighten when the two legs moved contracted. As a result, the composite part would build up potential energy, much like a bow or leaf spring, which then would generate

the force necessary to jump.

Hop 3 also proved to have several flaws that made it unsuitable for the project. The spring that was supposed to generate the jumping force would have made the system very rigid and stiff on a general basis. Making it hard to control the legs independently.

One of the main problems of this design was the construction of the bow-like spring itself. it needed to be able to bend without breaking, and at the same time be able to generate enough force to make the system jump. This would require extensive research into composite structures to find something suitable. While this is much likely possible, it would require further study, testing, and manufacturing. This is not a part of the scope of this project.

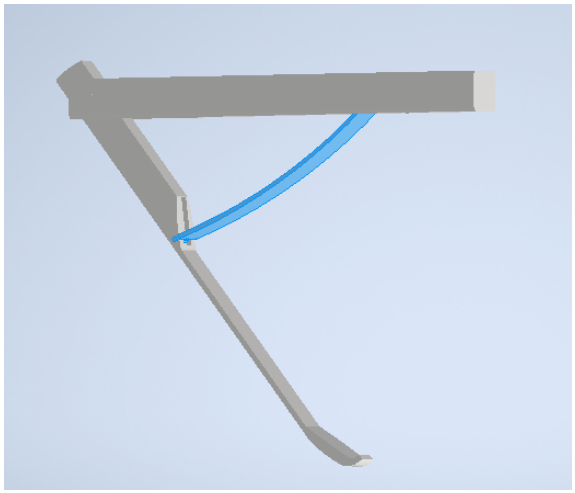

Figure 3.3: Conceptual leg design of HOP3.

Evaluations criteria of leg design	**HOP 3.0**
Potential Jumping Capabilities	Potential would depend on the mechanical properties of the composite
Jumping Locomotion	Potential would depend on composite capabilities to store energy and release it
Locomotion	Potential poor due to stiffness in composite
Mass	Potential law mass, dependent on weight of composite
Complexity	Leg design itself simple, composite unknown complexity
Machining/manufacturing	Unknown complexity due to composite

Table 3.4: Evaluation results for the HOP3 design based on the criteria.

3.3 HOP 4

This design has two motors that control the two upper legs. Both of these legs are then connected to their respectively lower legs, which again are connected to each other at the bottom with a third joint. Because the lower legs are connected, it is not necessary to have an actuator to affect the knee joint. This keeps the system in constant tension and makes it possible to control the configuration by only having actuators on the upper legs. This has several advantages. It keeps the inertia of the legs themselves as small as possible, making it theoretically possible to jump higher. It also removes the need for any motors, drives, or belts to actuate the lower joints and legs.

Jumping dynamics

The jumping dynamics are composed of two main elements. One is the moment generated from the actuators. The actuators will move the legs from position a to position b as shown in Figure 3.4, and then quickly contract to create a force that will propel the system upwards.

The other part of the jumping mechanism is the spring that is connected in between the two knee joints as seen in Figure.4. When the two actuators compress the system the spring will extend. The spring will build up potential energy that when the actuators release the counteracting torque will contract the system generating force and propelling the system upwards.

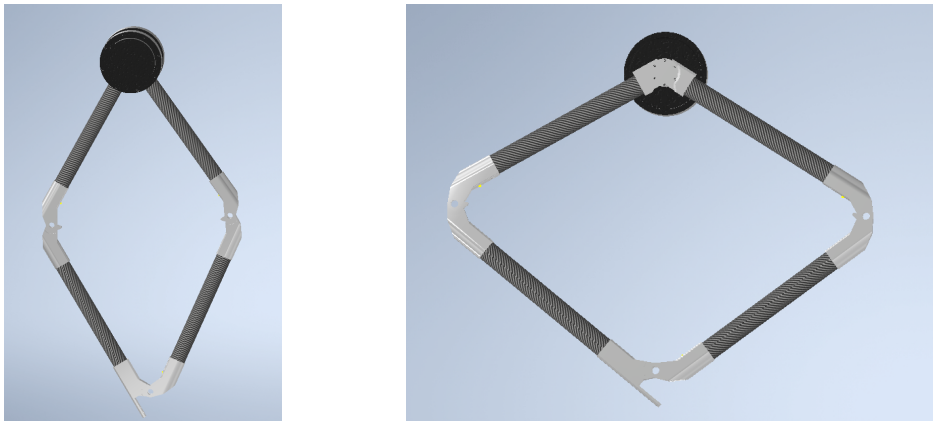

(a) Starting position of HOP 4. **(b)** Compressed position of HOP 4.

Figure 3.4: Jumping dynamics of HOP 4.

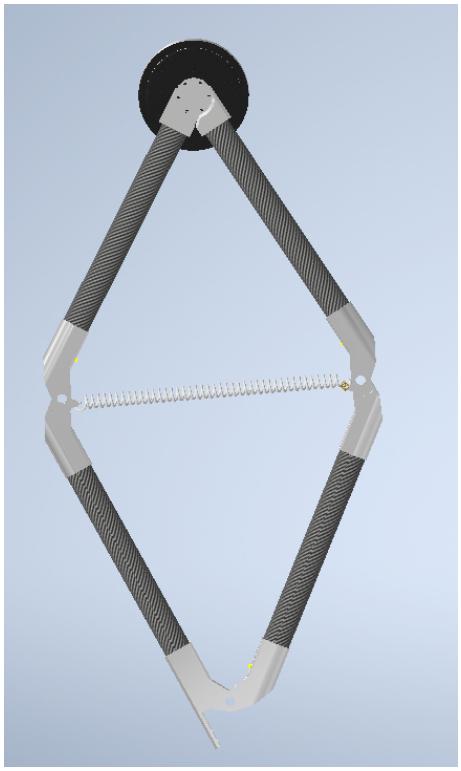

Figure 3.5: Conceptual Leg design of HOP 4.

Evaluations criteria of leg design	**HOP 4.0**
Potential Jumping Capabilities	Dependent on the force in spring, early tests show promise due to displacement potential
Jumping Locomotion	Spring would potentially have given capabilities of continuous jumping locomotion, FTR
Locomotion	Similar to normal quadrupeds, spring might cause increased energy usage, FTR
Mass	Few parts, potential low weight
Complexity	Medium complexity, due to few but some intricate parts that will need to act in tandem
Machining/manufacturing	Easy manufacturing, due to low complexity of individual components

Table 3.5: Evaluation results for the HOP4 design based on the criteria.

3.4 Final design selection

After several different designs have been discarded due to displaying potential insufficient capabilities with respect to the requirements. A final basic configuration for the leg design

is suggested. While the basic design configuration has been decided, there will be continuous work to improve and optimize it to achieve the best result possible. Therefore the design presented here may see altercations and changes during the optimization processes. To decide which one of the designs would be the suggested one for this thesis, all of the results from their individual evaluation criteria result would be scored against each other.

Evaluation criteria for design	**HOP1**	**HOP2**	**HOP3**	**HOP4**
Potential Jumping Capabilities	4	1	4	4
Jumping Locomotion	1	3	4	4
Locomotion	5	4	4	4
Mass	2	4	4	3
Complexity	2	3	1	3
Machining/manufacturing	2	3	2	3
Total Score	**16**	**18**	**19**	**21**

Table 3.6: Final results and scores of the design choosing process.

3.5 Component optimization

The process of optimizing the design start with localizing and identifying the different types of components and parts that will be needed for the design. To be able to optimize the design all the components will undergo several iterations and changes. When possible they will be 3D-printed to easier visualize them. During this process, there will be identified different requirements and specific properties for the individual components. These requirements will be used as tangible benchmarks for the performance of each different component iteration.

3.5.1 Joints

The joints in between the legs are designed to be easily connected with the legs. In case of damage or adjustments to the length, the legs can be removed from the joints. The joint and legs will be connected with an easily removable and modular joint. Both parts of the joint are shown in Figure 3.6.

(a) **(b)**

Figure 3.6: Early conceptual Joint design.

An early and crude design of the joint can be seen in Figure 3.6. The joint assembly consists of two separate joints that will be connected by a pin and bearings. The optimization process will consist of identifying the different important aspects of the joint individual components, as well as the overall assembly.

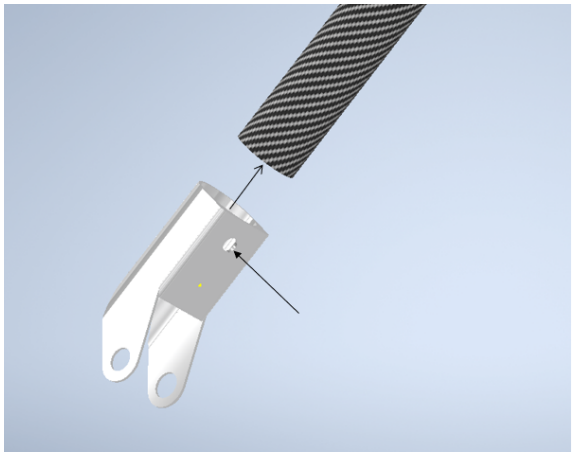

Figure 3.7: Conceptual design of leg joint insertion.

In Figure 3.7 it is seen where the joint will slide into place with the carbon fiber tubes that will act as the legs. An early idea was to use set screws to fasten the individual joint components to the carbon leg. But due to the brittleness of the carbon leg, this was discarded. One of the desired properties of the joint and carbon inserts is the ability to change the length of the carbon tube easily. This will be an important aspect of the optimization choices.

Joint Design Properties
Weight
Stiffness
Movement smoothness
Mechanical interface with joint assembly
Mechanical interface with carbon legs

Table 3.7: Important properties for the Joint component design.

3.5.2 Leg Insert

The leg insert will be the component that act as the connection between the motor and the carbon legs. While identifying the different problems this design would need to challenge it was noted that one of the main problems with the early design was having a sufficient range of motion, while not colliding with each other and still maintaining an equal axis to the motors. To be able to make the design as compact as possible, and having the carbon legs align to avoid bending and twisting during movement.

Leg Insert Design Properties
Weight
Stiffens
Impact and force absorption
Mechanical interface with motors
Mechanical interface with carbon legs

Table 3.8: Important properties for the Leg Insert component design.

3.5.3 Motor Housing

Since the component is highly dependent on its interface and adjutant parts a set of general requirements for its necessary properties have been set to design any potential future iterations. It will need to be able to fit and support the motors, in addition, to supporting the entire structure of the design.

Motor Housing Design Properties
Weight
Stiffens
Impact and force absorption
Mechanical interface with leg and body
Mechanical interface with Motors and Leg Inserts
Mechanical stops with respect to Body and Leg Body Connect

Table 3.9: Important properties for the Motor Housing component design.

3.5.4 Leg Body Connection

The mechanical interface between the leg itself and the motor inserted in the motor housing is responsible for hip adduction. It needs to be able to withstand the moment created in the motor with landings that are not perpendicular to the ground. As well as forces created in jumping and landing motions. To be able to create a suitable design for the motor housing, and to identify the different qualities that will be important. Not only for the current design but for improved iterations in the future. A set of requirements have been set.

Leg Body Connection Requirements
Weight
Stiffness
Mechanical interface with leg
Mechanical interface with body
Impact and force absorption

Table 3.10: Important properties for the Leg Body Connection component design.

3.6 Motor

One of the most important parts of any robotic system is the motors and actuators that are used to physically move and manipulate the components and control movements. The advancement of actuators in the last years has made it possible to make stronger, faster, and more compact robots. To choose the motors that would be used for the project following requirements were made to accommodate and meet the requirements of the leg design as a whole.

Motor selection requirements	
Torque	Torque must be high enough to give the wanted output
Mass	As little mass as possible is desired
Power density	The relation between mass and torque should be as high as possible
Interface	Interfaces must be compatible with other equipment
Size	As small size as possible is desired
Availability	The motors must be available for purchase in a reasonable time
Gearing	Integrated gearing desired

Table 3.11: Important aspects and requirements to account for in the Motor selection process.

Multiple different companies offer different types of motors with different specs. Different motors will be compared to each other. From this, the most suitable motor based on the requirements stated will be chosen.

RMD x8

RMD-X8 is a servo actuator module with integrated gearing and a FOC driver. It has a high power density and a compact structure. This motor has earlier been used by other projects in

NTNU [32]. However, the difficulty with acquiring these motors eliminates them due to the time limit of the project.

Maxon

Maxon is a company that delivers a wide array of brushless DC motors. However, these motors are not with integrated gearing. They offer to sell separate planetary gear that is compatible with the motors. However, this would include extra effort that had to be done to combine these to find the best solution to our system. Furthermore, the mechanical interface would be much more complex to be able to satisfy the implementation of not only the motor but also the planetary gear. For further work, the optimal torque, gearing, and power density may be found with thorough research and design from the Maxon system. But due to the requirement to use an integrated module, this may be done as future work.

T-motor

To start it was looked at the system of SpaceBok that had utilized a U8-KV85 motor. This is originally a drone motor. However, the team from SpaceBok has made their own planetary gear that allows them to use it as a suitable drive-train for their robot.

Chapter 4

Final Design HOP 4.4

With all the requirements being set for the different components of the design, it is possible to optimize all the components with respect to these. The parts in this section will present the individual suggestions for the optimized parts. This iteration of the design, HOP4.4, has been manufactured and assembled to test its properties in a real physical environment. All of the simulations and physical testing have also been done with the components presented here.

4.1 Joints

To be able to achieve the most out of the design all the components of the assembly must be correctly fitted. Factors such as damping and friction must be diminished as much as possible. This will be tested when assembling the components. This will be most evident in the joints of the design. Here the potential for wasted energy due to friction between the components will most evident. To achieve the highest energy output the joints are designed with this as the main focus.

4.1.1 Joint Assembly

The design consists of two main parts that are manufactured separately and then assembled by hand. This is the Joint-B Figure 4.6 and Joint-T 4.4. To make the parts as light as possible these parts have been made in POM plastic, also known as Polyoxymethylene or Acetal plastic (POM). This is a semi-crystalline, engineered thermoplastic. Due to its properties, it has very low surface friction, high stiffness, and high dimensional stability. Making it a viable substitute for heavier options of materials such as steel and aluminum.

The assembly consists otherwise of the Joint pin, two bearings, and two lock rings to hold the construct in place.

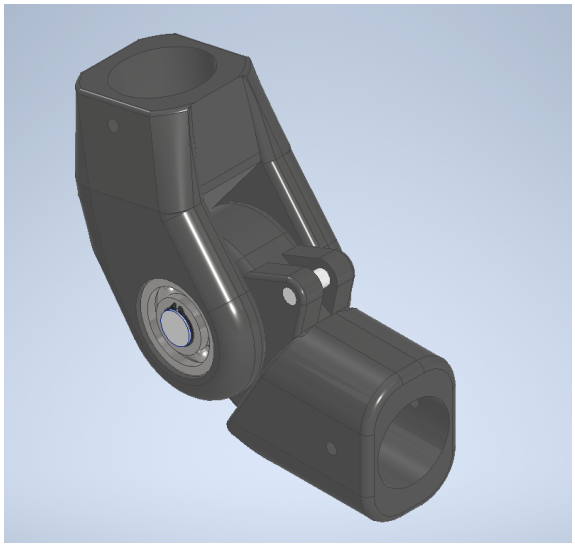

Figure 4.1: Joint component assembly.

While POM material has low friction, direct contact between the parts is not desirable. In addition to the added friction and energy loss, it will result in wear and potential damages or reduced longevity of the parts. This can alter clearances and fittings over time. To avoid this the Joint assembly is fitted such that the two different joints avoid contact with each other. In fig Figure 4.2 this clearance can be seen.

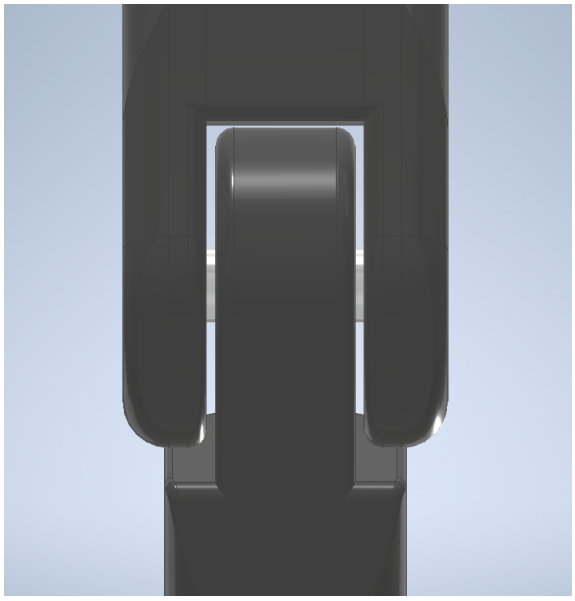

Figure 4.2: Clearance between parts in assembled joint component.

Joint Connection

An important aspect of this construct is that the distance of the clearance never changes or starts to drift. To ensure this, and that the two joints never come in contact, the Joint-Pin has a trace in the middle. By inserting a set screw through Joint-1 and into the trace the pin is locked in position. By inserting the lock rings on the side traces the pin is locked into place. And such, ensuring that the joint will not drift or move in any way.

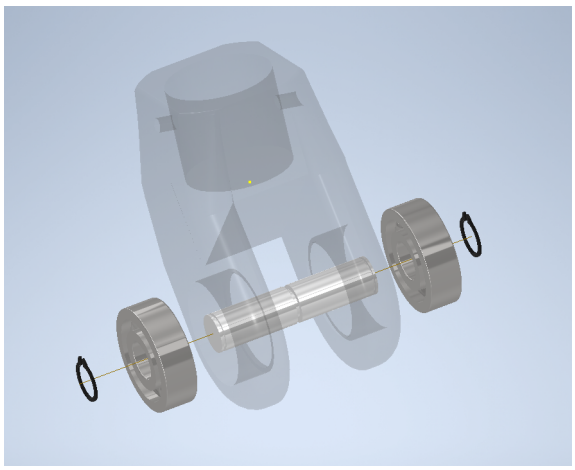

Figure 4.3: Exploded view of pin and bearing assembly for joint component.

4.1.2 Joint T

The upper joint, Joint-T, will be responsible for holding the bearings in place. A bearing will be placed in each of the holes that can be seen in Figure 4.4. The joints have been made to be as compact and light as possible. And still have a solid enough structure for any forces it will be exposed to.

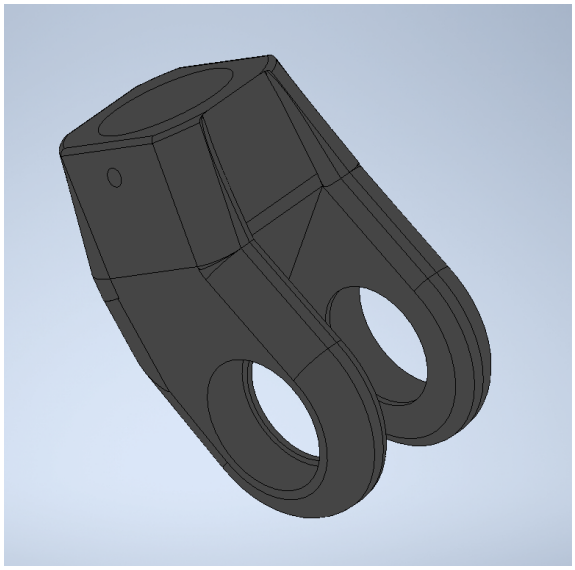

Figure 4.4: Single part; Joint T.

Joint T, Paw Connect

The Joint T, Paw Connect, is almost identical to the ordinary Joint T with the difference that it will act as the anchoring point for the paw assembly.

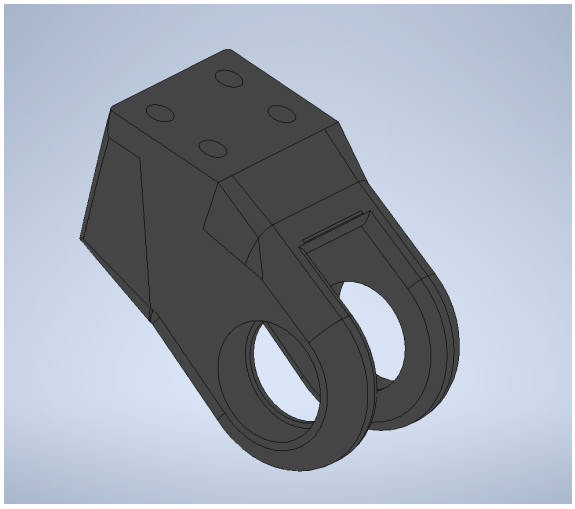

Figure 4.5: Single part; Joint T-Paw.

The paw assembly will be fastened with 4xM5 bolts to the holes that can be seen on the backside of the joint in Figure 4.5. As a result of this altering of the design, the Joint T-paw is slightly bigger than its other version, and also slightly heavier.

4.1.3 Joint B

Joint B is the lower joint part. It will inserted into the Joint T and connected to the bearings with a pin. The Joint B will have the spring insert as a vital component. It can clearly be seen in Figure 4.6.

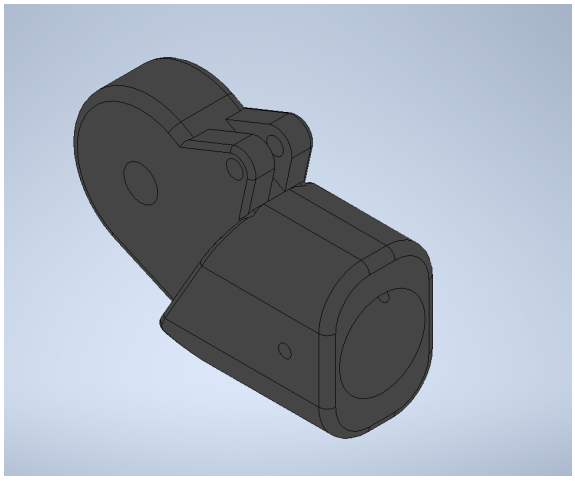

Figure 4.6: Single part; Joint B.

Spring insert

The spring insert will act as the anchoring for the spring in the design. To be able to make the design as modular as possible and having the opportunity to change the spring easily and without any specialised tools. A simple pin will be use as insert to hold the spring. In Figure 4.7 the spring insert can be seen with fitted pin.

(a) **(b)**

Figure 4.7: Joint T, Spring Insert.

4.2 Leg Insert

The Leg Insert will be responsible for transferring the torque from the actuators to the rest of the system. While it will need to be able to transfer the peak torque of the actuators. It will also need to retain its structural integrity while withstanding the forces made from the moment created by the spring forces.

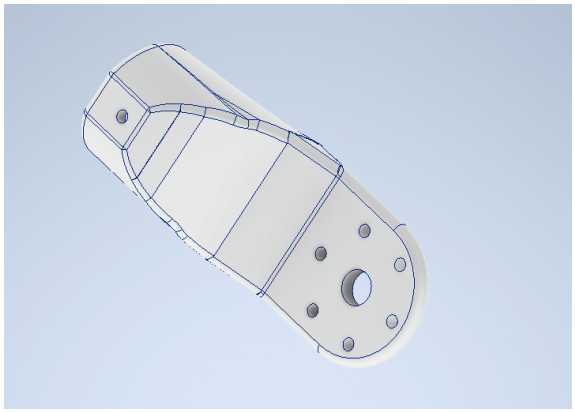

Figure 4.8: Single part; Leg Insert

The actuators are placed with their center at the same axis to create a balanced and equal work plane for the system. To facilitate this, and simultaneously have the carbon fiber legs acting in the same 2D plane as each other, the inserts are designed to have the same distance from the shared center between the motors. The leg insert consists of a flat surface where it will be connected to the motor and aligned with its neighboring leg insert and motor. To secure the carbon fiber leg, the leg fastener presented in Figure 4.10a will be used.

4.3 Legs

As discussed earlier one of the focal points of the design is to give all the components the lowest weight possible. This is extremely important for the legs, but as they also serve several other purposes other aspects and capabilities must be accounted for. To avoid drifting in the intersection between the other parts as well as deformation the legs must be rigid and have high stiffness. In addition to weight one of the most important aspects of the leg is that moment of inertia is as small as possible. Due to the simplicity of the leg design, it is possible to manufacture it of several materials.

Aluminum: With the requirements for the legs several design choices can be made. Aluminum would give the necessary strength and stiffens. It would be simple and cheap and manufactured, as well as being easy to alter with later iterations of the design. However, while aluminum is quite light it will be an added mass in comparison to other materials.

Steel: Steel will have many of the fulfill many of the same requirements as Aluminum. It stiffens and strength is even higher in fact, but the weight would be a major downside.

However, the strength would be significantly improved.

Carbon fiber: Since the most important requirement for the design is to achieve as low weight as possible, it is natural to find the lightest material that could potentially fulfill the requirements. This led to the choice of using carbon fiber tubes for the main leg components. Carbon fiber pipes have high directional strength and very high stiffness. This will ensure that there are no slipping and deformation in the design. Carbon fiber tubing is also the lightest of all the discussed materials.

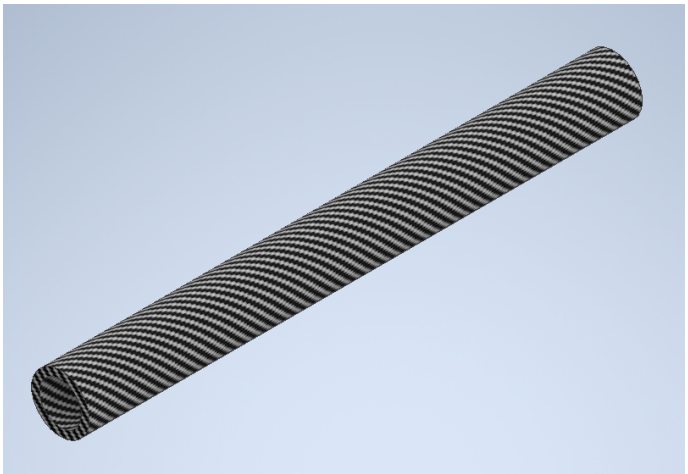

Figure 4.9: Single part; Carbon fiber Leg.

However, carbon fiber has some properties that can cause problems for the design. Due to their structure, carbon fiber tubes are quite brittle. And such assembly by directly inserting fastener screws or bolts could damage the structure. To solve this problem a component that can secure the carbon fiber tubes inside the joints, Figure 4.10a

Holes will be drilled through the carbon fiber tubes, the holes will be drilled to line up with the holes in the fastening component. By inserting screws through the tube and into the fastener, the fastener will be expanded and tightened the tube to be securely fastened inside the Joints and Leg Insert.

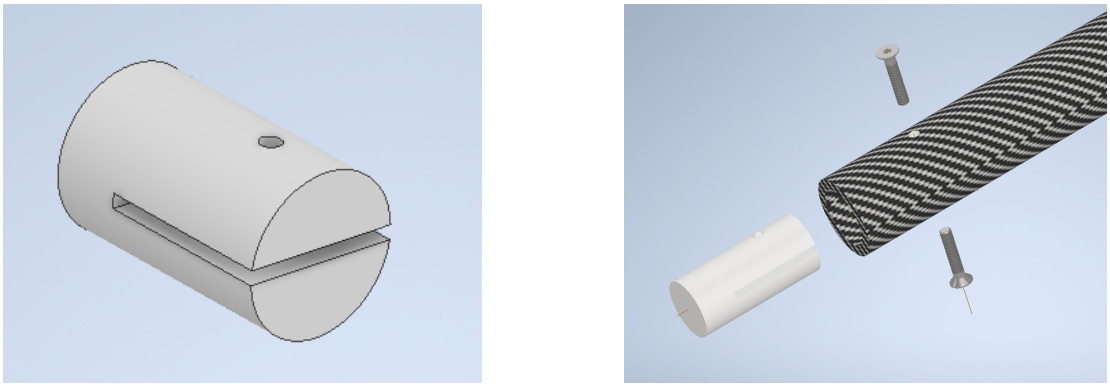

(a) Leg fastener **(b)** Fastener Assembly

Figure 4.10: Leg Fastener used in joints and leg insert.

This method has proven to be very useful, and physical testing has not given any sign of a problem with the connection method. Either in form of drifting or damages to either the joint or the carbon fiber tubing.

4.4 Motor Housing, Leg

The motor housing will act as the primary part of the motor support of the design, as it will house both motors. Since it is the only part connecting the two motors several design requirements are necessary and crucial for the design as a whole. The component is highly dependent on its interface and adjutant parts.

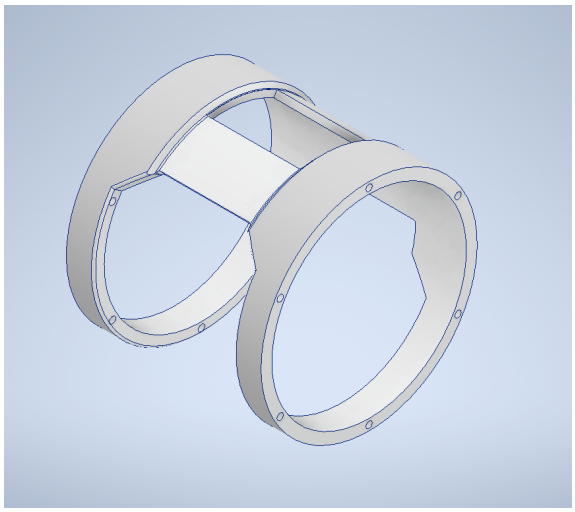

Figure 4.11: Single part; Motor Housing.

The current design of the motor housing has been made with an extensive focus on the weight. From Figure 4.11 and Figure 4.12b it can bee seen where material have been removed

to save weight.

While weight has been a focus, the stiffness and structural integrity of the component is crucial to ensure the rest of the system is held in place and functions properly. Therefore, as it can be seen from the Strength test Figure 5.32b the motor housing has a high general strength for potential forces.

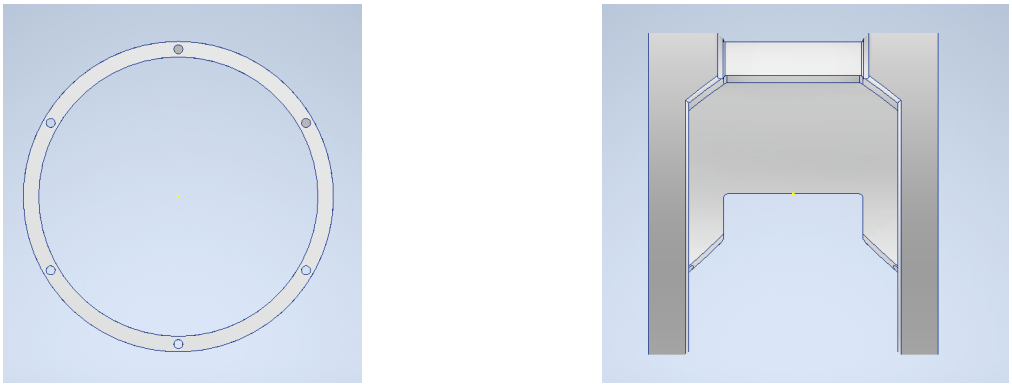

(a) **(b)**

Figure 4.12: Motor Housing; front and side view.

The Motor Housing Sides will be the components the motors are directly bolted into. With this specific design, the majority of the support on the motors will be on the Motor Housing. Therefore the Sides can be designed with the sole focus on securing the motors to the motor housing. As a result, the sides are made from POM to make it lightweight.

(a) **(b)**

Figure 4.13: Motor Housing Side.

The actuators will be secured with $8xM3$ to the Motor housing side. The motors will then be inserted into the motor housing a scan be seen if Figure 4.14a. Finally, the motor housing side will be bolted directly into the motor housing, and such securing the structure.

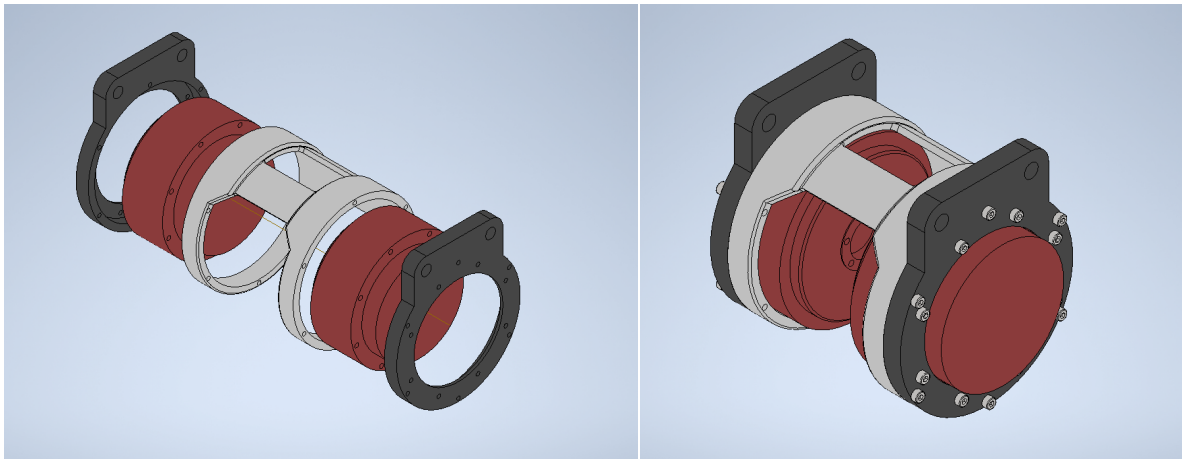

(a) **(b)**

Figure 4.14: Motor Housing Assembled with sides and motors.

4.5 Leg body Connection

The mechanical interface between the leg itself and the motor inserted in the motor housing is responsible for transferring the torque from hip adduction. It needs to be able to withstand the moment created in the motor with landings that are not perpendicular to the ground. As well as perpendicular forces created in jumping and landing motions.

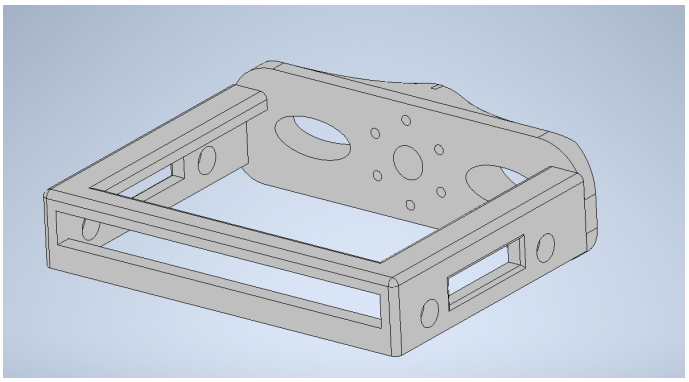

Figure 4.15: Leg Body Connection Assembly.

The component is made of two separate parts. One will be connected to the adduction motor in the Body Motor Housing. The other part will be the interface to the leg. As it can be seen in Figure 4.15 these two parts will be then fastened with each other.

Leg connect

Leg Connect will be the component acting as an interface between the Motor Housing Sides and the leg Body Connect. To save as much weight as possible only the material necessary for

remaining the structure meets the criteria for remaining structural sound during forces.

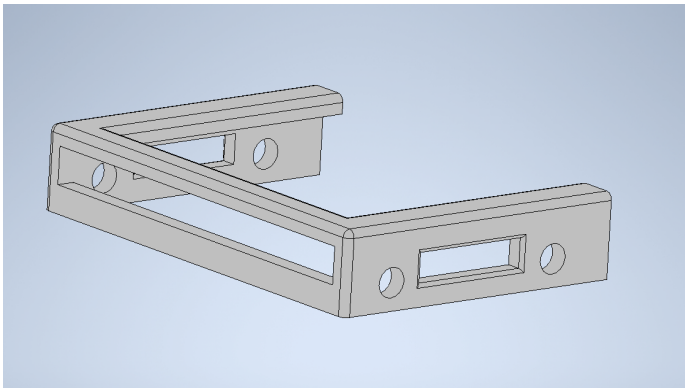

Figure 4.16: Single part; Leg Connect.

Motor Connect

Motor Connect is the only component connecting the leg design to the body design. It will be responsible for transferring any torque from the abduction motor to the leg. In addition to being strong enough for any forces in the leg to be transferred to the body without breaking or deforming.

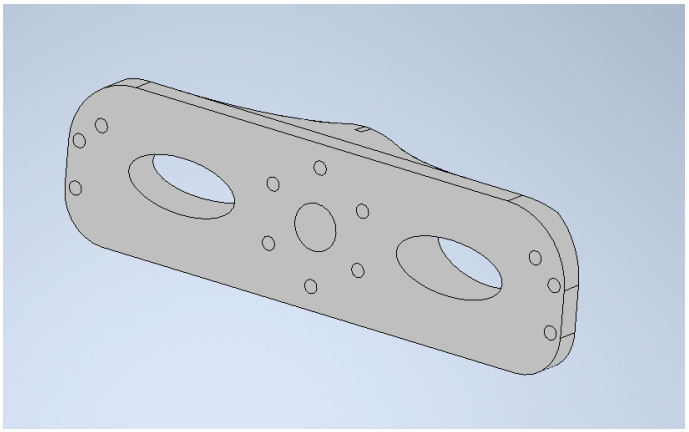

Figure 4.17: Single part; Motor Connect.

The connection is designed to give some clearance to the motor and the rest of the design. While giving this clearance the components are quite thick, therefore as it can be seen from Figure 4.17 material has been removed to minimize the weight as much as possible.

4.6 Paw

A key feature of the legged design is the choice of the paw that will be in direct contact with the ground. As earlier mentioned, wheeled locomotion will prove to be easily controlled and constructed. The legged design with a paw can have several advantages which can provide significantly better maneuverability, agility, and mobility.

There have been several different iterations of robotic paw design, and the current state of paw designs differs greatly for different robotic designs. Most of bipedal walking robots take advantage of flat paws with actuated ankles, examples such as ATLAS [7], Digit [33], HUBO [34], TALOS [35], NAO [36], Toro [37] and Walk-Man [38].

The reason for this design choice in bipedal robots is due to the fact that to stabilize them self they need to exert force on the ground, and therefore are dependent on having actuated flat paws. There are some exceptions to the bipedal paw designs, Hume [39] is a bipedal design with simple ball feet.

The case for quadruped-legged designs however is different. Their designs make stability and balance much simpler matters, they are not dependent on having paws that can exert force on the surface. Most quadruped-legged designs take advantage of the easier passive ball-shaped paw. Eg; ANYmal [1], HyQ [13], Spot [10] and MIT Cheetah [12]. While the passive ball-shaped paw is the most utilized configuration for quadruped-legged designs, there have been several different attempts at making flexible or adaptive paws that can provide capabilities that the standard passive ball shape can't. The "Adaptive feet for Quadrupedal Walkers [40] that have been tested in conjunction with the ANYmal [1]. Another example is the "Flexible foot design for a humanoid robot" [41].

The stability and locomotion capabilities of the robot as a whole will heavily depend on the design of the paw. While this is important there are several tasks that the paw design will need to account for.

Moment of Inertia

Due to the requirements that the robot design should be able to have reorientation and in-flight control capabilities, the paw must hold some mass. While the entire design of the rest of the leg is centered around having as small a moment of inertia and mass as possible. To be able to have an effective in-air flight control the paw, as they are the point furthest from the main body, will need to hold some mass to create enough force to manipulate the body as a whole.

While this is important, the solution of adding dummy mass should not be used. Therefore the challenge is to create a paw that will only have useful components, while still having enough mass to notably affect the moment of inertia at the end of the leg design. When making the design for the paw the requirements have to be made.

Paw Design requirements
Have capabilities that can contribute to the damping of the entire system
Have enough mass to create sufficient inertia for in-flight reorientation
Have sufficient grip to counter general slipping on surface
Be simple enough that it can be made for testing

Table 4.1: Important properties for the Paw component design.

While all of these requirements will be prioritized, a simple paw will be used in the beginning to start the physical testing. More complex assemblies and designs will be presented, however, for this version of the design, a simpler configuration of the paw will be used.

4.6.1 Carbon Flex foot

One of the possibilities for the paw design is to make the entire construct in carbon fiber composite. While this material is traditionally exposed to dynamical impact, with weak force absorption in omnidirectional aspects. However, there have been made advances in the prosthetic engineering field that have resulted in the "Flex-Foot Cheetah".

This product is used by amputee athletes in the Paralympics. Due to the shape and composition, it is not only able to absorb high impact forces, but also store the kinetic energy as potential, much like a spring [42].

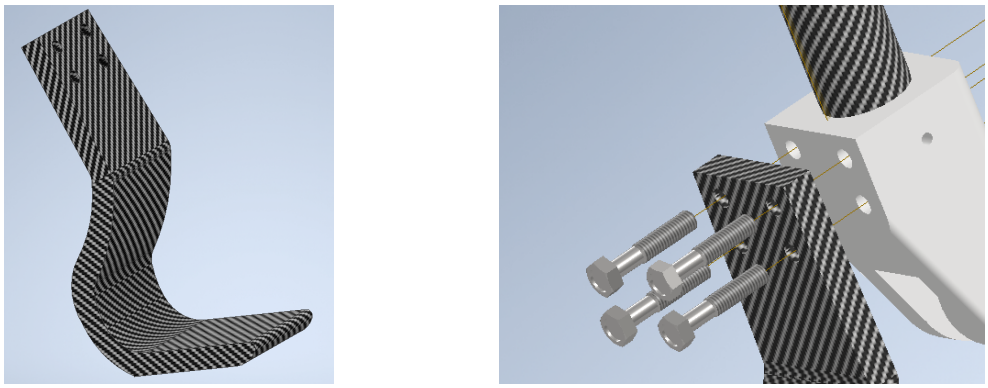

(a) **(b)**

Figure 4.18: Carbon Flex-Foot.

4.6.2 Ball-point foot

The most utilized type of foot for quadruped-legged robots is the ball-point, which uses a non-actuated foot. Quadruped-legged robots are not reliant on force-exerting feet such as bipedal designs are. Due to this fact that there is not necessary to create and design complex actuated feet. Instead, multiple concepts and designs for different ball-point have been made.

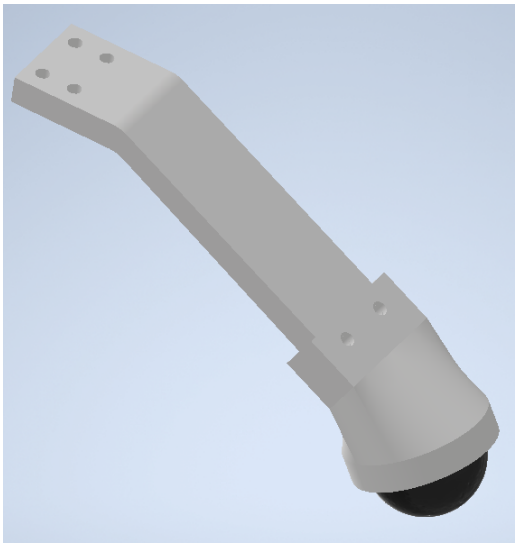

Figure 4.19: Ball-Point paw design.

4.6.3 Changeable sole foot

The design will in the beginning phases of physical testing depend on a simple foot design. This is because the earlier testing phases will focus on the jumping motion of the leg, as well as the general functionality and optimization of the design. With this in mind, a simple ball-point will be the most efficient for this phase. However, due to the different capabilities, the feet will need in the future this may not suffice for the foot design in later work.

To accommodate for this the "Changeable sole" design has been made. It will be able to alter all its properties, while still having the same mechanical interface as the other feet. With this design, it will be possible to change the length of the foot. The length will be a simple carbon fiber pipe, it will be fitted with the same fastening mechanism as the carbon fiber legs in the design. So no further altercations or designs are needed for this. Should the need arise, other materials with the same diameter can be used instead of the carbon fiber pipe.

(a) **(b)**

Figure 4.20: Changeable Sole Paw Components.

The sole of the paw will be fastened in the same manner as the part connected to the leg itself. The sole-insert is designed so any sole only needs 4xM5 to be fastened. Making it easy to change the sole. With the sole, it will be possible to change the properties of the foot that will have contact with the ground. Making it a solution that can be used for many different situations. The creations of soles can also be custom-made with specific properties in mind. Properties that have been discussed are different grips for different surfaces, different areas to accommodate for sinkage in soils, and different dampening functions.

Figure 4.21: Assembled Changeable Sole Paw, with a carbon fiber pipe as the adjustable length part.

4.7 Motor

The motor chosen for this project is also from T-motor. The AK70-10. It has a high torque with a peak of $25Nm$ and weight of $521g$ giving it excellent torque to weight ratio and power density. It is a fully integrated planetary gearing with a reduction ratio of $10:1$, making it ready for use without any further gearing or reduction necessary.

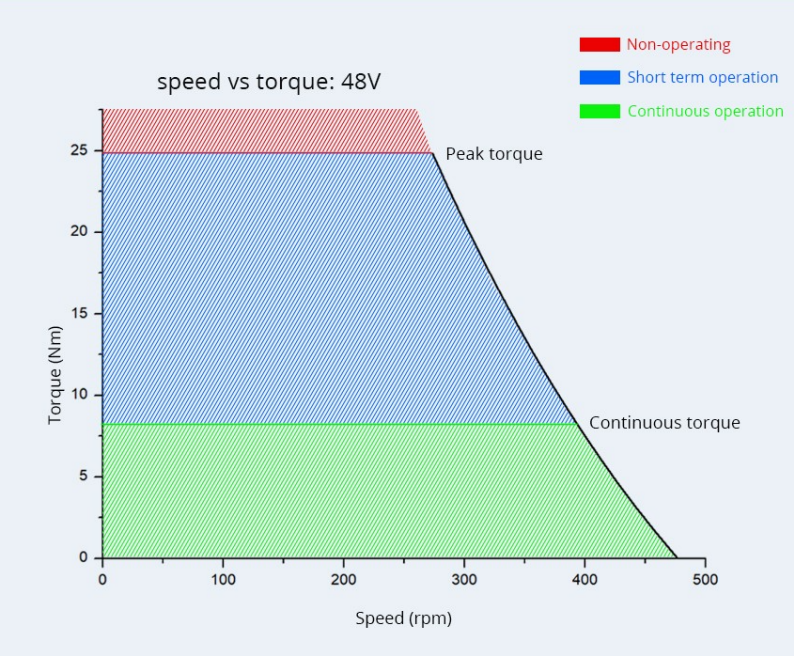

Figure 4.22: Torque vs speed of the AK70-10 [43].

As it is seen from Figure Figure 4.22 when utilizing the peak torque of the actuators it is possible to almost have an rpm of 300. This is a very important factor, as it is the speed the actuators can create for the system that will have a huge impact on the jumping capabilities of the system. This will be more covered in the simulation section. The motor of choice can be seen in Figure Figure 4.23.

Figure 4.23: CubeMars AK70-10 motor [43].

ESC and FOC

To be able to control and regulate the speed and angle of the actuators it is necessary to utilize an electronic speed controller (ESC). One of the benefits of the AK70-10 is that it comes integrated with an ESC, meaning there won't be a need to make or connect a separate component to the actuators for this purpose. In addition, the connector design has replaced the traditional wires to optimize installation. The contact interface is of a connector design with CAN protocol that makes it easier for connecting. As well as later the CAN protocol ban be utilized to control multiple of the same actuator easier.

The AK series actuators have as mentioned an integrated ESC in them. The one this uses is the Field Oriented Control, also called vector control, FOC. This is a special control method that improves the ability of the ESC.

Battery

To be able to use the actuators efficiently and have enough power to test the system properly. It needs to have sufficiently powerful and big enough batteries that can deliver sufficient power. The battery that will be used for the leg system test is a Gens Ace 6-cell battery, with a capacity of 2700mAh and a voltage of 22,2V. As the Actuators have a max operating voltage of 48v this setup will not be an optimal one. However, for the testing phase of the leg design, it will be sufficient.

The battery uses the XT60 connection, while the actuator uses the XT30 connection. This is the reason for the multiple connections presented in Figure Figure D.1. In Appendix D an overview of the electronics can be seen.

Controller

The controller that will be used for the testing of the system is an Arduino-R3. In addition to the Arduino controller, a CAN-BUS shield will be used to create an interface for the CAN connection from the actuator. The Arduino controller will send bit strings to the integrated controller in the motor via the CAN-Bus interface.

The reason for the use of Arduino is that it is an easily available and programmable controller that will work fine at the start of the testing phase of the system. In the future, other onboard PC will have to be considered for the whole system.

4.8 Leg Assembly

The final design of the jumping leg system has been the result of numerous iterations and design optimizations of all the different components. The components have all been strength tested and fitted to be compatible with the current last design iteration of the leg system.

During the project period the different components, while also beginning continuous optimization, have identified a set of requirements for the design. These requirements will be important for any future iterations of the different components.

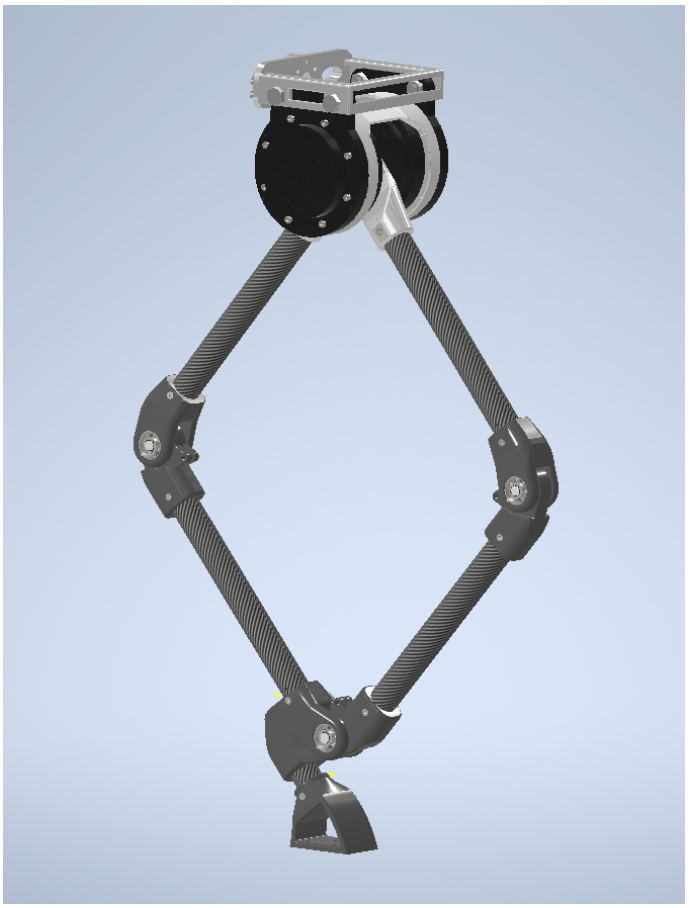

Figure 4.24: Fully assembled Leg.

The jumping mechanism for the first iteration of HOP4.1 is the same as the final design jumping mechanism. However, all the individual components have been modified and optimized.

4.8.1 Component and weight overview

When all the parts that are necessary for the design can be made an overview of all the different designs and their properties. While the physical robot will be made with the designs presented

in this chapter. Many iterations will be presented as alternatives to the current choices.

These different versions of the parts may alter in material, properties, sizes, and weight. All the parts are however made to be interchangeable with each other without having to make substantial changes to the interfaces and connections with the other parts. Making the entire design modular in nature. All the weights of the components have been found by the CAD program, Inventor.

Component overview, current iteration

Component	**Number of components**	**Component material**
AK70 Motor	2	
Joint T	3	POM
Joint B	2	POM
Joint B Paw	1	POM
Motor Housing	1	Aluminum
Motor Housing Side	2	POM
Carbon Fiber Leg	4	Carbon Fiber Tube
Motor Leg Insert	2	Aluminum
Leg Body Connect	1	Aluminum
Motor Body Connect	1	Aluminum

Table 4.2: Leg design component list.

Component	**Weight per comp [kg]**	**Weight all comp[kg]**	**Comp pct [%]**
AK70 Motor	0,521	1,042	51
Joint T	0,052	0,104	5,1
Joint B	0,052	0,104	5,1
Joint B Paw	0,056	0,056	2,7
Motor Housing	0,156	0,156	7,6
Motor Housing Side	0,045	0,09	4,4
Carbon Fiber Leg	0,045	0,18	8,8
Motor Leg Insert	0,065	0,13	6,4
Leg Body Connect	0,081	0,081	4
Motor Body Connect	0,1	0,1	4,9
Total Weight		**2,043**	

Table 4.3: Leg design weight overview list.

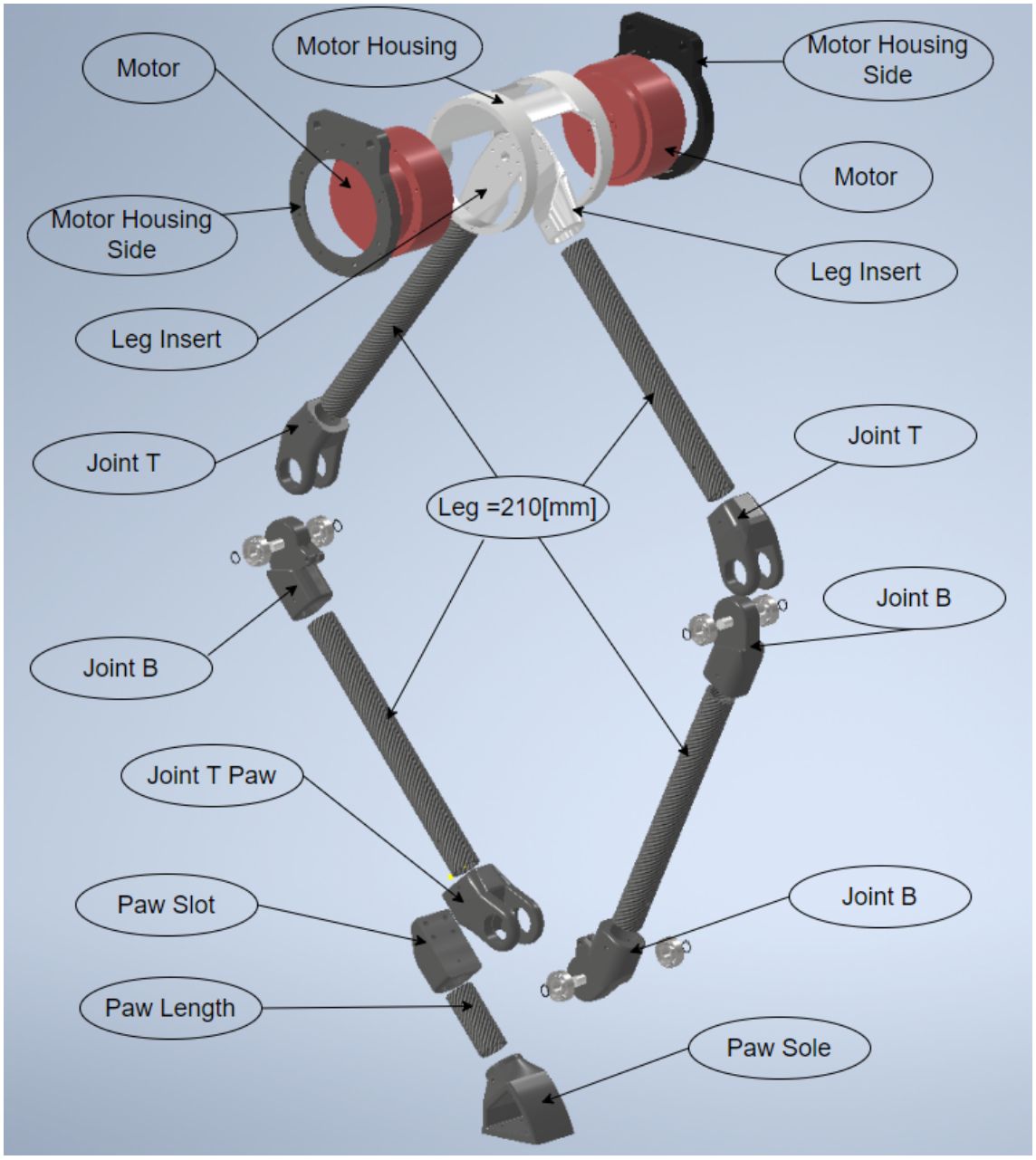

Figure 4.25: Exploded view of full design with notations.

4.9 Body Design

During the design process for the leg, a conceptualized design for a body was been made. Due to the fact that the thesis's main focus is on the Leg design and control. The body has not been optimized or manufactured. Due to the more conceptual take on the body design as opposed to the optimized leg design. As the different designs of the body have not been made it can't be made specific requirements for the properties of the design of the components. Therefore it has rather been identified important aspects the design will need to meet regardless of the future iterations.

4.9.1 Motor Housing Body

The motor housing will be an essential part of the design. It will be the component that connects the leg to the body and hence will serve several important aspects of the design. To be able to create a suitable design for the motor housing, and to identify the different qualities that will be important. To optimize the design for the current and future iterations set of important aspects have been made to the design.

Important Aspects of motor housing design
Weight
Impact and force absorption
Compatibility with rest of body
Mechanical interface with the leg
Mechanical interface with leg body connect

Table 4.4: Important aspects for future designs of Motor Housing Body.

As with the rest of the design. weight will be crucial for the full-body design choices. Over several iterations, the most weight-efficient design with regards to the current availability of material and machining was found to be POM, carbon fiber, and aluminum. The body motor housing is suggested to be made in POM. With this as a core it can be inserted into a metal casing that will act as a stiffener and absorb the different forces it will face. While the design of the leg itself is capable of absorbing forces that are created by falling and vertical impacts, the forces will need to be absorbed into the body itself as well. With this in mind, there has been created a suggested configuration for dampening the motor housing and the rest of the body.

The first part created with the body is the motor housing. Due to this design approach, the rest of the body will need to be designed in a manner that compliments the housing. This is to increase the absorption of forces, while also optimizing the weight of the final robot design. The mechanical interface between the leg itself and the motor inserted in the motor housing is responsible for hip adduction. It needs to be able to withstand the moment created in the motor with landings that are not perpendicular to the ground. As well as forces created during jumping and landing impacts.

With the most important aspects of the design located, it will be possible to design components. And also identify how they will affect the performance. Future iterations will possibly be

very different, however, the important aspects will be similar as long as the original full robot requirements are the same.

Dampening and impact absorption

During the jumping movement, and especially the impact from landings, the robot will experience a considerable force. The leg design itself is capable of absorbing forces quite efficiently. This is due to its two actuators with the same axis both breaking by applying a counter torque to the moment affecting the motors, as well as the spring. However, while the leg itself may prove sufficient for dampening it's important that the motor housing have dampening properties to maximize the entire design's dampening potential.

With this in mind, the motor housing itself will not be screwed or directly fastened to the sides or the front. It will instead have some room to move inside. By giving it this clearance and the possibility to move it can be implemented dampening functions. Due to limited time, there have been made several iterations of a dampening design. Where a rubber padding will be utilized if the other designs prove to be non-feasible to incorporate due to being too time-consuming to manufacture, assembles, and tested efficiently.

Spring dampening

The design that has the potential to give the highest dampening effect is the spring dampening design. Small slots will be inserted into the motor housing and the surrounding sides. Inside the slots, springs will be fastened. When the housing experience a force the spring will compress and dampen the impact on the motor housing and the rest of the body. The springs that will be used in this design have been simulated and found after taking into account several factors that are crucial for the design.

Body Motor Hosing spring
The springs can not have a travel distance that is smaller than the potential distance it can move inside the design
The clearance of the slots to each other must be larger than the travel distance of the springs, in regards to the previous point
The slots need to act as a mechanical hard stop to enable the springs to exceed their maximum travel distance
The motor housing in POM must not act as the hard stop. The slots inserted in the motor housing must hit the metal sides, not other way around

Table 4.5: Requirements for the Body motor housing springs for the dampening configuration.

To find springs that will meet the criteria a simulation in Simulink Multibodies has been made and utilized. It will simulate the drop of a given mass with the spring coefficient. One of the major problems this model however faces is that the dampening coefficient has in this case to be found by experimentation, making it impossible to incorporate it correctly in this simulation. Therefore several dampening coefficients have been used. The result of this is that while the frequency is greatly influenced, the maximum amplitude (travel of the spring) is not

affected to the same degree. Therefore the spring has been chosen with this mind.

The springs are however only installed on the top and the inner side of the motor housing. The reasoning for this being the force direction will primarily concentrate here on the impact of the landing. Due to the design and potential compensating in position for landing this is the direction most of the forces will be. It is important that the clearance between the slots are large enough to compensate for the travel in both directions.

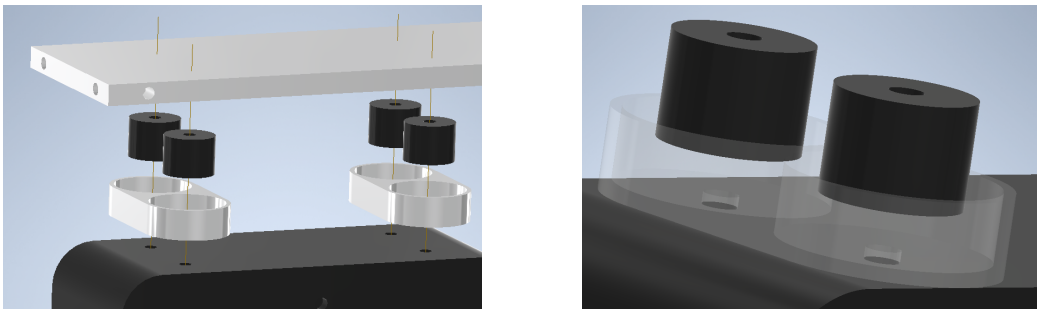

(a) Assembly of dampening configuration. **(b)** Spring slots overview.

Figure 4.26: Conceptual design of the Motor Housing Body spring dampening construction.

For the remaining two sides rubber will be placed. In addition, to act as extra dampening it will press the motor housing in place, securing the design and giving it better stability. And hindering it to travel any other way than the spring sides.

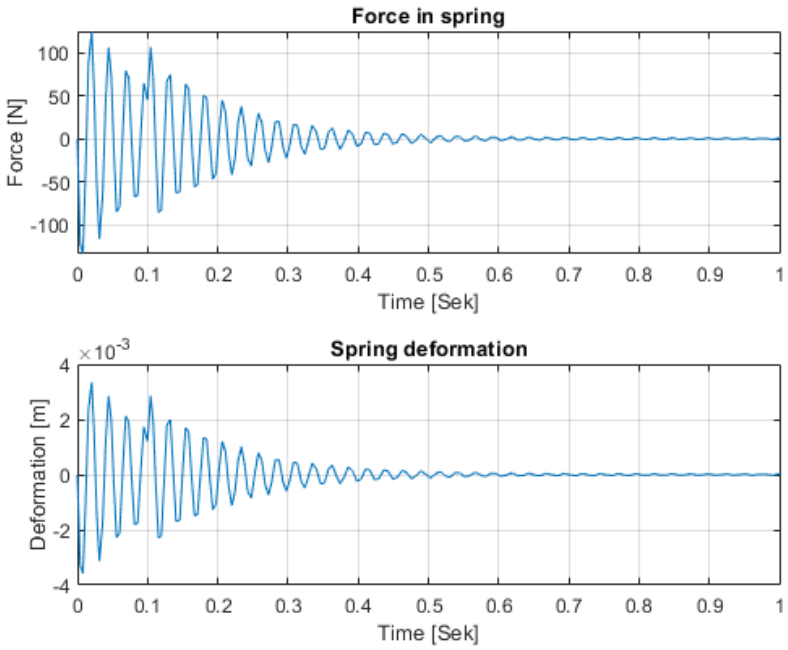

Figure 4.27: Spring Dampening Results, Body Motor Housing.

As it can be seen from the results in the graph, a drop from $1m$ will result in a deformation of the spring to a maximum of approximately $4mm$. However, due to the design and dampening from the rubber, this would be difficult to incorporate into the simulation. With this in mind as long as the traveling distance boundaries are within the maximum deformation of the simulation this is the only thing that matters. With this in mind, a spring with the following qualities has been chosen.

Material	Piano thread
d - Thread [mm]	1.60
De - Outer diameter [mm]	9.60
Di - Inner diameter [mm]	6.40
L0 - Non loaded length [mm	14.50
Ln - Max loaded length [mm]	9.00
Sn - Max travel [mm]	5.50
Fn - Max load at Ln [N]	211.82
K - Spring constant	37.27

Table 4.6: Body dampening spring parameters.

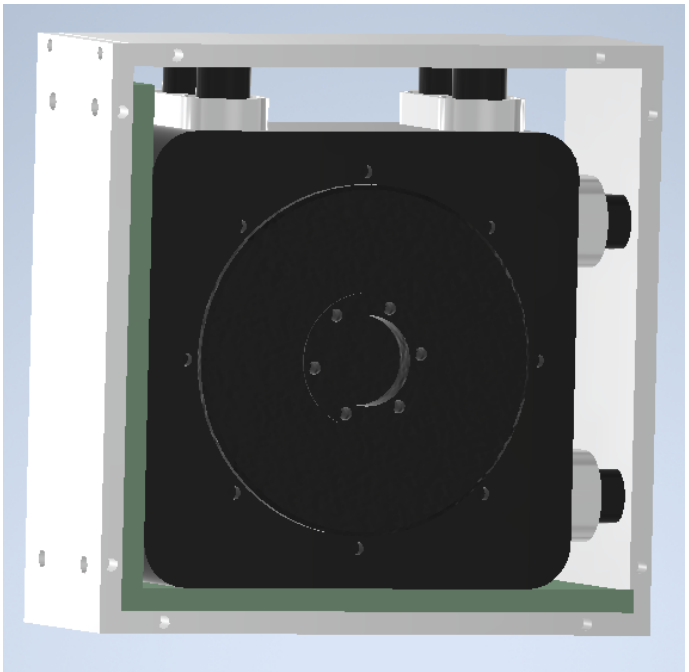

Figure 4.28: Conceptual spring dampening design for Motor Housing Body.

As mentioned earlier, if the described spring system will be too difficult to implement. All the sides can be lined with rubber. As the slots are screwed into the housing and sides these can be removed and placed easily as the design will require.

4.9.2 Front

The front of the robots will need to serve multiple factors. With the current design, it will need to act as a fastener for the motor housing and secure the motor housing with the sides. One of the challenges with the interface between the front, motor housing, and the sides. Is to allow the motor housing the possibility to travel and move to utilize the spring dampening system. While still securing it in such a way that doesn't shift move out of position or damage the design.

To be able to create a suitable design for the motor housing, and to identify the different qualities that will be important. Not only for the current design but for improved iterations in the future. A set of requirements have been set.

Body Front important design aspects
Weight
Ability to stiffen and brace the body design
Mechanical interface with the motor housing
Mechanical interface with rest of the body

Table 4.7: Important aspects for future designs of Body Front.

As with the rest of the components in the design, the most important is to reduce the weight to a minimum. While This has been the number one priority for the earlier components, due to the importance of structural integrity crucial to the design as a whole it may be necessary to use a material that favors strength overweight. While the leg design has a natural dampening due to its design, the body doesn't have the same properties. This is a situation that will apply to many of the body components, as strength and stiffens may have to be prioritized over weight.

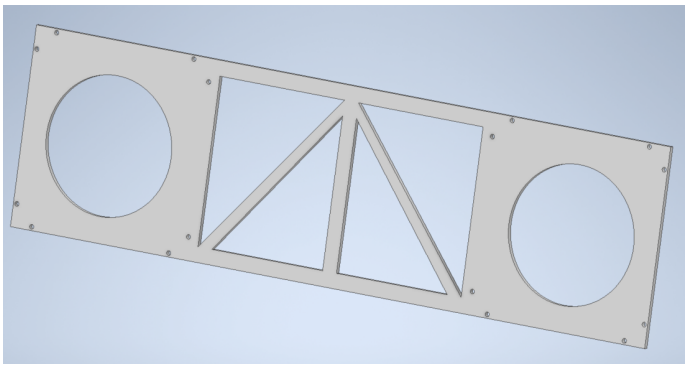

Figure 4.29: Conceptual Body Front design.

The front will mainly act as a support structure that will stiffen and connect the two motor housings. Due to the current design, it will not be directly fastened into the motor housing. But instead the surroundings side structures. The reason for this is so the motor hosing can move freely inside the motor hosing sides.

The structure of the front can easily be cut out of plates of the chosen material. While this design has been chosen to have both high structural integrity and save weight, as much of the material has been cut from the middle of the component. With the future design, it can be saved more weight or gained a higher strength by changing how much has been cut away. v AS can be seen from Figure 4.30 the motor is not placed in the center of the outer parts of the front. This is to give it clearance with regards to the front and motor housing while it moves. Doing this will avoid collision between the motor and the front. Due to the fact it can only travel upwards and to the left, it is placed in a off-centered position that allows for this.

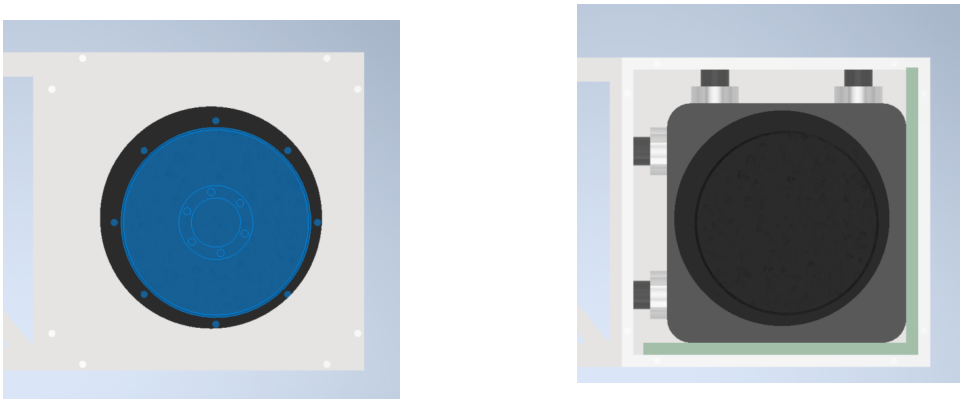

(a) Body front mounted, motor in blue.

(b) Placement of motor and dampening configuration.

Figure 4.30: Body Front with Motor Housing assembled.

Two identical fronts will be placed on both sides of the motor housing. As can be seen in Figure 4.31 As the housing itself is not secured by any other means, they have to be held together by the front. It will be fastened with 8xM3 screws in identical ways for both sides

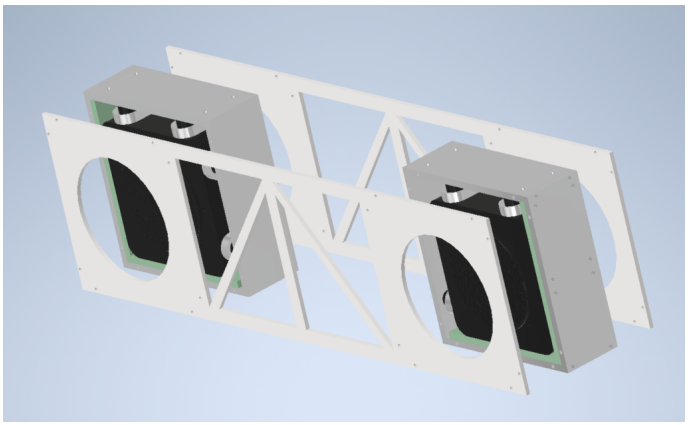

Figure 4.31: Body Front Placement on the Motor Housing Body.

4.9.3 Side

One of the most structurally important parts of the body as well as the entire robot design is the sides. They will act as the main support for the entire system, and they will need to withstand all the forces that the design will be exposed to.

To be able to create a suitable design for the motor housing, and to identify the different qualities that will be important. Not only for the current design but for improved iterations in the future. A set of requirements have been set.

Body Side important design aspects
Weight
Ability to withstand all the forces the design will be exposed to
Mechanical interface with rest of the body

Table 4.8: Important aspects for future designs of Body Side.

However, with this design, it is easy to change the carbon fiber pipes to other materials of the same dimension, e.g aluminum, plastics, and steel. The slots in which the pipes will be connected to the body will be made of POM in this iteration. They will be screwed directly into the sides of the motor housing. The pipes will then be inserted and fastened in the same way as the previous pipes.

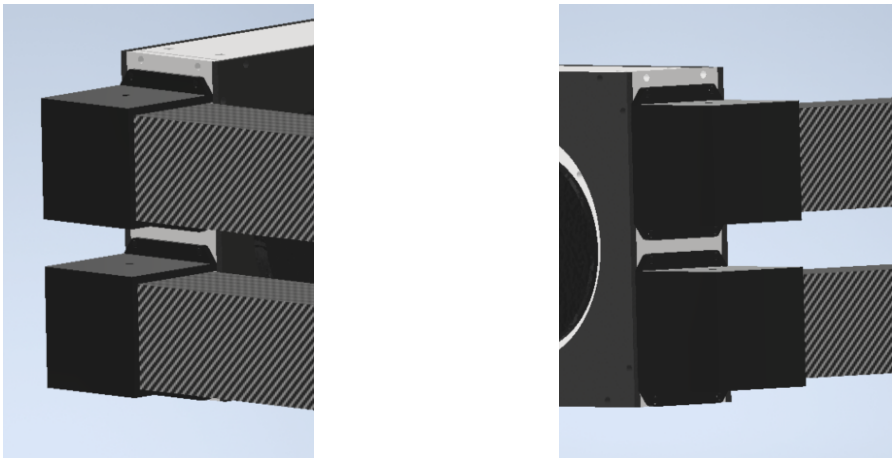

(a) **(b)**

Figure 4.32: Body Side, tube inserts assembled and fastened to the Motor Housing Body.

To be able to make a design that can be modular in nature, and such make it easy to change the sides. The current sides are rectangular 40x40mm carbon fiber pipes which will be fitted into slots and then fastened. They will be fastened in the same way that the carbon fiber pipes of the leg design with a fastening component inserted into the pipes.

One of the most important aspects as has been discussed numerous times is the weight. Therefore the design is made in such a way that the slots can be made for other dimensions, without altering the motor housing sides. Therefore multiple iterations can be tested without

changing the much more complex design and multiple interfaces of the motor housing components.

4.9.4 Carbon top and bottom

The suggestion for a conceptual body design would be to use carbon fiber plates to strengthen and stiffen the entirety of the structure. By using sandwich composite carbon fiber plates the weight could also be reduced when compared to the usage of standard carbon fiber plates.

Body Top/Bottom important design aspects
Weight
Ability to stiffen the entire body structure
Ability to withstand impacts and any forces that will affect the body and entire robot

Table 4.9: Important aspects for future designs of Body Top and Bottom components.

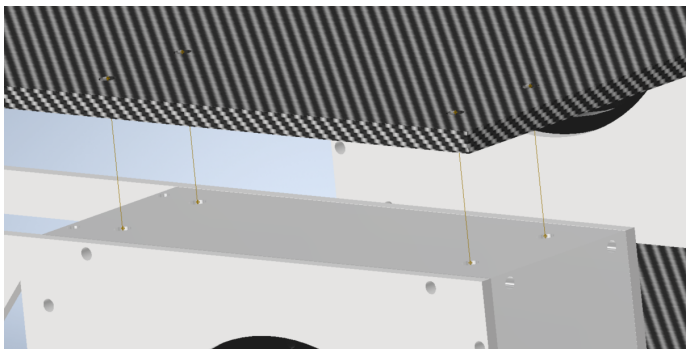

Figure 4.33: Body insert top motor housing.

The conceptual body with the carbon fiber plates placed on the top and bottom can have been designed and modeled. While this body design is a very early iteration it may be used as a base for the different needed parts and components that will be needed for the future full-body design.

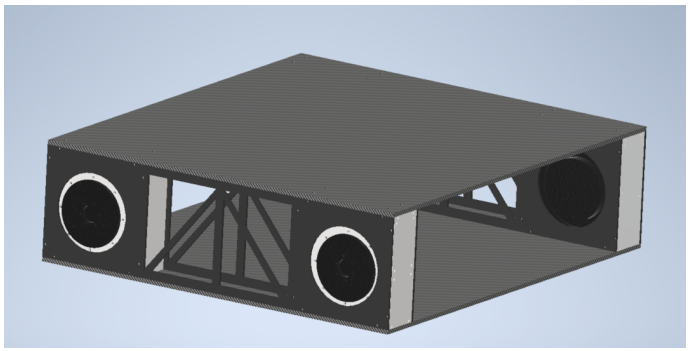

Figure 4.34: Conceptual design of a full Body assembly.

Chapter 5

Simulation

5.1 Forces in the system

During the various movements of the leg, it will experience several different forces. To be able to conduct stress test simulations. These forces will need to be identified to give as accurate as possible representations of the actual forces to which the system will be exposed.

When the forces have been identified, the different parameters generating these can be altered to change the abilities of the system.

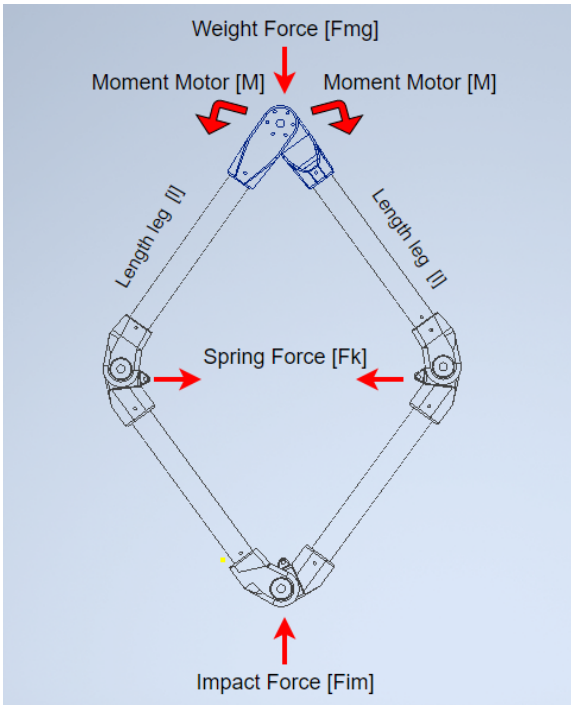

Figure 5.1: Overview of forces acting on the system, and the forces created from motors and springs.

The critical force on the system is the weight of the design. This will create forces that act through the entire leg design. By altering the weight of the body and the motors, the reaction forces in the leg will change. Due to the joint around the motors being the acting pivot for the system, all the parts seen in Figure 5.1 have been neglected for this calculation due to their low weight and positioning with regards to acting forces and moments in the closed kinematic chain.

The torque from the motors is the main counteracting gravity and the spring force. While they will be needed for all movement and actuating, the spring will be able to hold a mass by itself. Meaning the system can stand upright without the use of continuous torque from the motors. Giving the potential to save power while standing still. The actuators will need to act both clockwise and counterclockwise depending if the design should compress or extend.

With the current design choices, the spring will be chosen to have a non-loaded length that will coincide with the starting angle between the two top legs, $beta$. The spring force will increase the more the angle $beta$ increases. The size of the spring must be chosen to fit within the maximum distance it can extend in the system. This can be changed by changing the length of the carbon fiber legs. The spring coefficient must be chosen such that the motors can extend the spring. An important factor is the weight of the design, as this will add to the force that is needed to extend the spring.

The impact force will be the force the system experiences from drops and similar collisions during its movements. By simulation the force created during these collisions with the potential deformation of the system an average impact force can be found. This force can be used to design components that can withstand specific heights and different masses.

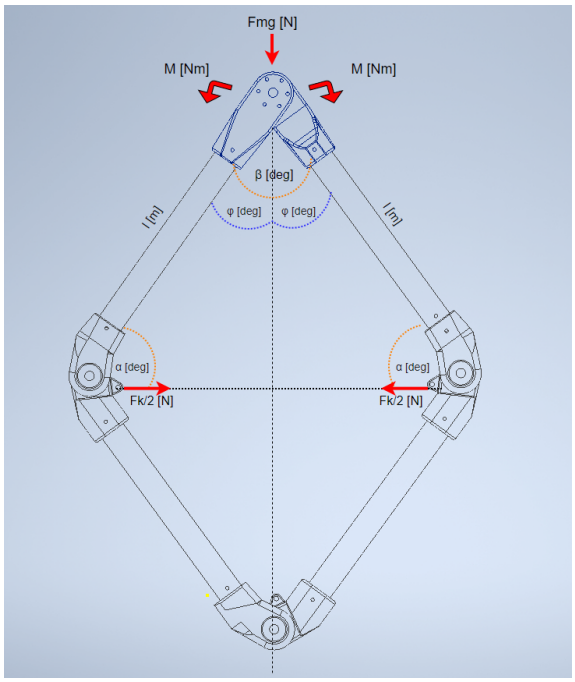

Figure 5.2: Force from weight, motors and spring with correlating angles.

The system is further broken down to illustrate the different forces acting on the system. As well as the notation and nature of the different forces. A FBD can be drawn to deconstruct the different forces and start to identify the different forces acting in the system.

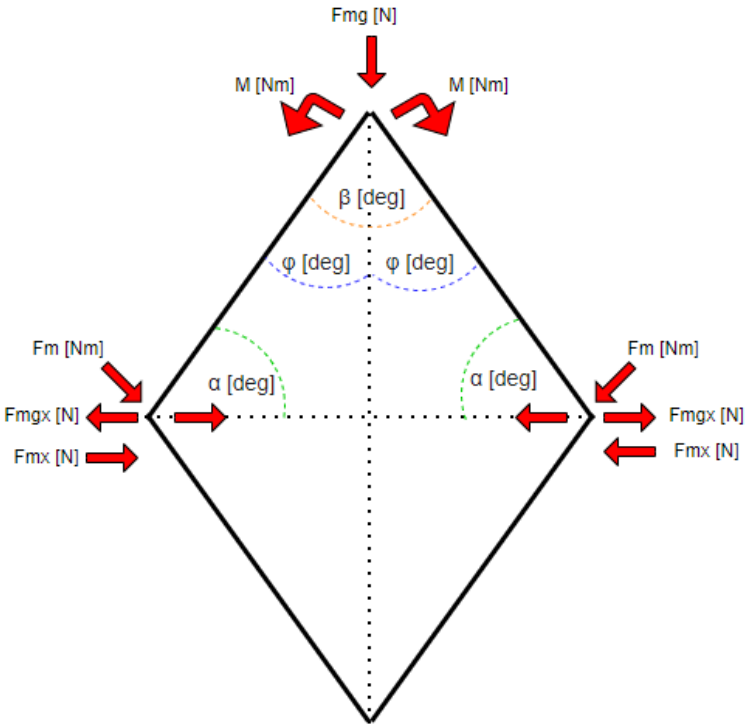

Figure 5.3: An FBD of the force overview.

Forces made in spring by deformation

Most of the forces will be calculated with respect to the β, the reasoning behind this is that this makes it compatible with the physical system. Where the β angle can be found with only the motors encoder. Gives the possibility to have an overview of the different forces without the use of sensors. $Spring_{min}$ and $Spring_{max}$ are the minimum and maximum length of the spring, and SGC is a constant that compensates for geometrical influences in the components that effects the distances and angles in the calculations.

$$x_{min} = spring_{min} + SGC \tag{5.1}$$

$$x_{max} = spring_{max} + SGC \tag{5.2}$$

$$\beta_{min} = \arccos \frac{l^2 + x_{min} - l^2}{2ll} \tag{5.3}$$

$$\beta_{max} = \arccos \frac{l^2 + x_{max} - l^2}{2ll} \tag{5.4}$$

Maximum and minimum angle of beta are found to be able to base the rest of the calculations on thees. The angle is dependent on the spring and the legs that are chosen. β_{min} and β_{max} are the minimum and maximum angles corresponding to the lengths of the legs l and $Spring_{min}$ and $Spring_{max}$.

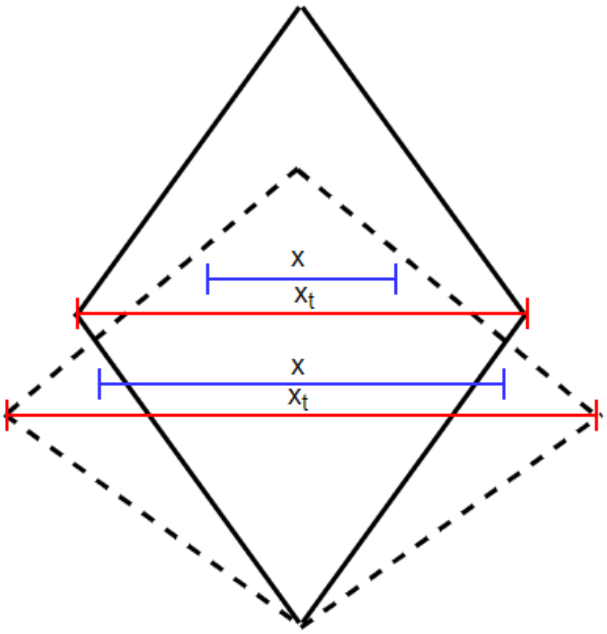

Figure 5.4: Visualization of changing distances in the system during compression.

$$x_t = \sqrt{l^2 + l^2 - 2ll * \cos(\beta)} \tag{5.5}$$

$$x = \sqrt{l^2 + l^2 - 2ll\cos(\beta)} - (SGC + x_{min}) \tag{5.6}$$

The force in the spring is a result of Hook's law, therefore the displacement with respect to the original length is found. Due to the geometrical structure of the leg, it is necessary to include a geometrical coefficient to compensate for this during the calculations. X_t is given as the geometrical length of the whole spring axis, Figure 5.4, x is the displacement with respect to only the spring. With the displacement. Hook's law can be utilized to find the force F_k in the spring.

$$F_k = xk \tag{5.7}$$

To find the torque needed to counteract the spring force, it is necessary to find the moment generated by the spring with respect to the moment around the motor axis. The α angle is found as a result of the length of the spring axis and the leg length.

$$\alpha = \frac{l^2 + x_t^2 - l^2}{2x_t l} \tag{5.8}$$

The force of the weight will act as a supplement when the motors are applying torque to extend the spring. This force needed to be added when the moment needed for extending the spring is calculated. Decomposition of the weight forces and difference with respect to spring force. With F_{mg} force from gravity, F_{km} force created in motor from spring, F_{mgx} force created from gravity deconstructed for the spring direction, F_{kmm} is the resultant force from gravity, moment and the spring in the spring direction.

$$F_{mg} = \frac{mg}{\sin(90 - \beta/2)} \tag{5.9}$$

$$F_{km} = F_k l \cos(\alpha) \tag{5.10}$$

$$F_{mgx} = F_{mg} \cos(\alpha) \tag{5.11}$$

$$F_{kmm} = F_k - F_{mgx} \tag{5.12}$$

The moment needed from the motor to counteract the force in the spring and expand it is stated as the moment created from the resulting forces M. As this is the entire force generated, each motor of the design will need to generate half this moment.

$$M = F_{kmm} l \cos(\alpha) \tag{5.13}$$

By dividing this by two the torque needed in each motor is found. The graphs are showing the moment needed for each motor to provide to stretch the spring at a given length. Otherwise, the force created in the spring can be seen based on its displacement as well as the angle of β. With these forces identified the components such as spring fasteners and joints can be designed and optimized based on the type of spring chosen, and visa versa.
One of the most important aspects of the design is the system's ability to extend the spring to create the force needed for jumping. Therefore the spring can not be too strong and hinder this movement.

Force from weight and impact

Due to the design of the system, the max weight it can withstand without collapsing is dependent on the length of the legs, the torque of the motor, as well as the length and coefficient of the spring.

The other aspect of the design is the distance the system will contract when experienced during weight being added or the impact from collision forces. The torque form the motor

in the spring direction. When sustaining weight the spring force and the actuators will both contribute to this goal. The force created from the motor in spring direction F_{Mx} is stated.

$$F_{Mx} = \frac{Torque_{motor}}{l} \cos(\alpha) \tag{5.14}$$

The force from weight is deconstructed in the spring direction.

$$F_{mg} = \frac{mg}{\sin(90 - \beta/2} \tag{5.15}$$

$$F_{mgx} = f_{mg} \cos(\alpha) \tag{5.16}$$

The maximum weight the system can hold without collapsing as a result of the α angle. This weight is the max weight the system can hold before the spring and actuators will fail.

$$mass_{max} = \frac{((F_{Mx}2 + F_k)\sin(\alpha)}{\cos(\alpha)g} \tag{5.17}$$

The average impact force on the system during impact will be a result of the energy from the potential fall. To be able to analyze the energy must be converted into force in N. The vertical compression will act as the deformation, and hence absorbed the force based on the deformation of the system.

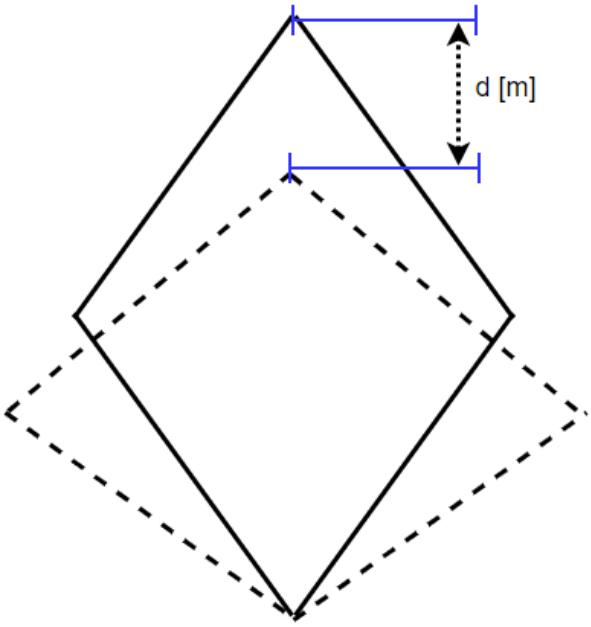

Figure 5.5: Lateral displacement of the system during compression.

The length the system can be compressed is found by simple geometry.

$$d = 2 * (l \sin(\alpha_{max})) - lsin(\alpha_{min})) \tag{5.18}$$

The average impact force, AIF, the system will experience from a given height and mass.

$$AIF = \frac{m * g * h}{d} \tag{5.19}$$

5.2 Design parameters optimization

This section will be focused on the utilization of the scripts created from the force decomposition to identify how the system will react to different parameters being changed.

With this information, it will be easier to optimize the design for any future iterations. When optimizing the parameters there will be used a constant weight of the system of $5Kg$. While this will be the standard for the current optimization, it is only a placeholder for the true weight that has to be found from any future full design.

To be able to optimize the current system the only parameters that will be changed are the length of the legs and the spring coefficient. For all the calculations a motor torque of $24[Nm]$ has been used. Testing showed the average output from the motors is greater than this. However, due to not overshooting any of the results, a little more conservative value has been used in the motor torque.

Optimal Configuration parameters
Spring minimum distance
Spring maximum
Total body mass
Gravity
Leg length
Spring Coefficient

Table 5.1: Parameters that affect the results of the optimization simulations.

For the current iteration of the design different configurations of leg length and spring coefficient have been tested to see if there are any correlations or notable trade-offs between design choices.

Current iteration of the design; $Leg210[mm]$

From Figure 5.6a it can be seen that the current spring coefficient of $0.88[N/mm]$ is well under the maximum motor torque of $24[N/mm]$. With the current leg lengths a coefficient of $1.2[N/mm]$ would be possible as seen in Figure 5.6b.

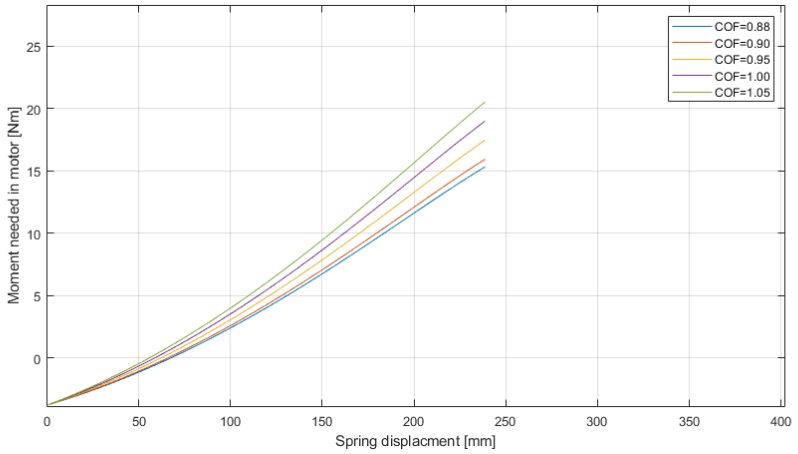

(a)

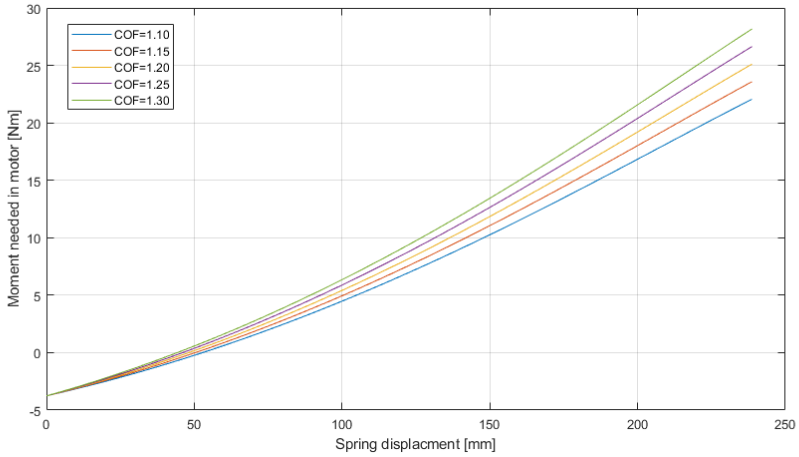

(b)

Figure 5.6: Moment in motor; *Leg=210[mm]*.

From the optimized choice of $COF = 1.2[N/mm]$ a maximum mass of $\approx 30.60[Kg]$ can theoretically be supported. With the current choice of $0.88[N/mm]$ the maximum mass that can be supported it limited to $\approx 25.8[Kg]$. This is presented in Figure 5.7.

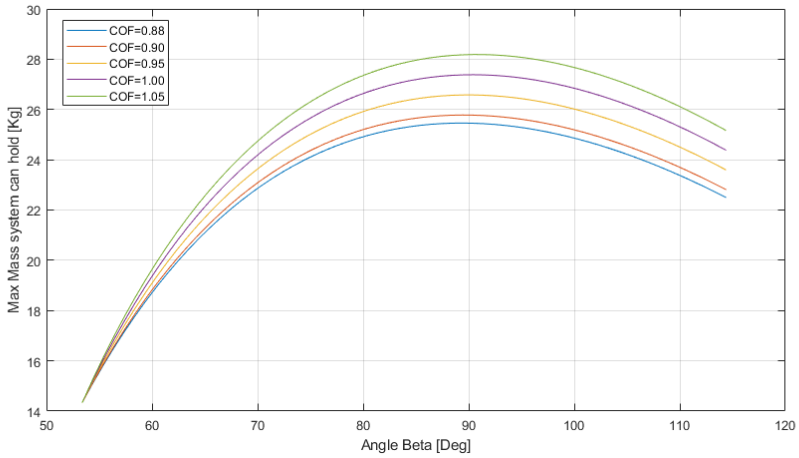

(a)

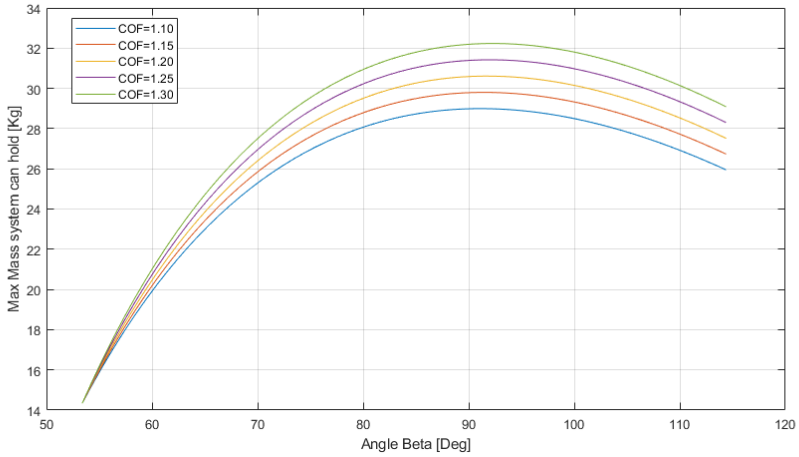

(b)

Figure 5.7: Max mass, *Leg=210[mm]*.

Current iteration of the design; $COF[0.88N/mm]$

From Figure 5.8 it can be seen that the moment needed in the motor will decrease with shorter legs. As a result, with shorter legs, the spring coefficient can be higher, which again will result in a potentially higher force with the stronger spring. While shorter legs seem to be able to generate a higher moment from the given torque of the motor, short legs may also cause problems. Should the leg get too short the geometry of the system will start to converge to begin not feasible. As it can be seen from the $Leg = 185$ results and downwards, a descent after the apex of the moment curve appears. This is due to the angles between the legs needing to be larger to reach full displacement. This may be counteracted by having a smaller spring.

However due to this, while the $Leg = 170$ shows the most promise purely based on the moment, it's recommended to not go below the distance of $Leg = 180$ with the current con-

figuration of spring length.

While the moment needed is decreased with the shorter legs, the maximum mass is also decreased with shorter legs. This means the shorter legs will result in a lower potential supported mass.
This is a trade-off that will need to be taken into consideration when choosing the optimal parameters for the design.

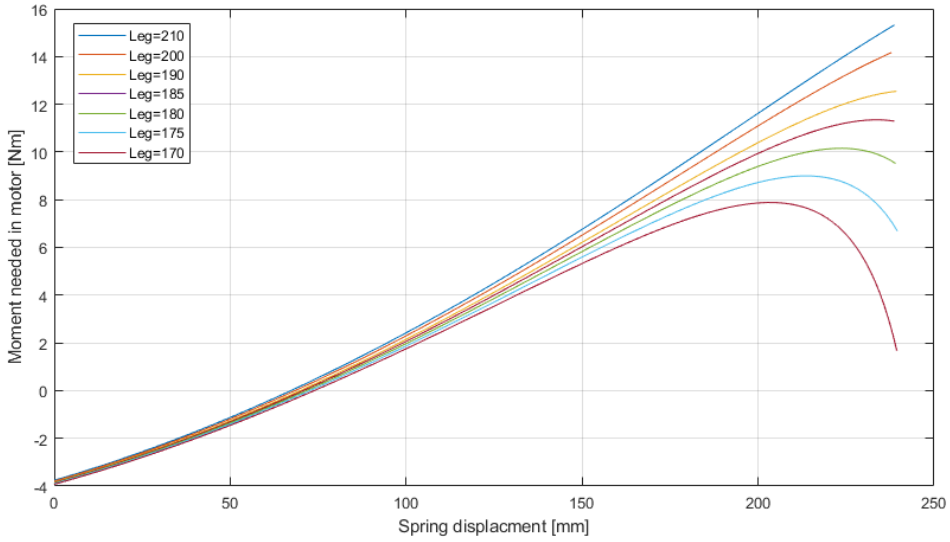

Figure 5.8: Moment in motor; *COF=0.88[N/mm]*.

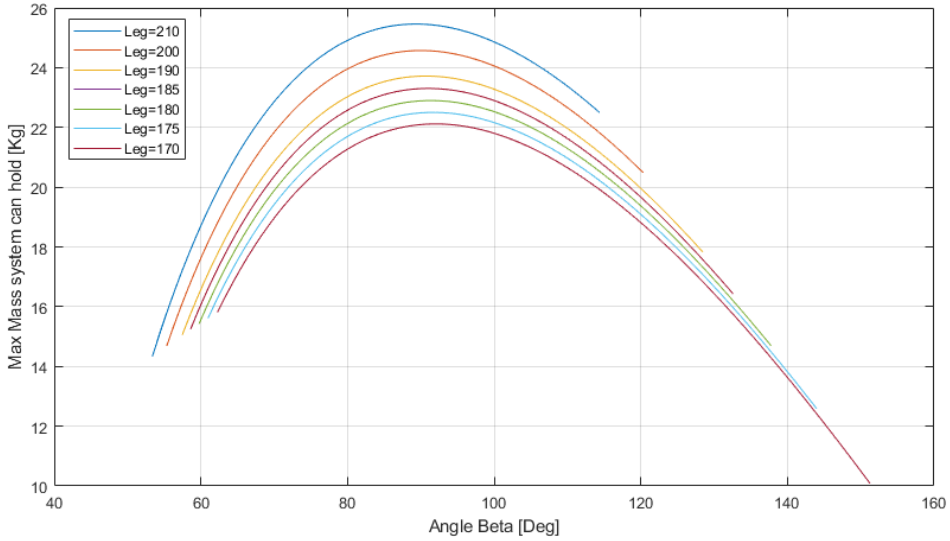

Figure 5.9: Max mass; *COF=0.88[N/mm]*.

Results for potential optimized iteration; $Leg180mm$

From Figure 5.8 a leg length of 180$[mm]$ was chosen as a candidate for the optimal design. Results shows this as a good length with regards to avoiding the steep descent of mass that occurs for the shortest lengths, as seen in Figure 5.9. This length is also outside the are were the geometrical complications have a severe impact on the moment and mass, as seen in Figure 5.8 and Figure 5.9

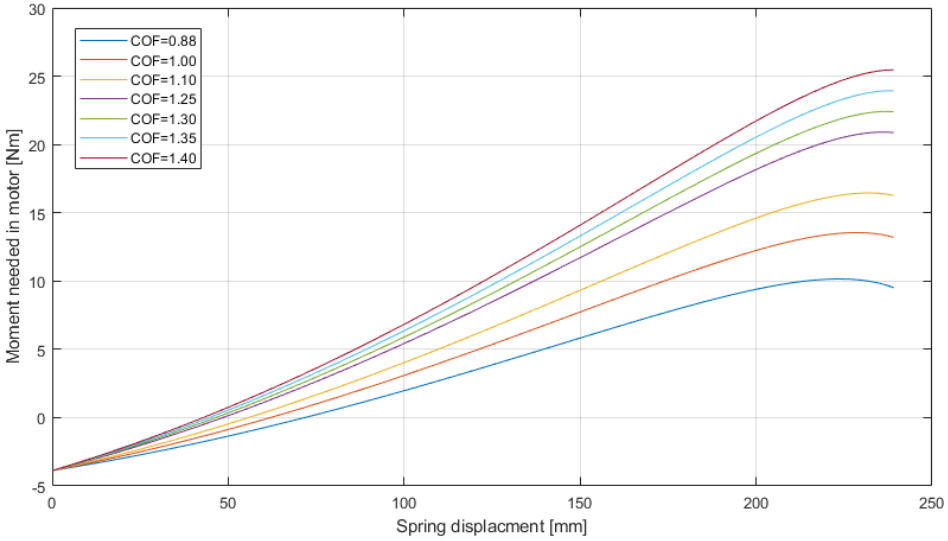

Figure 5.10: Moment in motor, *Leg=180[mm]*.

From the several iterations in Figure 5.10 it can be seen that is possible to have a spring coefficient of 1.35$[N/mm]$ with this configuration. This will result in a supported mass of 28, 59$[Kg]$ while creating a spring force of 322.72$[N]$.

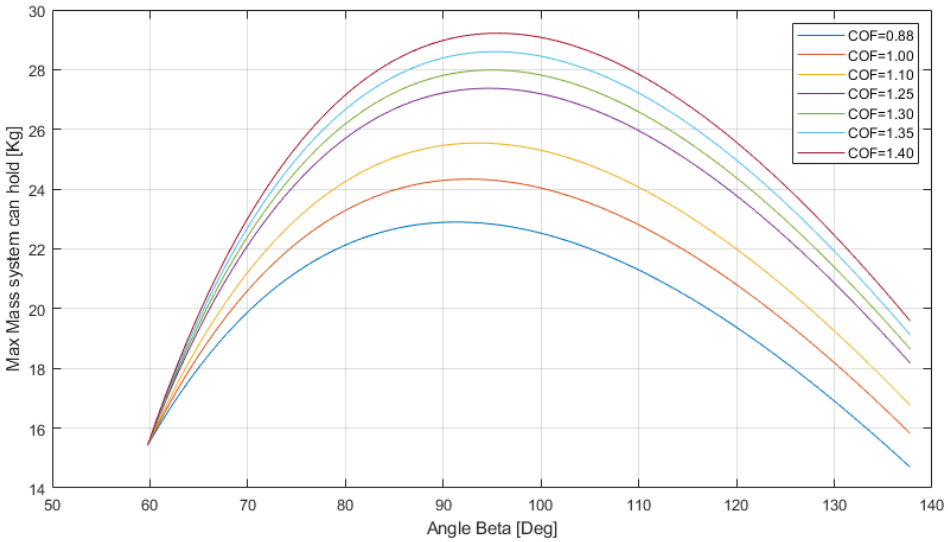

Figure 5.11: Max mass; *Leg=180[mm]*.

To compare the potential optimized design and the current iteration. The difference in force created with the different parameters has been evaluated.

In Table 5.2 the current iteration that has been built is presented, alongside the optimal spring choice for the current leg. The optimal spring choice for $Leg = 180[mm]$, and also the optimal choice for $Leg = 170[mm]$. Even though the simulations may indicate that this length can cause problems for the geometry, it may be possible to incorporate the parameters if a spring with a smaller total frame, but the same displacement is found.

As it can bee seen from Table 5.2 the optimized iteration for the current leg length can produce 26.7% more force. While the optimized $Leg = 180[mm]$ can generate 34.9% more force.

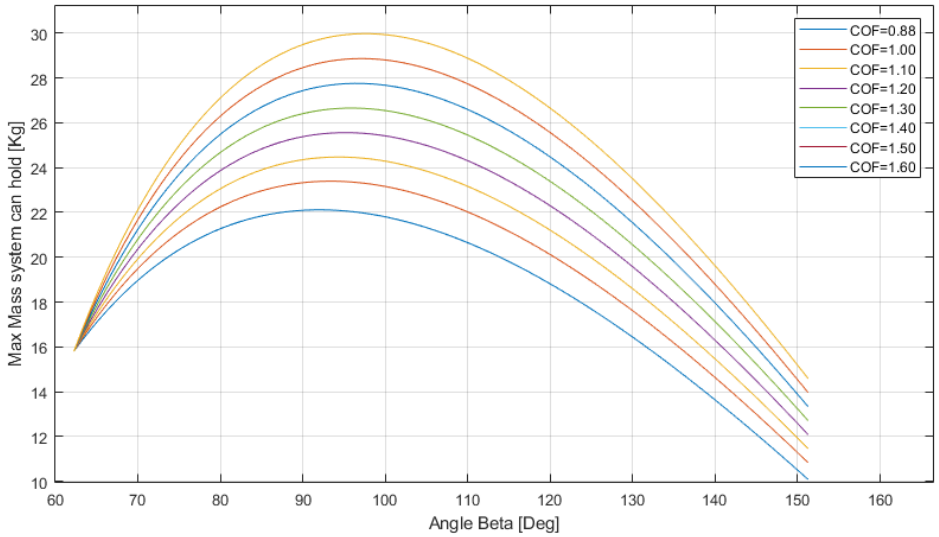

Figure 5.12: Moment in motor, *Leg=170[mm]*.

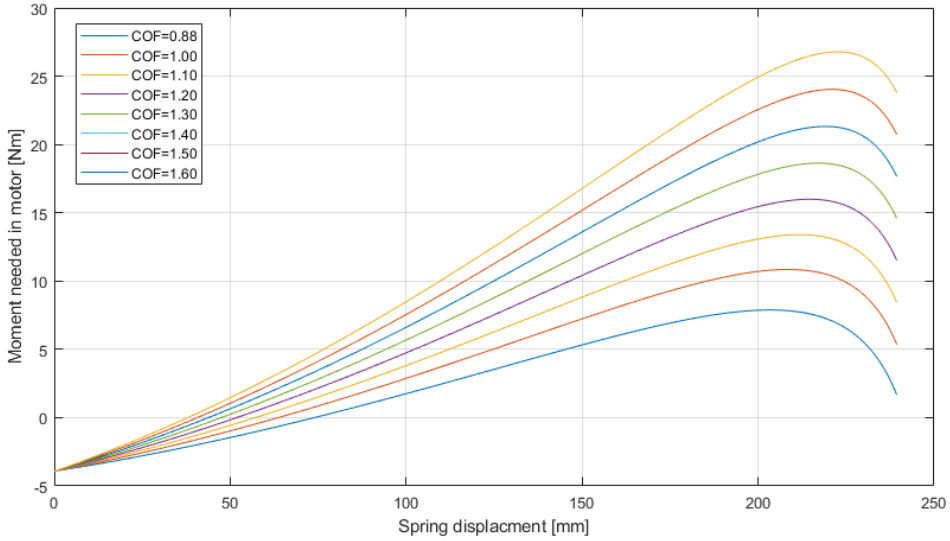

Figure 5.13: Max mass, *Leg=180[mm]*.

Iteration	Length[mm]	COF[N/mm]	Moment[Nm]	Spring Force[N]	Force diff[%]
Current	210	0.88	15.32	210.05	
Optimised 1	210	1.20	23.90	286.5	26.7
Optimised 2	180	1.35	23.91	322.72	34,9
Optimized 3	170	1.50	24.04	358.04	41,3

Table 5.2: Results of several iterations with different lengths and COF.

Spring force created with different leg lengths

The spring force for different leg lengths. Ultimately the potential jumping capabilities of the system will be determined by the amount of force the leg can generate in the spring and its actuators.

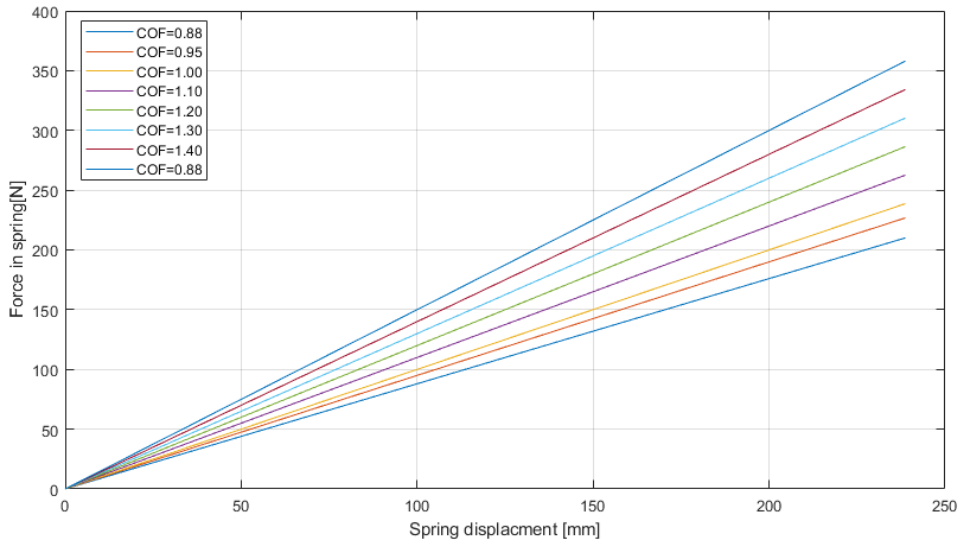

Figure 5.14: Force generated in spring.

Leg length	Max COF[N/mm]	Max Moment [N/m]	Max mass[kg]	Spring force[N]
Leg=210[mm]	≈ 1.20	≈ 23.58	≈ 30.60	≈ 286.5
Leg=200[mm]	≈ 1.20	≈ 23.90	≈ 29.29	≈ 285.41
Leg=190[mm]	≈ 1.25	≈ 23.91	≈ 28.69	≈ 299.15
Leg=180[mm]	≈ 1.35	≈ 23.91	≈ 28.59	≈ 322.72
Leg=170[mm]	≈ 1.50	≈ 24.04	≈ 28.8	≈ 358.04

Table 5.3: Spring force generated.

5.3 Strength Testing

The most crucial aspect of the stress analysis, Inventors Stress Analysis has been used, is to locate critical points in the system. Since the forces the system will experience have been located, these can be imposed on the system to locate where the system is most prone to breaking. As well as how much these areas and components can withstand before breaking.

With the different simulations, the forces for different leg design configurations can be found. With this info, components can be optimized with respect to weight and the forces they would need to withstand.

Von Mises Stress will show how much stress the parts will be exposed to in MPa, this will give an indicator for how much stress the system will encounter during the given force.

Displacement will show how much the system will move from its original positioning when prone to the forces. This will help locate areas that may be of structural importance when optimizing the system. It is however important to identify parts that will suffer from displacement, and areas that naturally will move with added loads.

The Safety factor is an indicator of how much more stress the system can handle. The lower the safety factor the closer the area is to breakage. Should the safety factor fall below 1.0 this will indicate breakage.

5.3.1 Spring Fasteners

One of the most crucial parts of the design is the Spring fasteners. There is the only component securing the spring to the rest of the system. The only forces the spring fasteners will be susceptible to are the forces created in the spring. As such the force is easily calculated to form the simulation in section 5.1.

With the current spring and leg length configuration, the maximum force is now 250N generated in the spring. However, since the current design will be optimized and subsequently exposed to much higher forces in later designs, the inserts will be tested with higher forces.

Since the damage potential to the system in its entirety is so high, due to it being the only component holding the spring in place, it's important to ensure structural integrity should unexpected forces occur. Such as falling, impacts, twisting, and bending during testing and movement. With this in mind, the spring insert has been brute designed with strength as a focus, as opposed to solely weight.

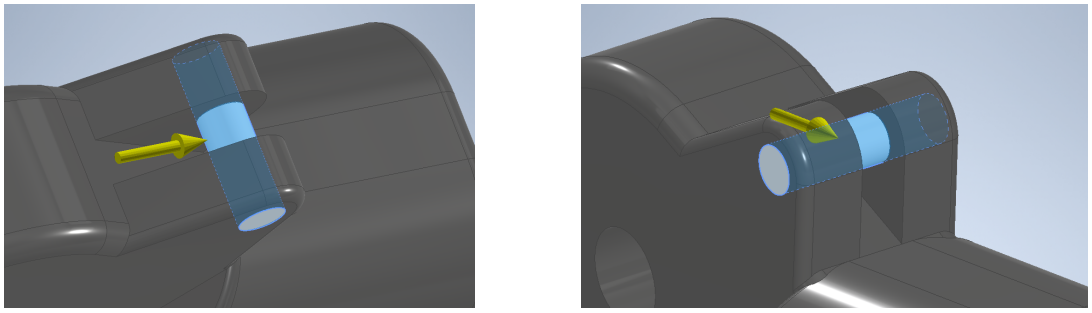

Figure 5.15: Spring Fastener Force localization

In Figure 5.15 the force direction and localization on the component have been visualized. A force is applied to the pin that will secure the spring to the insert. This will simulate correct force localization during tension where the spring will exert its force on the spring insert. The numerical results of the FEM analysis can be seen in Table 5.4. VMS, Displacement, and as a result of a force of 700[N].

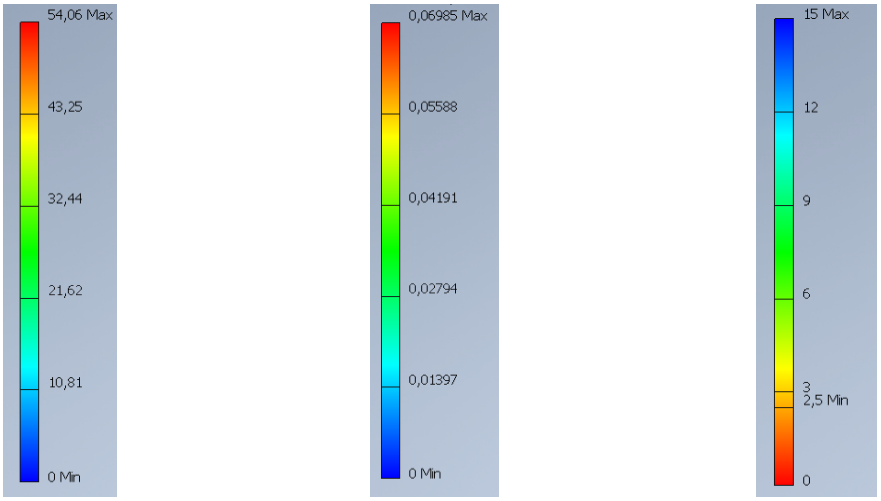

(a) Von Misses Stress [MPa] **(b)** Displacement [mm] **(c)** Safety factor

Figure 5.16: Heatmap Results stress test analysis; Spring Insert

FEM Analysis: Spring Insert	**Force: 700 [N]**
Von Misses Stress [MPa]	54,06
Displacement [mm]	0,006985
Safety Factor	2,5

Table 5.4: Results stress test analysis; Spring Insert

Von Mises Stress

The results indicate stress that accumulation are primarily focused in the pin itself as can be clearly seen from Figure 5.17a and Figure 5.17b . There is also high concentration around the bottom of the insert as can be seen in Figure 5.17b.

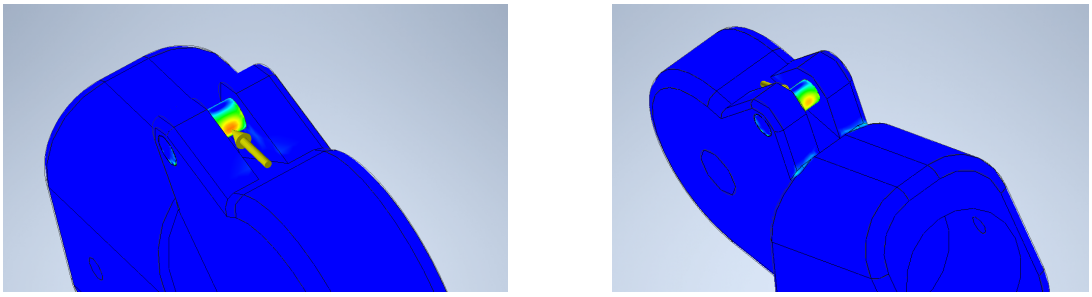

(a) **(b)**

Figure 5.17: VMS; spring insert.

Displacement

Its clear to see that any eventually displacement will be in the contact point between the pin and the fastener. The displacements however, as can be seen from the table, is so small that it should pose no problem.

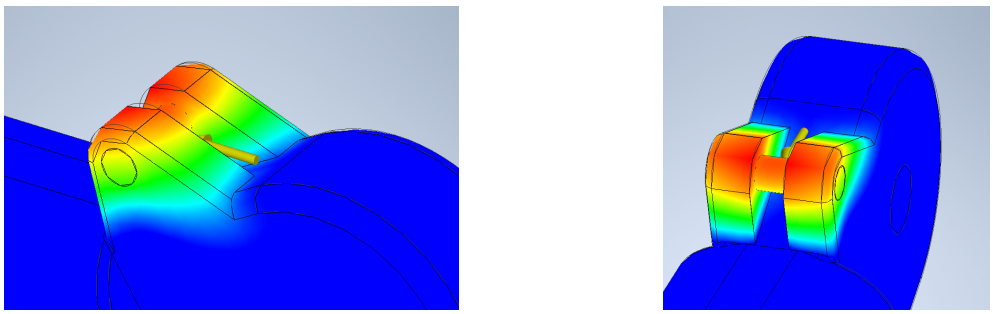

(a) **(b)**

Figure 5.18: DS; spring insert.

Safety Factor

From Table 5.4 it can bee seen that the system have a SF of approximately 2.5. While this suggest the structure is fairly safe from breakage and deformation, other unforeseen forces can damage the component.

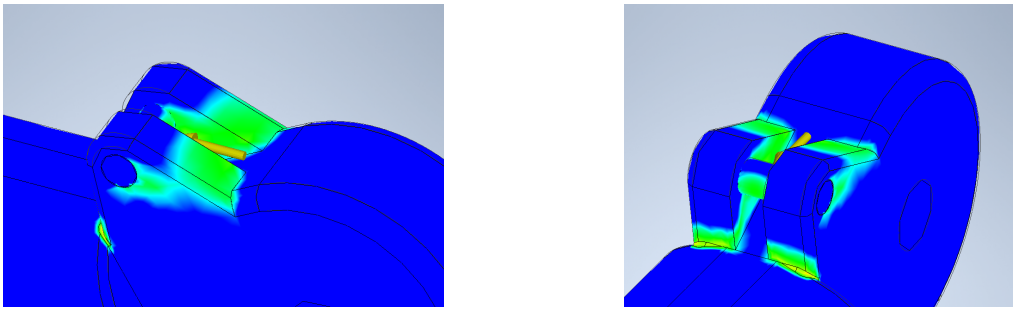

(a) **(b)**

Figure 5.19: SF; spring insert.

The component has been exposed to a suggested force of 700$[N]$ along its natural force direction during the potential tension in the spring. From the analysis, the direct spring force of the system should not impose any structural complications. However, due to the component's exposure and importance, it has been designed with a focus on strength.

5.3.2 Carbon fiber leg

The carbon fiber legs have been exposed to 500$[N]$ each as seen from Section 5.3.2. This will represent the bending moment they will experience during the spring extension.

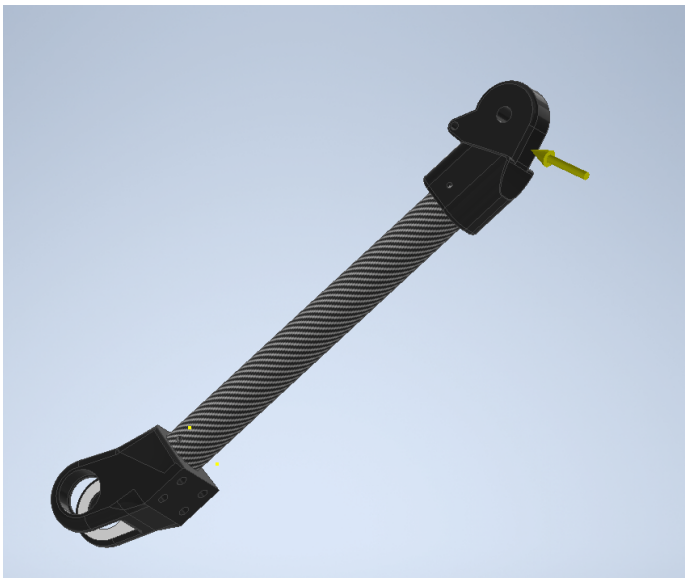

Figure 5.20: Leg Force Localization.

As it can be seen from Figure 5.3 the leg will be exposed to a bending moment. This moment will occur both as a result of the force generated in the spring during both jumping and supporting mass. The legs have been applied a force of 500$[N]$.

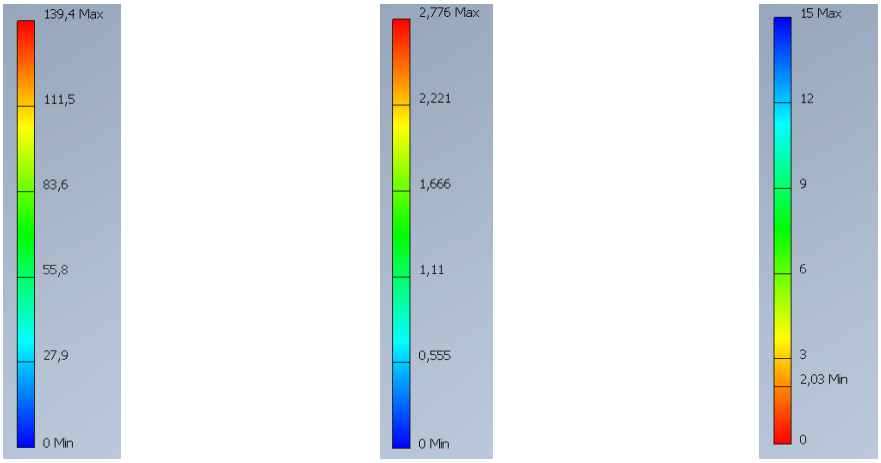

(a) Von Misses Stress [MPa] **(b)** Displacement [mm] **(c)** Safety factor

Figure 5.21: Heatmap results stress test analysis, Leg.

FEM Analysis: Leg	**Force: 500[N]**
Von Misses Stress [MPa]	139,4
Displacement [mm]	2,776
Safety Factor	2,03

Table 5.5: Results stress test analysis; Leg.

Von Mises Stress

The stress can be seen to accumulate in the lower joint inserts. From Figure 5.22 it is shown that the stress is increasing along downwards the leg.

The highest forces is in the insertion of the leg and the joint. An important notion of the design is that the screw insert for the leg fastener is placed perpendicular on the bending moment, as shown in Figure 5.22a. Otherwise the potential force consternation around the screw hole may compromise the structural integrity of the leg.

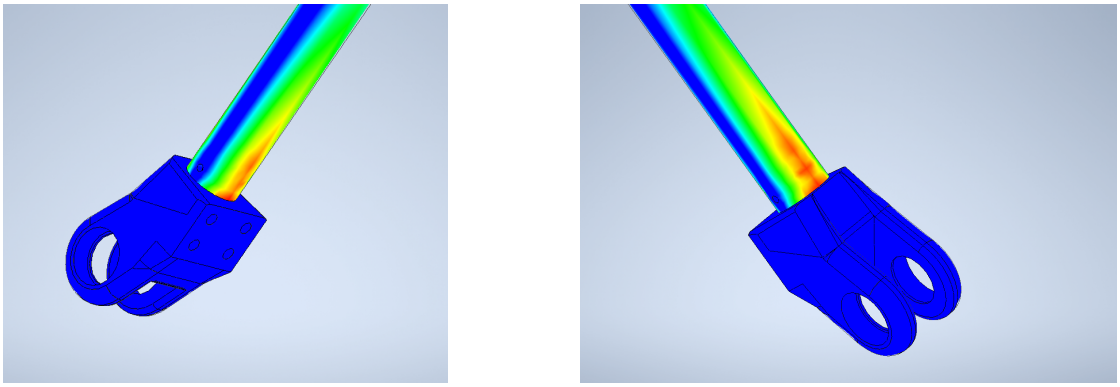

(a) **(b)**

Figure 5.22: VMS; Leg

Displacement

The only notable displacement is the movement of the upper joint. No displacements are shown for the leg itself concerning other components.

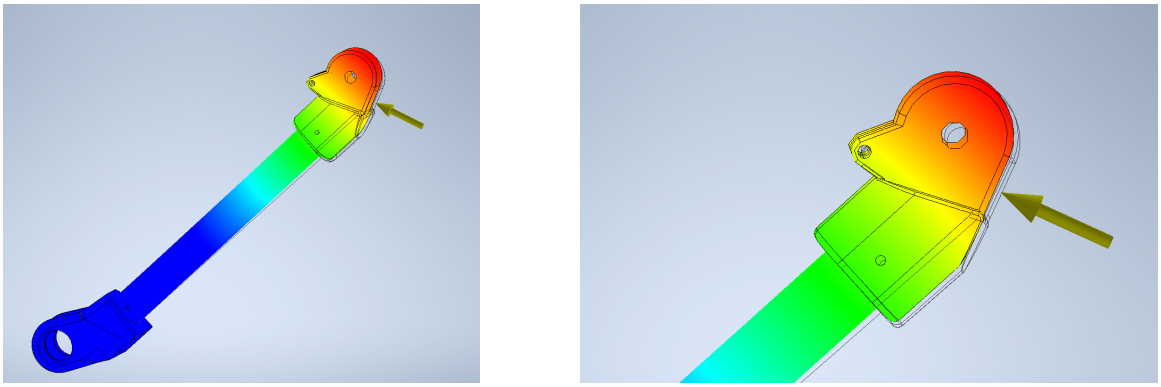

(a) **(b)** 1b

Figure 5.23: DS; Leg

Safety Factor

With a safety factor of 2.03 as seen in Table 5.5, it has good clearance before breakage.

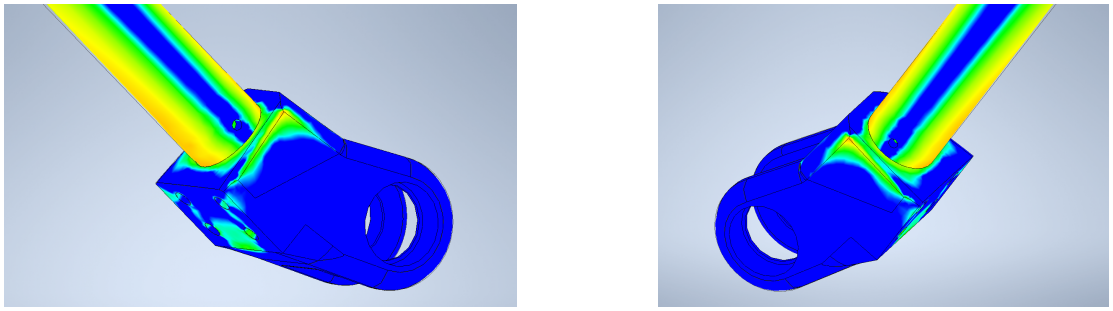

(a) **(b)**

Figure 5.24: SF; Leg.

5.3.3 Leg Insert

The leg insert will be the only connection between the motors and the rest of the system. It is necessary to ensure that any forces created in the system don't exceed the forces the leg insert cant handle.
For this purpose, the leg insert has undergone extensive testing with multiple analyses.

The initial analysis focuses on the potential forces that will occur when the leg is acted on by the torque of the motors, as a bending force from the inserted leg will impose this force on the insert.

(a) **(b)**

Figure 5.25: Leg Insert Force localization.

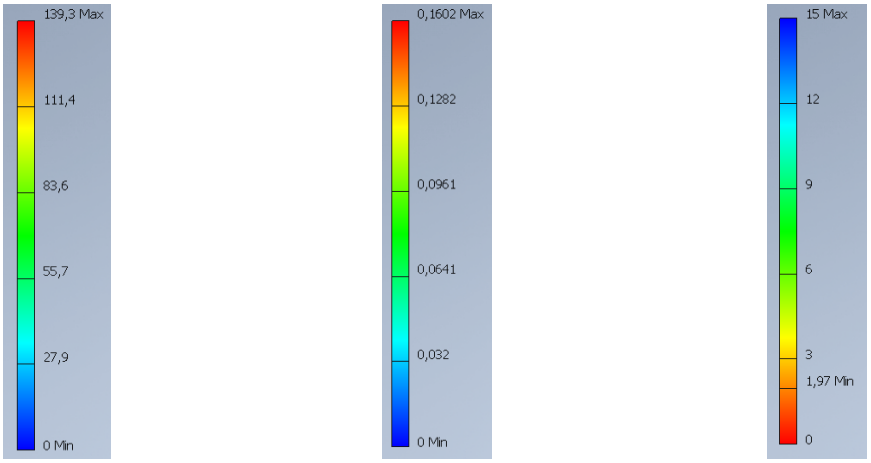

(a) Von Misses Stress [MPa] **(b)** Displacement [mm] **(c)** Safety factor

Figure 5.26: Heatmap results stress test analysis, leg insert.

FEM Analysis: Leg Insert	**Force: 320[N]**
Von Misses Stress [MPa]	139,3
Displacement [mm]	0,01602
Safety Factor	1,97

Table 5.6: Results stress test analysis; Leg Insert.

5.3.4 Von Misses Stress

The Stress-induced on the insert accumulates in the top slope intersection. as well as the bolt hole placed closest to the force.
The bolt hole was removed to assess the resulting forces with this design change. As a result, none of the results was improved.

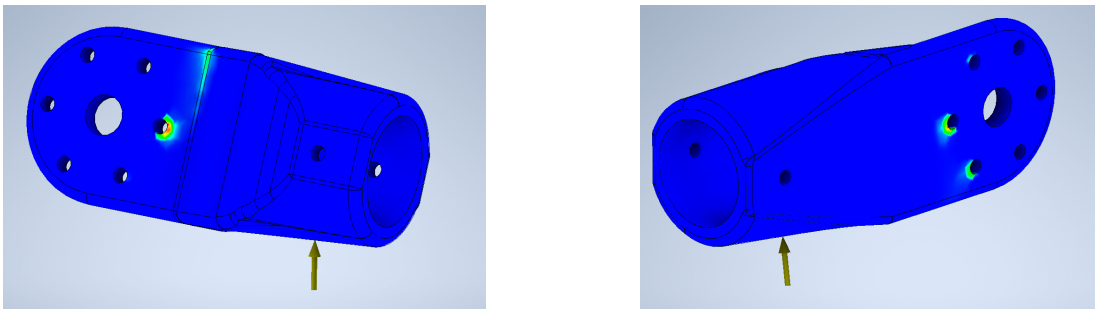

(a) **(b)**

Figure 5.27: VMS; Leg Insert.

Displacement

From the placement of the displacement accumulation and the results, 5.28, proved it will not impose problems on the design.

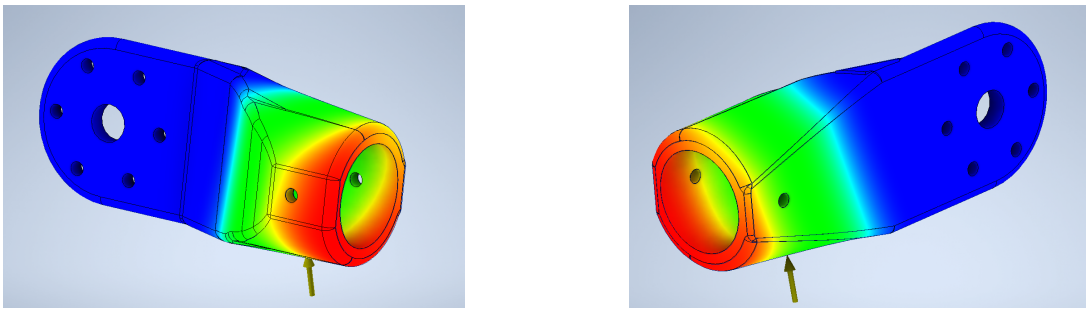

(a) **(b)** 1b

Figure 5.28: SF; Leg Insert.

Safety Factor

As with VMS the safety factor can bee seen to be at it's lowest around the bolt hole. Leg Insert have been tested with a force of 320[N]. With this force the SF is approximately 1.97, 5.6

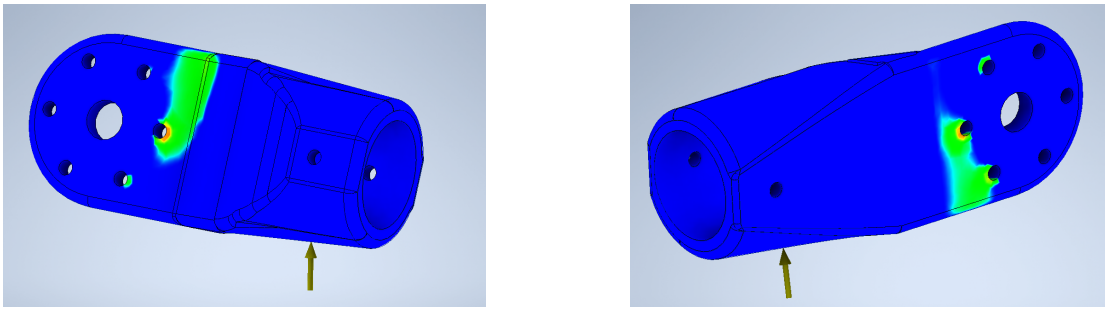

(a) **(b)**

Figure 5.29: SF; Leg Insert.

5.3.5 Motor Housing

The interface between the leg and body motor will experience several different forces. With its structural importance as the only connection between the body and the leg, it must be able to withstand all the forces the system experiences, as well as the body.

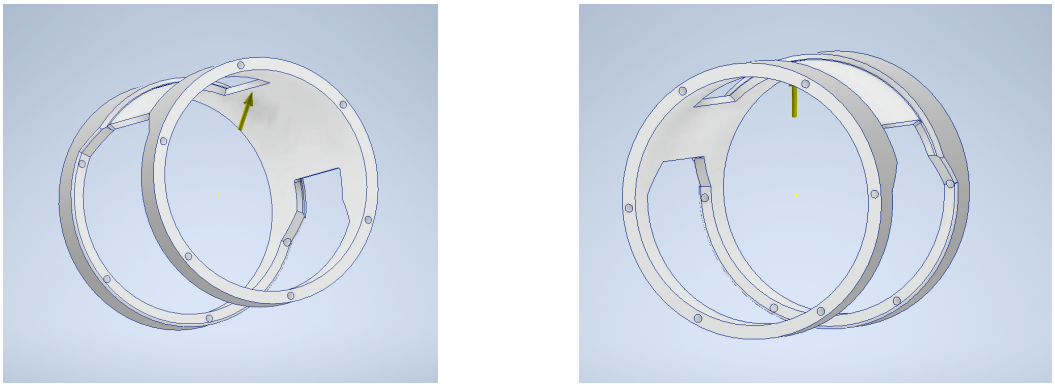

(a) **(b)**

Figure 5.30: Motor Housing Force Localization.

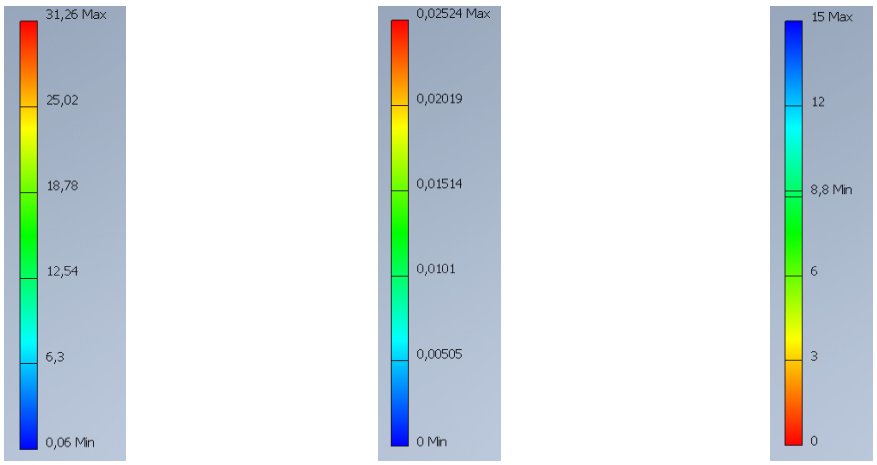

(a) Von Misses Stress [MPa] **(b)** Displacement [mm] **(c)** Safety factor

Figure 5.31: Heatmap results stress test analysis, motor housing.

FEM Analysis: Motor Housing	**Force: 2000[N]**
Von Misses Stress [MPa]	31,26
Displacement [mm]	0,02524
Safety Factor	8,8

Table 5.7: Results stress test analysis; Motor Housing.

Von Misses Stress

The VMS created from an internal force of 2000$[N]$ from the inside proves to pose few problems for the component. It can be seen with little effect on the design, with a maximum stress of $31,26[MPa]$. This indicates that none of the forces that can be created in the system will

cause a problem for the motor housing. From Figure 5.32b the force accumulation can be seen in the corners of the intersection between the two halves.

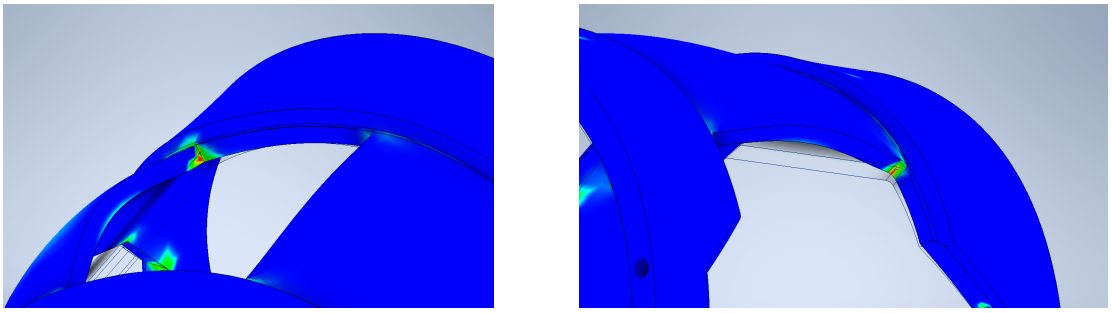

(a) **(b)**

Figure 5.32: VMS; Motor Housing.

Displacement

Displacement will be present in the thinnest part of the housing. However, with the amount of displacement that presented itself during FEM analysis, it's very little.

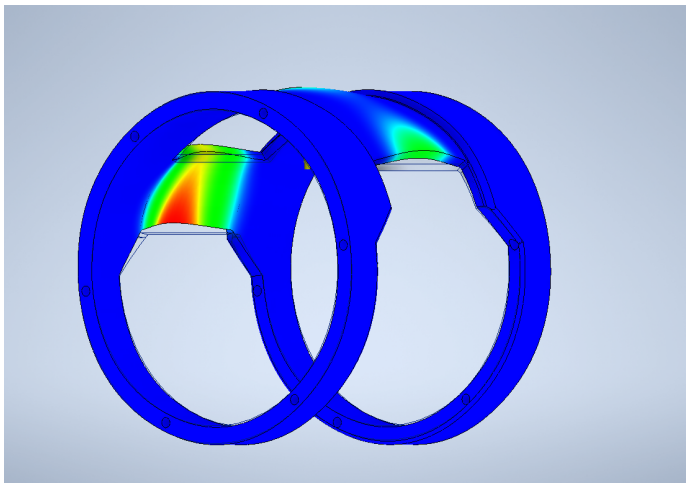

Figure 5.33: Displacement; Motor Housing.

Safety factor

Lowest safety factor is present similar with the highest VMS, however so high that it is not a problem.

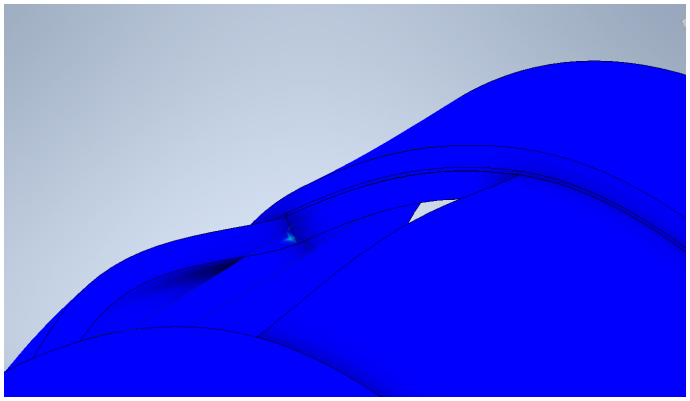

Figure 5.34: Safety Factor; Motor Housing.

5.3.6 Leg Body Connection

To find the limit for forces that can be transferred from the leg to the body it's necessary to find the amount of force the Leg Body Connection can handle before breakage.

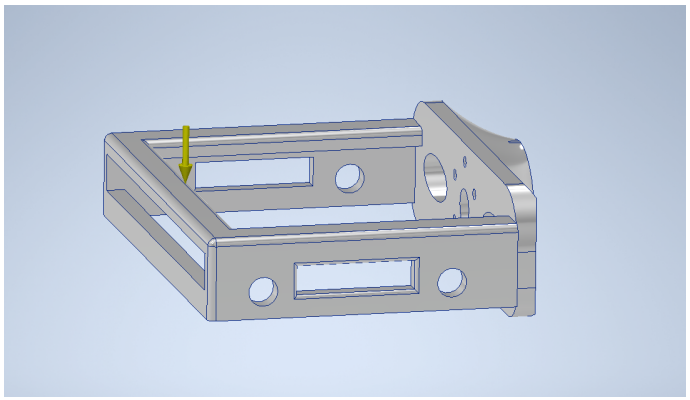

Figure 5.35: Leg Body Connection Force Localization.

The connection will need to withstand the forces created by the entire leg design during any movement. This is the only component that will connect the leg to the 3DOF body motor, and such will need to support the entire weight of the design during impacts and forces.

FEM Analysis: Leg Body Connection	**Force: 950[N]**
Von Misses Stress [MPa]	130,8
Displacement [mm]	1,043
Safety Factor	2,1

Table 5.8: Results stress test analysis; Leg Body Connection.

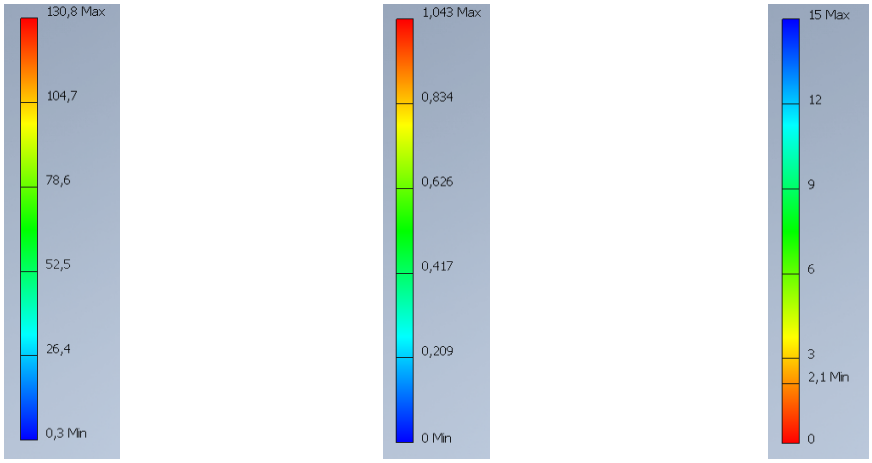

(a) Von Misses Stress [MPa] **(b)** Displacement [mm] **(c)** Safety factor

Figure 5.36: Heatmap results stress test analysis.

Von Misses stress

The stress can be seen to accumulate at the interface between the leg and body connections. Besides for this no other part of the structure seems to be exposed to any significant stress that will cause problems. Future iterations any then focus on the interface are for optimization.

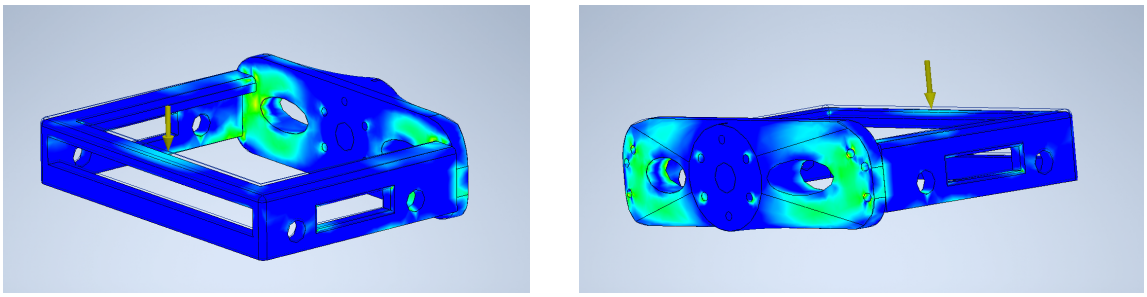

(a) **(b)**

Figure 5.37: VMS, Leg Body Connection.

Displacement

While the displacement is concentrated at the front of the leg connection the displacement is so small that it will pose no problems.

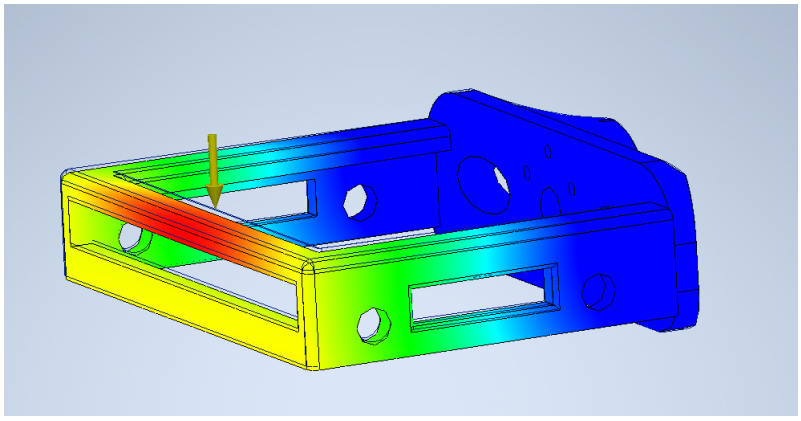

Figure 5.38: Displacement; Leg Body Connection.

Safety factor

The safety factor can be seen to accumulate in the same areas as the stress was. Further implying this will be an important area for future iterations optimization.

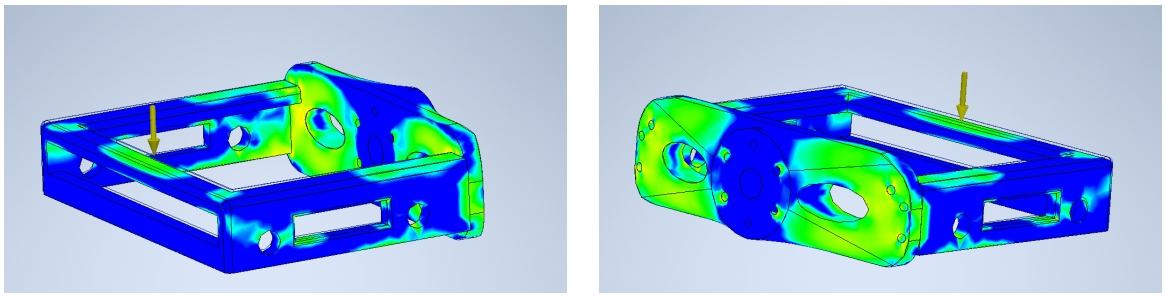

(a) **(b)**

Figure 5.39: Safety Factor; Leg Body Connection.

5.3.7 Maximum Impact Force

The maximum impact force of the system will be highly dependent on the configuration choices for the design. The simplicity of the design makes it easy to change either the spring length and coefficient or the length of the carbon fiber legs. The current physical configuration has been stress tested to find its potential maximum strength.

The maximum weight the system can hold can be found with the static analysis shown earlier. However, the dynamic responses of the system during the impact forces are more volatile and difficult to do a more accurate stress test analysis. Therefore the components will be presented with a maximum suggested force with a safety factor to be certain the parts are within their structural limits.

Since there have not been set any concrete goals for the strength of the system. The maximum force that can be implemented will be presented as a result of an optimization based on the strength simulations and weight reduction as the main focus.

FEM Analysis Results	**Force**	**VMS [MPa]**	**Displacement [mm]**	**Safety Factor**
Spring Insert	700[N]	54,06	0,006985	2,5
Carbon fiber Leg	500[N]	129,4	2,776	2,03
Leg Insert	320[N]	139,4	0,01602	1,97
Motor Housing	2000[N]	31,26	0,02524	8,8
Leg Body Connection	950[N]	130,8	1,043	2,1

Table 5.9: FEM Analysis Results for all components.

From the FEM analysis, it has been made evident that the weakest part of the structure as a whole is the leg insert. All of the components have been tested to find the maximum amount of force they can be exposed to before closing in on a safety factor of approximately 2. Some parts have not been tested for this due to it being unnecessary because of the difference in strength.

The maximum force required to yield a safety factor of $1,97$ for the leg insert was not any more than $320[N]$. Due to the mirrored design of the system, this yields a total force of $640[N]$ for the entire system. With this, it can be calculated the maximum force the spring can generate before the leg insert will reach critical stress.

For future iterations, it may be necessary to strengthen the Leg Insert. Not only because of the forces emerging from the system itself, but also unforeseen impacts and collisions that will affect the system.

Chapter 6

Modeling

6.1 Kinematics

6.1.1 Closed kinematic chains

Due to the connections of the robotic system. The robot has closed-kinematic chains, as a result of the bilateral position constraints. Similar problems can be found in Delta robots [44] and other four-bar linkage design [45]. The Underactuated Robotics book [46] explains and walk-through the basics for such problems. Stating these conditions and how they differ from other kinematic constraints makes it possible to work further on the general equation for the closed kinematic chain system utilized in the design.
Constraint equation

$$\boldsymbol{h(q)} = 0 \tag{6.1}$$

For the case of the closed kinematic chain, the kinematic constraint where the endpoint of one chain is equal to the location of the other chain. By incorporating this constraint the equations of motion can be stated.

$$\boldsymbol{M(q)\ddot{q} + C(q,\dot{q})\dot{q}} = \tau_g\boldsymbol{(q) + Bu + H^T(q)}\lambda \tag{6.2}$$

Where $\boldsymbol{H(q)} = \frac{\partial h}{\partial q}$ and λ are constraint force. Using this it can be stated as.

$$\boldsymbol{M(q)\ddot{q}} = \tau(q,\dot{q},u) + \boldsymbol{H^T(q)}\lambda \tag{6.3}$$

By using

$$\boldsymbol{\dot{h} = H\dot{q}} \tag{6.4}$$

$$\boldsymbol{\ddot{h} = H\ddot{q} + \dot{H}\dot{q}} \tag{6.5}$$

λ can be solved by observing the constraint $\boldsymbol{h} = 0$ and such also , $\boldsymbol{\dot{h}} = 0$ and $\boldsymbol{\ddot{h}} = 0$. By inserting Equation (6.3) into Equation (6.5) yields.

$$\lambda = -\boldsymbol{(HM^{-1}H^T)^{+}(HM^{-}\tau + \dot{H}\dot{q})} \tag{6.6}$$

This matrix will be in many cases full rank, for instance, in the case of multiple independent four-bar linkages, and such the inverse can be used. Should the matrix drop rank the pseudo-inverse selects the solution smallest constraint forces.

6.1.2 Forward Kinematics

As been shown there has been extensive research on these kinds of problems with closed-chain designs, and the kinematics that has been derived can be based on these earlier work as [47] and [48]. As shown in Figure 6.1 the coordinate relationship has been established for the end-effector position expressed in the $R-frame$. The end-effector has been placed at the end of the paw of the design, and as such, the object of study is the position of the paw with respect to the $R-frame$ frame which has been placed around the axis of the aligned housing motors.

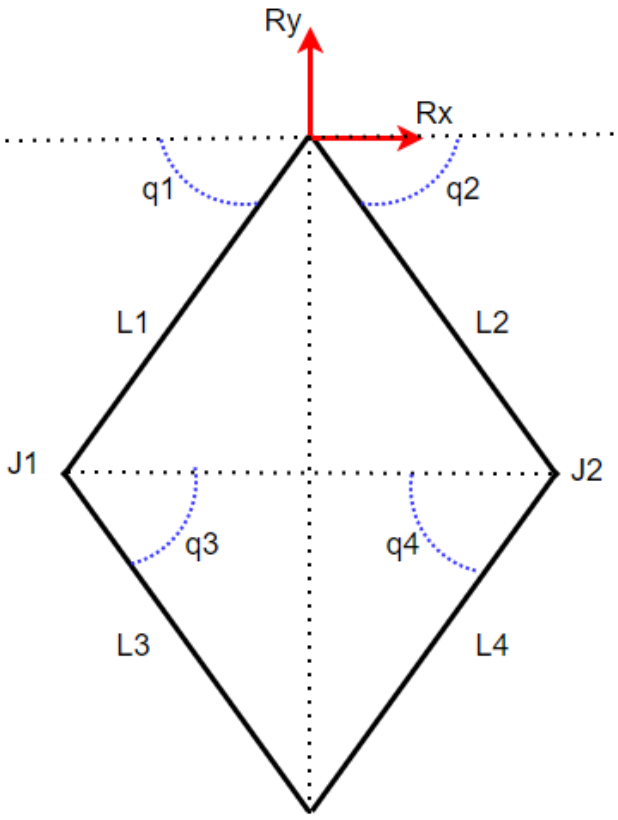

Figure 6.1: Closed chain overview.

While most D2 delta designs have a given distance between their actuator that manipulates $q1$ and $q2$, the aligned motor axis of the chosen design eliminates the need for any consideration of this distance.
The model of the motion relationship can be stated as

$$-L_1\cos(q_1)+L_2\cos(q_2)+L_3\cos(q_3)-L_4\cos(q_4)=0 \tag{6.7}$$
$$-L_1\sin(q_1)-L_2\sin(q_2)+L_3\sin(q_3)+L_4\sin(q_4)=0 \tag{6.8}$$

The end-effector coordinates stated as $P(x,y)$ are to be solved by using the angle actuated angles q_1 and q_2. To yield these coordinates the relationships between angle q_3, q_4 as a result of q_1 and q_2 must be stated.

$$A=L_1^2-L_2^2+L_3^2+L_4^2 \tag{6.9}$$
$$B=-2L_1L_3\sin(q_1)+2L_3L_4\sin(q_4) \tag{6.10}$$
$$C=-2L_1L_3\cos(q_1)-2L_3L_4\cos((q_4)) \tag{6.11}$$
$$D=2L_1L_4\sin(q_1)\sin(q_4)+2L_1L_4\cos(q_1)\cos(q_4) \tag{6.12}$$

Which can be presented as the following with the utilization of trigonometrical manipulation.

$$\tan(q_3)=\frac{2\tan(\frac{q_3}{2}}{1-\tan^2(\frac{q_3}{2})=\frac{2\zeta}{1-\zeta^2}},\sin(q_3)=\frac{2\zeta}{1+\zeta^2},\cos(q_3=\frac{1-\zeta^2}{1+\zeta^2}$$

The angle relationship as mentioned gives the following relationship equation

$$A+B\sin(q_3)+C\cos(q_3+D=0 \tag{6.13}$$

By exploiting the trigonometrical manipulation this yields.

$$A+B\frac{2\zeta}{1+\zeta^2}+C\frac{1-\zeta^2}{1+\zeta^2}+D=0 \tag{6.14}$$

$$\zeta=\frac{-B\pm\sqrt{B^2-(A-C+D)(A+C+D)}}{A-C+D} \tag{6.15}$$

$$q_3=2\tan^-1\zeta \tag{6.16}$$

$$q_2=\sin^-1\frac{-L_1\sin(q_1)+L_3\sin(q_3)+L_4\sin(q4)}{L_2} \tag{6.17}$$

This then can be solved for the end-effector coordinates $P(x,Y)$ with respect to only the actuated angles q_1 and q_2.

$$\begin{cases}P_x=L_4\cos(q_4)-L_3\cos(q_3)\\P_y=-L_4\sin(q_4)-L_3\sin(q3)\end{cases} \tag{6.18}$$

The closed kinematic chain of the design can also be presented as the following system of equations. With the same end-effector position expressed in the $R-frame$ as the previously stated position equations

$$\begin{cases}P_x^2+P_y^2-2(L_1\cos(q1))P_x-2L_1\sin(q1)P_y+L_1^2-L2^2=0\\P_x^2+P_y^2-2(L_1\cos(q2))P_x-2L_1\sin(q2)P_y+L_1^2-L2^2=0\end{cases} \tag{6.19}$$

6.1.3 Inverse kinematic

The position of end-effector point $P(x, y)$ from the reference frame. From the reference frame position vectors of joint points.

$$J_1 = (L_1 \cos(q_1) \qquad L_1 \sin(q_1))^T \tag{6.20}$$
$$J_2 = (L_1 \cos(q_2) \qquad L_1 \sin(q_2))^T \tag{6.21}$$

With the input angles as the actuated angles q_1 and q_2, the inverse kinematic can be solved with the following constrains equations.

$$(x - L_1 \cos(q_1))^2 + (y - L_1 \sin(q_1))^2 = L_2^2 \tag{6.22}$$
$$(x - L_1 \cos(q_2))^2 + (y - L_1 \sin(q_2))^2 = L_2^2 \tag{6.23}$$

For the forward kinematics, the end-effector point was found by the depending relationships of q_1 and q_2. For the inverse kinematics the relationships of the $P(x, y)$ coordinates, and the subsequent corresponding angles q_1 and q_2.

$$a = L_1^2 + y^2 + x^2 - L_2^2 + 2xL_1 \tag{6.24}$$
$$b = -4yL_1 \tag{6.25}$$
$$c = L_1^2 + y^2 + x^2 - L_2^2 - 2xL_1 \tag{6.26}$$

$$\rho = \frac{-b_1 \pm \sqrt{b^2 - 4ac}}{2a} \tag{6.27}$$

For which for a know position point $P(x, y)$ the inputs for the given point can then be obtained by

$$q = 2 \tan^{-1} \rho \tag{6.28}$$

6.2 Workspace

One aspect of the design is the reach of the paw, and the workspace the end-effector can operate in. While this should be an important focus in future iteration and design choices the current iteration of Hibert has not been designed with this as a focus.

The different parameters for the workspace of the leg have however been identified and will need to be taken into consideration in future design choices.

Parameters affecting workspace
Length of carbon tubes in leg
Length of carbon tube in paw assembly
Size of paw
Mechanical stops in motor housing

Table 6.1: Parameters that will affect the size and shape of the workspace.

Due to the bilateral constraints and closed chain kinematics, it has been observed that the increase in length of the leg and paw will extend the workspace. However, it will also increment the extent of the minimum distance of reach with respect to the $R-frame$.

The graphs represent the outermost borders of the workspace, any area inside the graphs is part of the workspace.

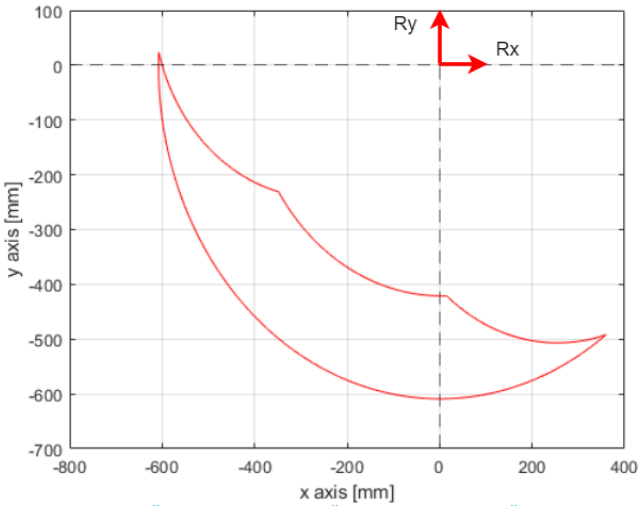

Figure 6.2: Calculated workspace of Leg.

The main aspect of the end-effector capabilities in the outermost values in either direction is the physical restrictions that are imposed on the legs due to mechanical stops. These mechanical stops can be seen in red in Figure 6.3.

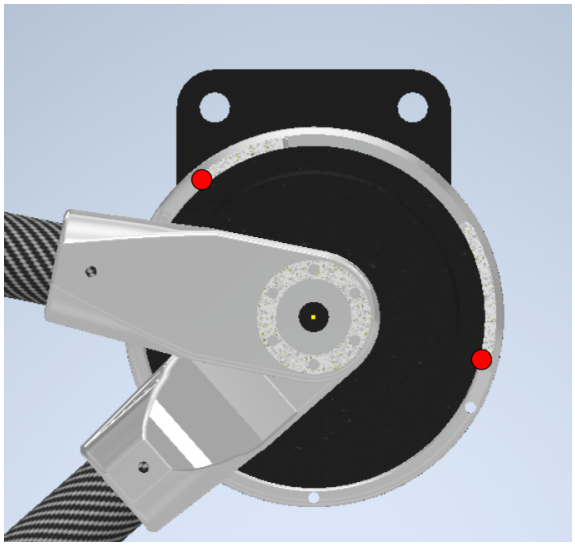

Figure 6.3: Mechanical Stops imposing the workspace, marked in red.

6.2.1 3D-workspace

The workspace has also been presented in a 3D environment. This was done by plotting the numerically found points in Inventor. And afterward revolving the area to simulate the complete 3D workspace. This makes it simpler to envision the potential of the leg design as a manipulator.

While this allows envisioning the workspace in 3D, it also makes it possible to incorporate the actual design with a 3D-CAD model. By doing this the physical movements of the leg design can be compared to the numerically plotted workspace with the forward kinematics.

To illustrate the full potential of the leg the workspace has been revolved without any restraints or suggested mechanical stops for the abduction DoF. While this shows the entire workspace, future design and iterations will have to account for the body and adjutant legs to hinder its potential workspace and movement.

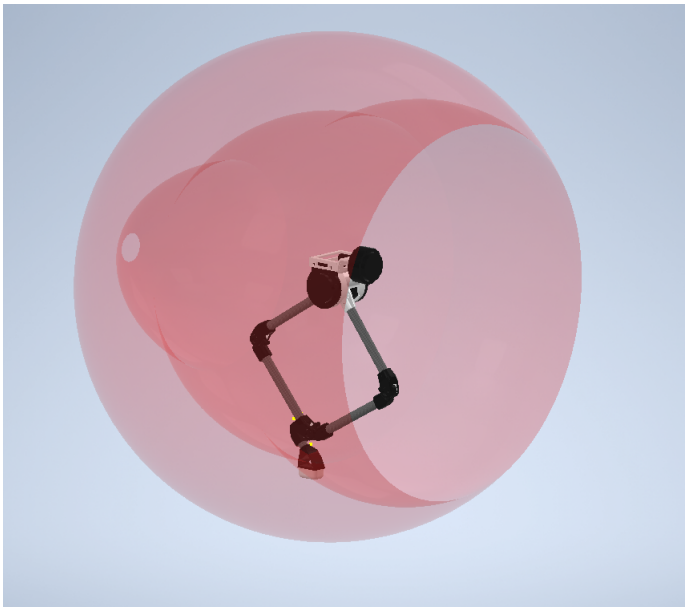

Figure 6.4: 3D-Workspace.

During testing, it was found that the numerically calculated workspace had some divergence from the 3D-CAD model's movements. In Figure 6.5a the full extension of the leg can be seen to be quite accurately aligned with the border of the workspace. However, in Figure 6.5b the contracted leg can be seen to diverge from the border by quite some margin.

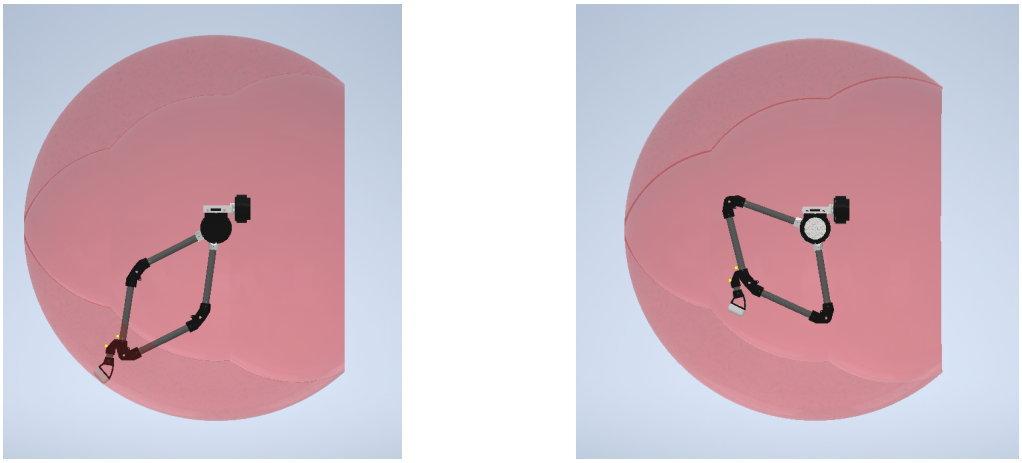

(a) Aligns with the outer borders. **(b)** Inner borders don't coincide with leg.

Figure 6.5: 3D-Workspace alignment with leg assembly.

Further analysis showed that the distances found from the 3D-CAD model and then used in the calculations were found for the fully extended leg configuration. However, due to the design of the leg the distances from the knee joint B and the paw, L4. Was not consistent throughout the movement. Therefore as the distance changed the constant lengths that were set for the calculations were incorrect. This is a problem for the future control of the system, as constant distances cant be used as of now without creating an offset to the physical results.

6.2.2 Real representation workspace

To simulate the real workspace the distance from the knee joint to the paw end effect has been presented as a time-dependent non-constant value between the maximum and minimum distance of the said distance.
Should the entire workspace be simulated with the minimum the results would be similar in shape, however with some differences.

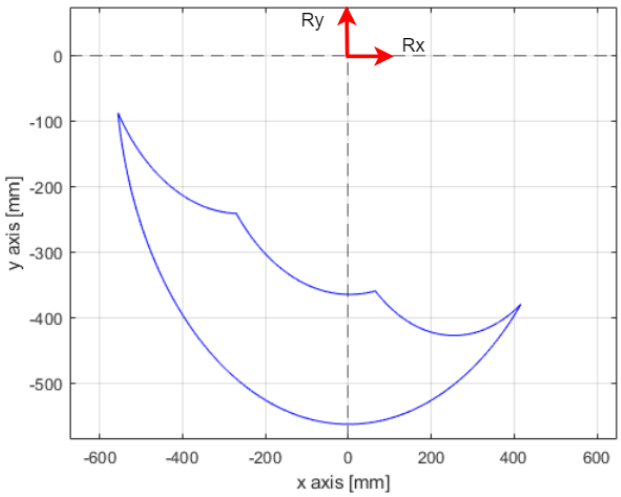

Figure 6.6: Workspace; minimum leg distance.

The differences between the maximum and minimum leg distance have been illustrated. It can be seen that the results differ quite a lot.
With future modeling, this is something that will need to be accounted for. As can be seen the results of using constant lengths on all leg parameters.

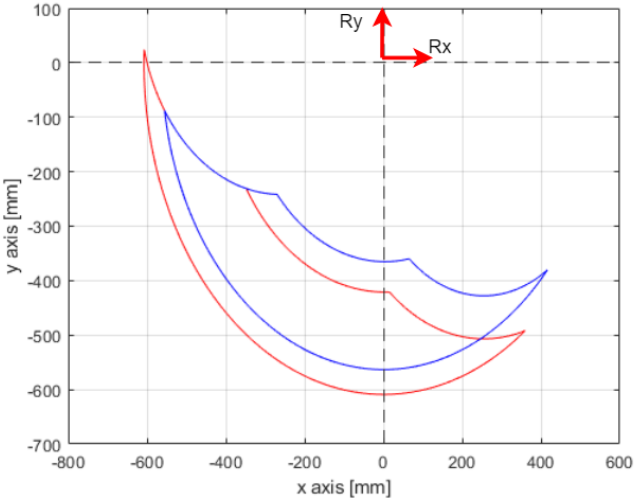

Figure 6.7: Workspace; Minimum VS Maximum

The real representation of the workspace as a merging of the minimum and maximum workspace can be seen in Figure 6.8. To simulate this utilizing the forward kinematics the distance has to be stated as a non-constant distance. That changes based on the angles $q1$ and $q2$ throughout the movement.

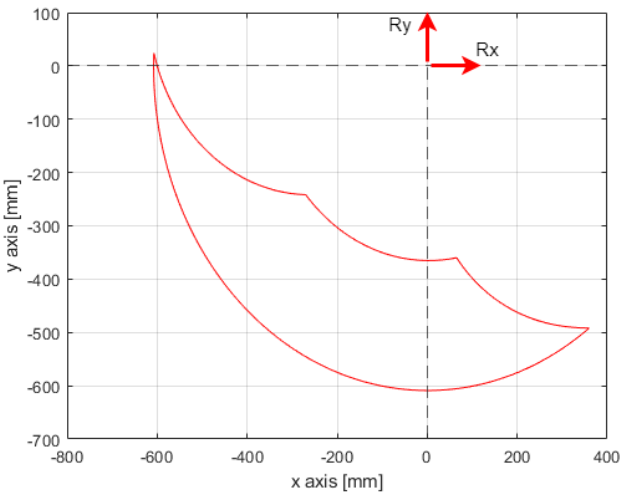

Figure 6.8: Workspace; real representation.

By projecting the new 2D workspace to a 3D representation it's clear to see that it is a much better fit with the 3D-CAD model limits.

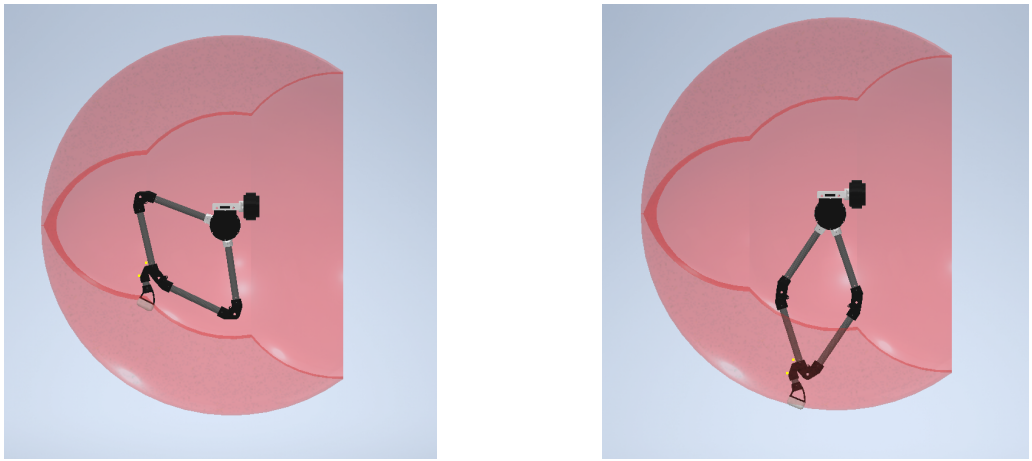

(a) **(b)**

Figure 6.9: 3D-Workspace Accuracy with real representation.

6.3 Jumping Simulations in Simscape Multibody

Simscape Multibody has been used to simulate a jumping motion of the leg design. This gives the possibility to see how the system will act in a physical environment, as well as allow different configurations of the design to be tested. While this is not an optimal testing environment due to the negligence of friction and uncertainties of the design such as dampening in spring and components.

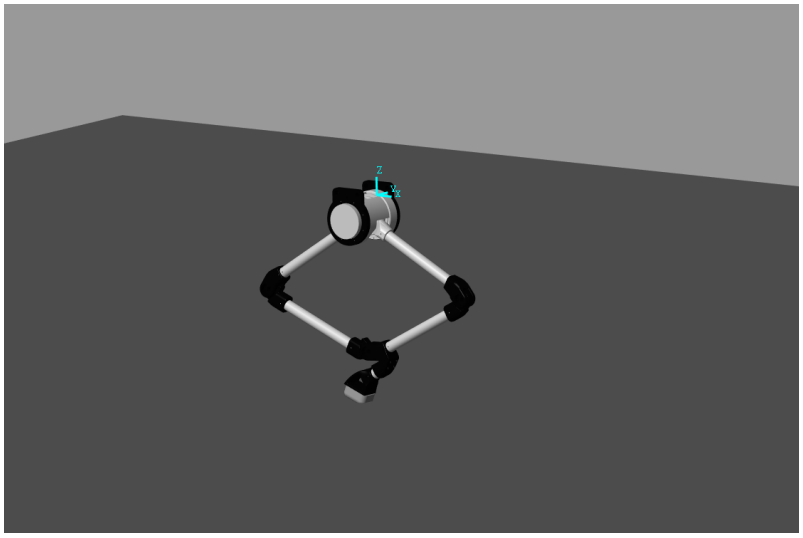

Figure 6.10: Leg design placed in the Multibody simulation environment.

The leg design has been placed on top of a solid block that will act as the ground for the simulation. The world frame for the simulation has been placed in the motor housing, as can be seen from Figure 6.10 and Figure 6.11. Due to this, the results will be presented as the distance from the world frame and to the relevant frame for the component that is being evaluated.

All of the simulations that have been conducted have been passive jumps. This means that the motors are not activated and don't contribute to the result in any way. The only force generated in the system during these tests is the spring. Which starts full extended and then contracts at the start of the simulation to create the jumping force.

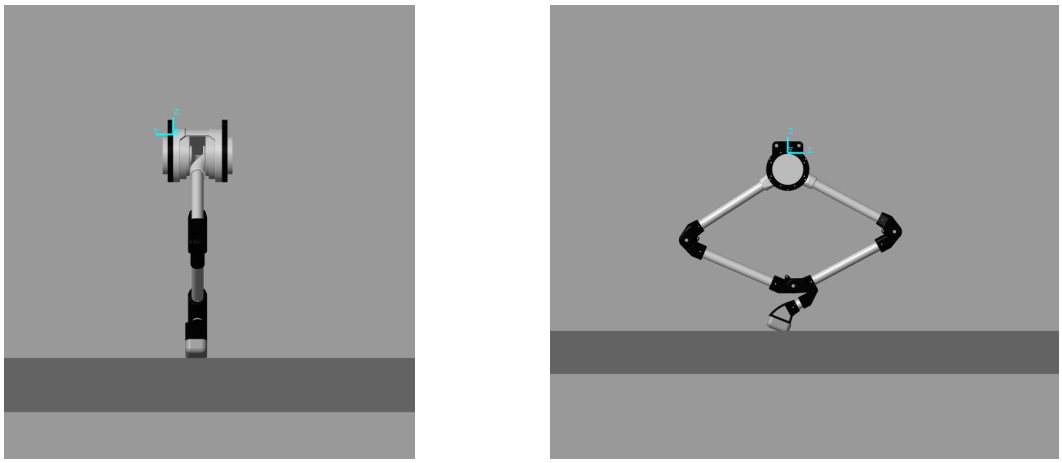

(a) **(b)**

Figure 6.11: World frame in blue placed on the Motor Housing in the Multibody simulation environment.

The height of the body starts at 0 because the world frame and motor housing frame are aligned at the start of the simulation. Due to the fact that none of the motors have actuated the leg is inherently unstable, and will as a result fall after the jump. Resulting in the negative results of the body height with respect to the world frame at the end of the simulation.

With the current configuration, the body will have a travel distance of approximately $0.757m$. With regards to the ground, which is located $0.325m$ below the world frame, this results in an approximate height of $1.082m$.

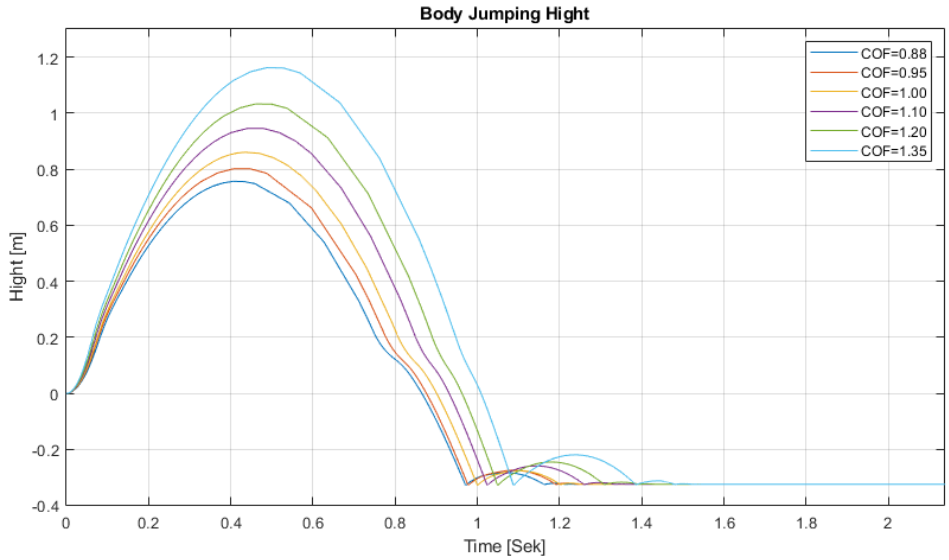

Figure 6.12: Body jumping height for different spring COF.

Several different spring coefficients have been simulated to evaluate the jumping potential of the leg design.

COF[N/mm]	Height; World frame[m]	Height; Ground[m]
0.88	0.757	1.082
0.95	0.802	1.127
1.00	0.860	1.185
1.10	0.946	1.271
1.20	1.038	1.363
1.30	1.162	1.487

Table 6.2: Height measurements for the Motor Body during the jumping simulations.

In addition to the motor housing, the translation to the paw has been mapped. Because the motors are not affecting the dynamics, the leg design will be fully extended after the initial contraction of the spring. Several different spring coefficients have been simulated to evaluate the jumping potential of the leg design.

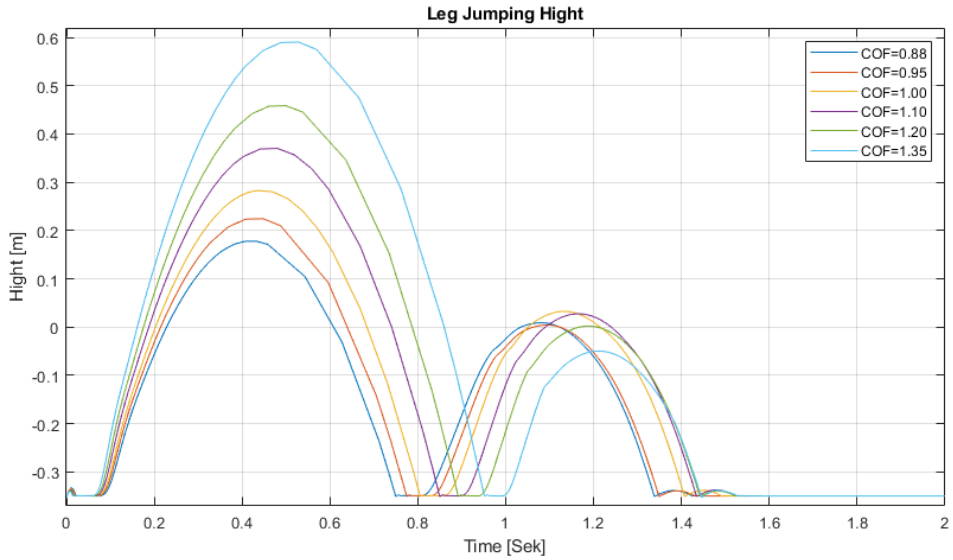

Figure 6.13: Leg jumping height for different spring COF.

COF[N/mm]	Height; World frame[m]	Height; Ground[m]
0.88	0.177	0.502
0.95	0.224	0.549
1.00	0.283	0.608
1.10	0.370	0.695
1.20	0.459	0.784
1.30	0.590	0.915

Table 6.3: Height measurements for the Paw during the jumping simulations.

Another important value that will be important for the current design and for any future control or benchmarks evaluations. is the velocity of the system. The velocity of the motor housing has been mapped to give an insight into not only the velocity. But with the velocity known the force the system exerts on the ground, as well as the energy the system has during jumps can be calculated. Several different spring coefficients have been simulated to evaluate the different velocity of the leg design.

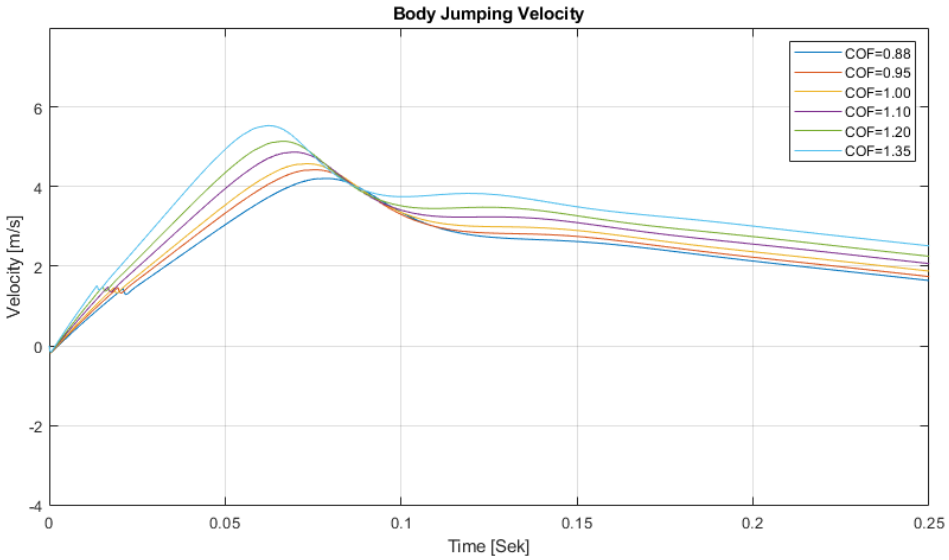

Figure 6.14: Body jumping Velocity for different spring COF.

COF[N/mm]	Apex Velocity[m/s]	Apex Velocity Time[s]
0.88	4.194	0.077
0.95	4.417	0.075
1.00	4.564	0.072
1.10	4.863	0.069
1.20	5.134	0.066
1.30	5.525	0.063

Table 6.4: Velocity measurements for the Motor Body during the jumping simulations.

One way of finding the force the paw will create during the lift-off is with the velocity. It can be seen from Figure 6.15 that the velocity graph has been shifted to start at 0.05s. This is done because the contact simulation between the ground and paw creates unreadable results before the paw experiences lift-off from the ground. Several different spring coefficients have been simulated to evaluate the different velocity of the leg design.

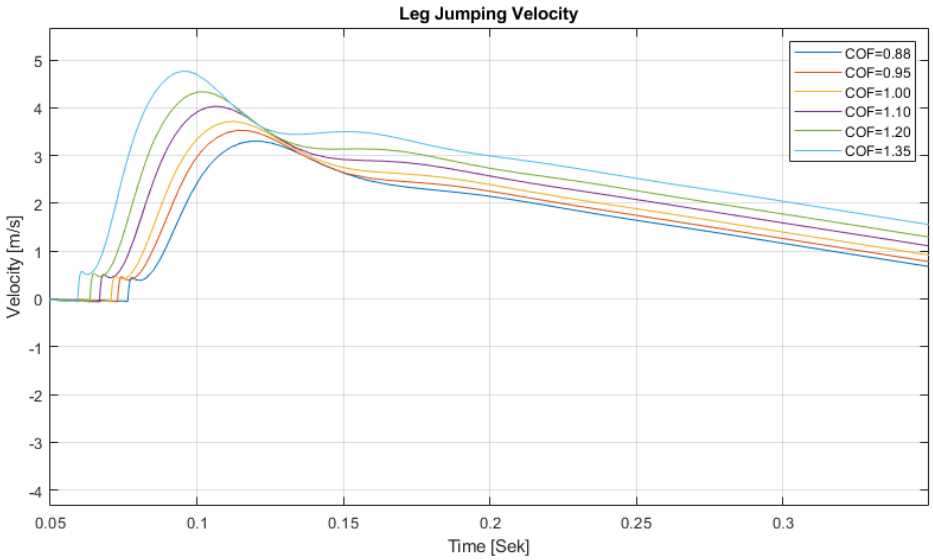

Figure 6.15: Leg jumping Velocity for different spring COF.

COF[N/mm]	Apex Velocity[m/s]	Apex Velocity Time[s]
0.88	3.298	0.122
0.95	3.527	0.114
1.00	3.712	0.113
1.10	4.035	0.106
1.20	4.331	0.101
1.30	4.763	0.095

Table 6.5: Velocity measurements for the Paw during the jumping simulations.

Chapter 7

Physical Testing

To be able to truly evaluate the full leg design it will need to undergo extensive physical testing. This is an aspect of the design process that can help uncover potential flaws in the design, and give a visualization of the design in person. The physical testing has been conducted at the robotics lab at NTNU by using the Qualisys motion capture system. To be able to test the capabilities of the design as well as the external components. Extensive testing was done on all the different parts. In addition to the mechanical parts that have been manufactured in-house and ordered mechanical parts such as the carbon pipes.

All the parts for the design have either been ordered and then altered, or made in-house by the workshop. Due to this if any parts should need to be altered they could be fixed without special orders. The component assembly proved to be non-complicated and all the parts, interfaces, and tolerances have all been tested and fitted to be working optimally.

The test that will be conducted and presented on the leg design in this thesis has been chosen to be compared to the tests done in the simulations. As a result of this approach, the following experiments will be conducted. The reason for the order of the physical test is in increasing order of potential damage to the design, and therefore ensure some tests are done before any potential damage occurs.

- **Workspace**
  The workspace was computed by utilizing the forward kinematics that was derived in Chapter.6. By plotting the workspace with the physical design it can be estimated the accuracy of the mathematically computed workspace compared to the true physical representation.

- **Passive jumping**
  The passive jumping was simulated in the Simulink Multibodies environment. The passive jumping will be conducted by manually compressing the design and then realizing it. This will give an indicator of how the system behaves in real environments compared to the simulated one.

- **Drop Test**
  To estimate how the design would react when dropped from heights there was conducted a drop test. The design was elevated to different heights and dropped down.

7.1 Workspace

To find the experimental workspace the tracking ball was placed at the end of the paw. The design was then moved through all its movable space. The workspace can be seen to not have its frame of origin at the origo as the calculated one had. This is because to evaluate the movement of the end-effector a frame of origin had to be made. Since the calculated workspace has been stated with an origin frame at the center of the aligned motor axis. The R frame of the experimental workspace also has this as an origin. Due to the elevation of the motor housing, the frame is placed approximately 1110mm above the origo in the Y-axis.

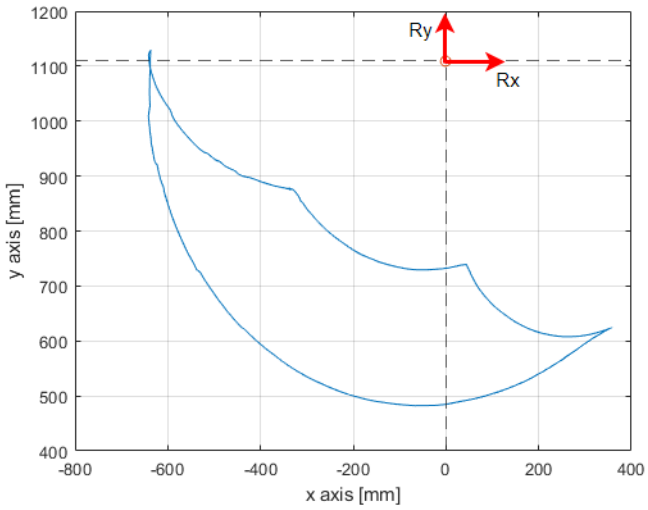

Figure 7.1: Experimental Workspace from motion capture.

The workspace has earlier been calculated by using the forward kinematics. To evaluate the accuracy of the calculations to the experimental results from the physical testing the workspace has been superimposed to estimate the overlap and fit of the two workspaces.

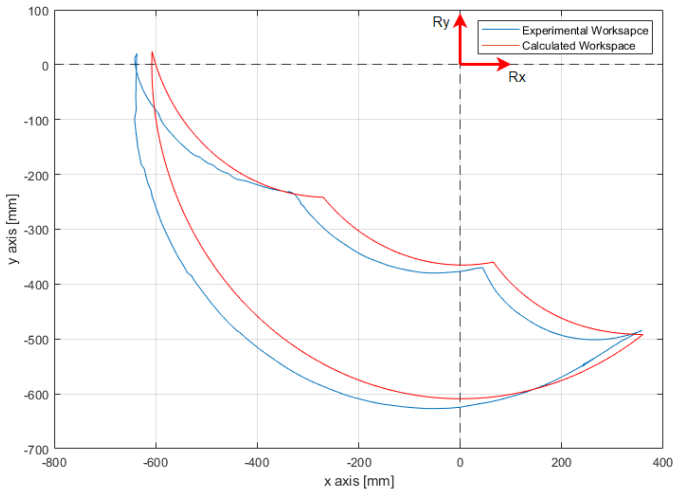

Figure 7.2: Workspace experimental and calculated superimposed.

The superimposed graphs in Figure 7.2 show that the experimental and calculated results of the workspace are not perfectly aligned. One of the reasons for this can be the positioning of the tracking sensors during the experimental results. If the sensor is placed differently from the end effector point that has been chosen for the calculated simulation of the workspace the results will differ. Other reasons can be the calculated result errors in its chosen parameters of lengths and angles or errors in the kinematic calculations.

7.2 Passive Jumping

The passive jumping test was done by compressing the design manually and securing it at its fully compressed stage, with the spring extended to the same length as the simulations, and then releasing it.

The test was done multiple times to compare and see if there would be any differences or patterns in the test. Tracking sensors were placed on both the motor housing and the paw. By tracking both the motor housing and the paw these can be compared to the same points in the simulation.

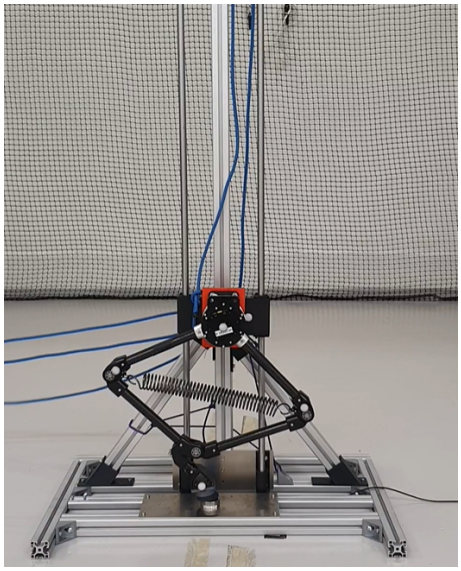

Figure 7.3: Fully compressed start position of passive jump test.

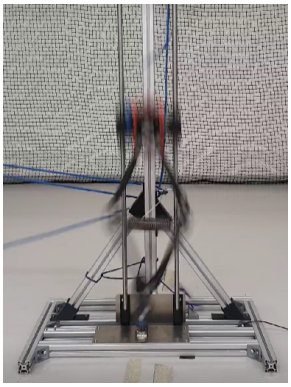

(a) Point of lift-off.

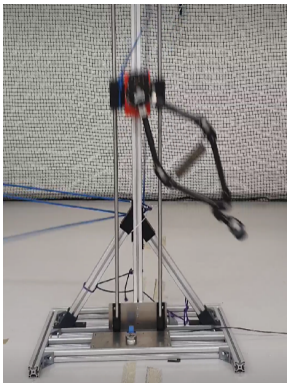

(b) Paw rotation at max height.

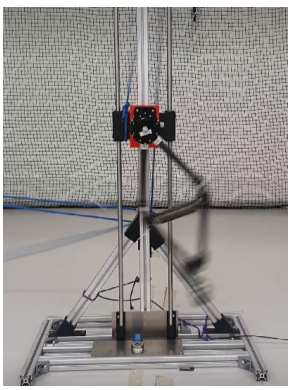

(c) Max height reached, paw rotating.

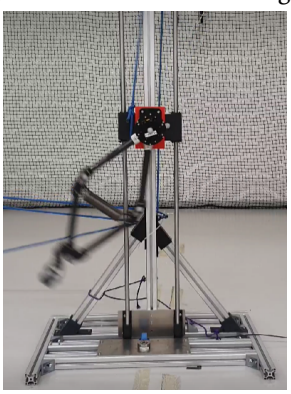

(d) After complete test.

Figure 7.4: Passive Jump screenshots throughout the movement during the test.

The height of the motor housing was measured to see how high the motor housing would travel during the jump. Since the housing and paw is relative to each other in the physical workspace, the motor housing have a starting position at approximately 500mm Y-axis. And reaching an approx height of 1050mm.

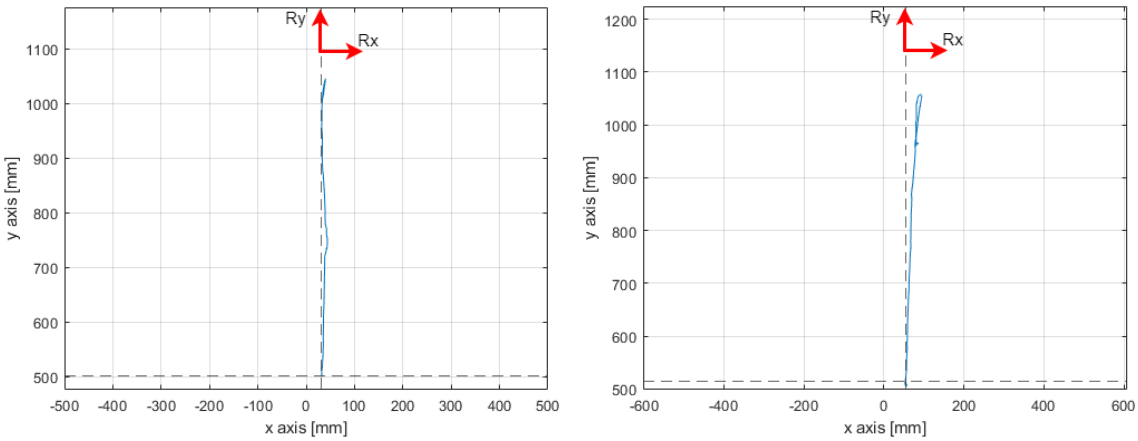

(a) **(b)**

Figure 7.5: Body tracking result from passive jumping tests.

Passive Jumping Test Body	Apex height [mm]	Height from base frame[mm]
Test 1	1057,46	543,98
Test 2	1044,78	531,3

Table 7.1: Body traveling result from passive jumping tests.

While the motor housing is secured on the testing rig and is therefore constrained to be moving in a solely vertical motion. The paw can move freely in the horizontal and vertical directions.

The tracking shows that the paw will not travel in a straight path, but rather travels forward quite a distance as tracked in Figure 7.6. This rotation is a result of the geometrical construction of the design. Since the end effector of the paw is not centered directly below the motor axis there will be created a lever arm. The longer lever arm will cause a rotation in the system during the passive jump, as can be seen in the graphs.

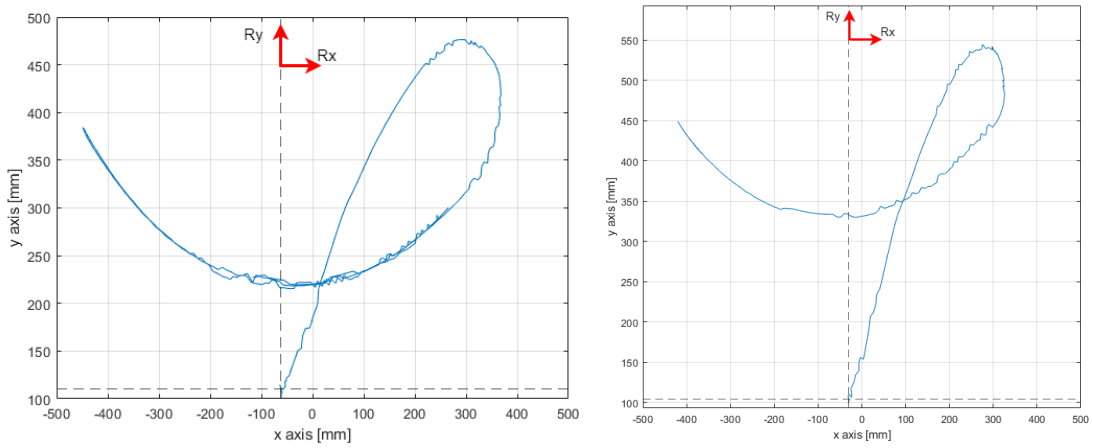

(a) **(b)**

Figure 7.6: Paw tracking result from passive jumping tests.

Passive Jumping Test Paw	Apex height [mm]	Height from base frame[mm]
Test 1	540,46	436,14
Test 2	476,37	372,05

Table 7.2: Paw traveling result from passive jumping tests.

During the passive jump test a force sensor was used to measure and evaluate the force created during the jump. It can bee seen that the compressed system is making a force of approx 125N, and during the launch the force is increased to approx 136N

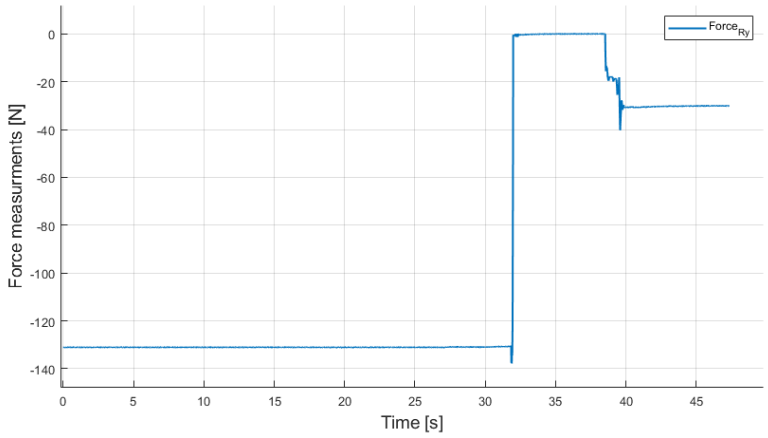

(a)

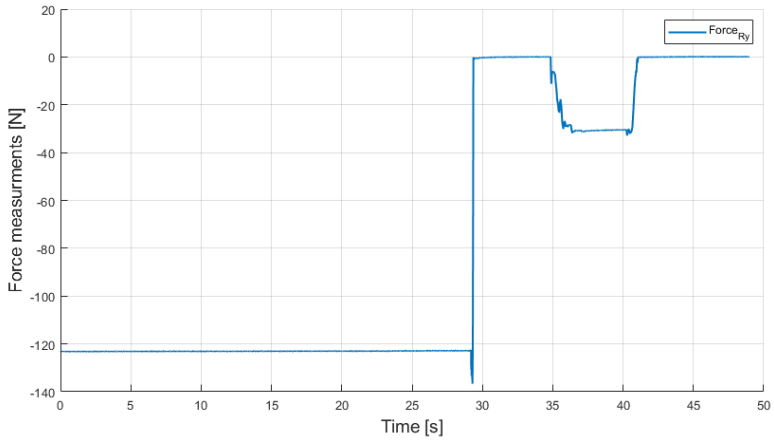

(b)

Figure 7.7: Passive Jump test force sensor results.

Passive Jumping Test Force	**Constant pressure force[N]**	**Lift off force[N]**
Test 1	131,09	137,831
Test 2	123,06	136,66

Table 7.3: Passive Jump test force sensor results.

7.3 Drop Test

The drop test was done by elevating the design to different heights before releasing it and letting it drop in free fall. This test was conducted to observe several aspects of the design. The force that would be generated at the impact would be measured by dropping the leg onto the force sensor. How the design would react to begin dropped and to see that all the parts and assembly would stand the impact.

Three different tests were done from three different heights. None of the heights damaged the design in any way.

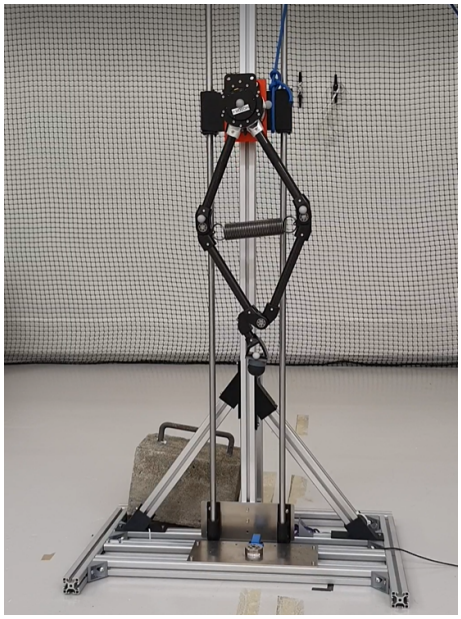

Figure 7.8: Start positing of drop test.

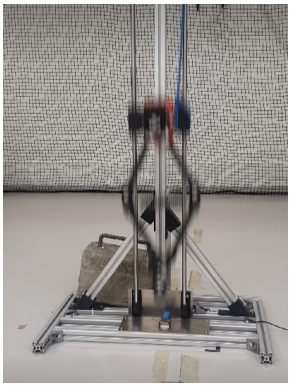

(a) Mid drop.

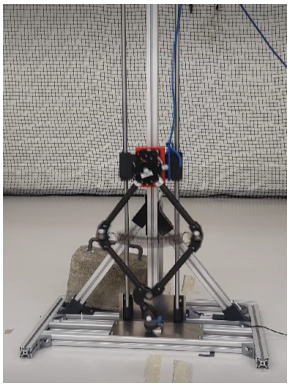

(b) Impact with ground.

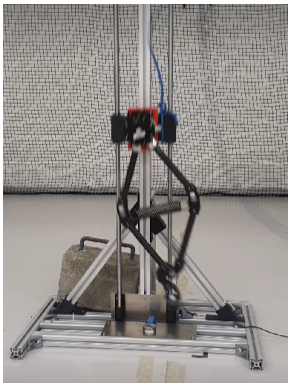

(c) Bouncing after impact.

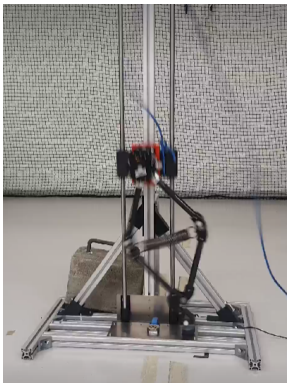

(d) Standstill after test.

Figure 7.9: Pictures series of a drop test from drop to standstill.

Drop Test Force	Drop Height[mm]	Impact force[N]
Test 1	200	325,31
Test 2	300	502,17
Test 3	400	598,37

Table 7.4: Drop test force sensor results.

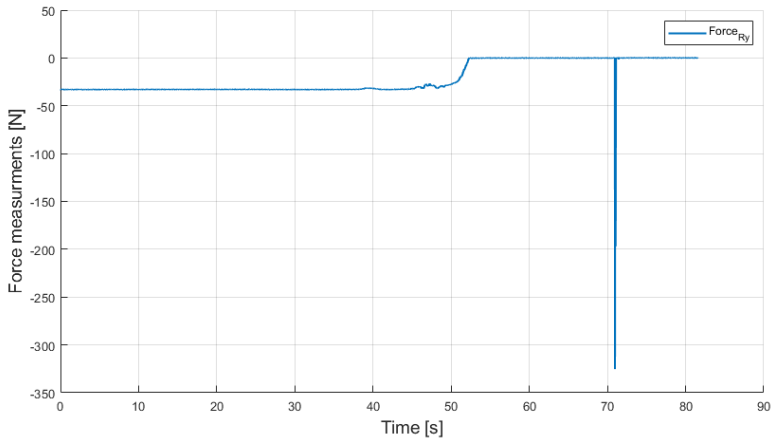

(a) Drop Test [200mm]

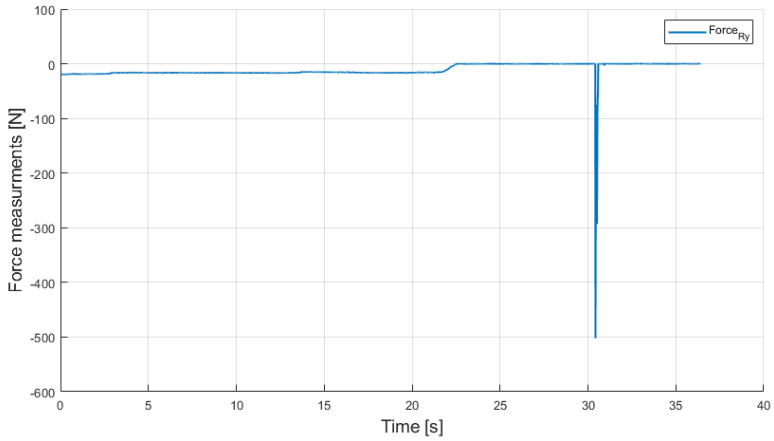

(b) Drop Test [300mm]

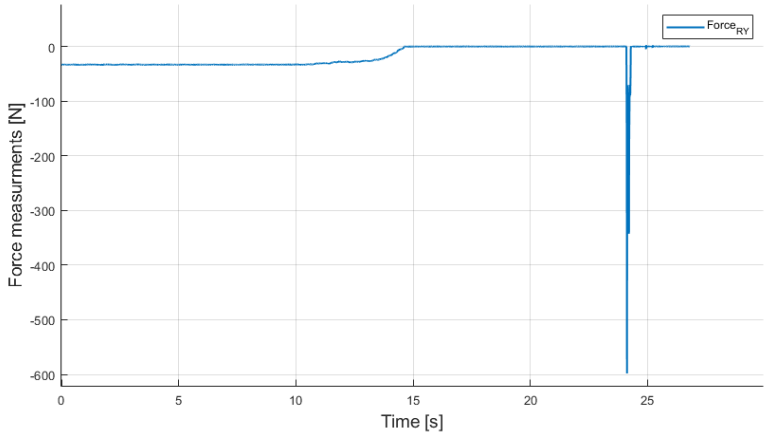

(c) Drop Test [400mm]

Figure 7.10: Results from force sensor form the drop tests.

7.4 Physical test sources of errors.

The physical testing and result made it evident that the testing set-up has shortcomings and factors that can affect the results of the tests. These have been identified and can be used to improve the physical testing setup for future testing.

Testing rig: The testing rig introduces some friction during the jumping and drop test. This will cause the system to perform worse during jumping and is one of the reasons for the difference in results for simulations and experimental tests. During drop tests, it can break the design and reduce the impact.

Mechanical interface: The mechanical interface between the leg design and testing rig proved to be too loose for the testing. During passive jumping, there would be created movement in the interface that would further increase the friction in the system.

Spring and joints: The spring will not have ideal properties as it is during the simulations as it will have friction during compression and extension. While the joints have been designed to have as little friction as possible, some friction will always be present.

Chapter 8

Conclusion

The development of legged robotics has over the years received increased attention. They have proven to be able to complete more complex tasks, such as traversing difficult terrain. This has been especially the case for quadruped-legged robotic systems. Different quadruped robotic designs have proved excellent maneuverability, stability, and locomotion abilities.

In this thesis, a new leg design for a quadruped robotic system has been proposed. The design is a result of an extensive literature review regarding similar quadruped robotic design, their drawbacks, and design choices that complement the requirements of the specific design. A clear focus of the leg design would be jumping and dynamical jumping locomotion. Before the final leg design, several iterations were conceptualized and analyzed based on their positive and negative attributes. The final design was chosen as the result of the solution that best met the requirements set for the final design. It was made as a modular assembly of all its components. This approach has made it possible to optimize individual aspects of the design, without making huge design altercations and rather changing out the desired individual components.

Multiple simulation scripts have been developed to analyze the abilities of the design with different parameters. Simulations for the optimization of the design have been used to present different iterations. Physical testing on the system proved the design had the potential to deliver on the requirements that were set. This includes jumping capabilities, dampening abilities, and the potential for accurate actuation. The design also demonstrates the capabilities of withstanding the impact of larger drops without sustaining any damage.

A design for dynamical jumping and locomotion has been proposed as an alternative to the more classical design of quadruped robotic systems. With the optimization of the leg design as well as the making of a correlating body, the full robot could one day be made to fully test its capabilities.

8.1 Future work

The next step in the process of the HOP project would be to use the simulations to find the optimal design parameters for the design. The scripts can be used to build an optimization tool for the design, giving the possibility of inputting wanted inputs to achieve design parameters. To further test the capabilities of the system it will need to be fully actuated with the motors.

When jumping capabilities of the 2-DOF system have been achieved it can be connected to the 3-DOF abduction motor that will be attached to the body. The body design will ideally be made to give the system additional dampening, especially in directions the leg cant provide sufficient dampening to withstand impacts. With the full design, assembled control systems will need to be made to enable the full design to have locomotion of both normal and jumping nature.

Bibliography

[1] M. Hutter, C. Gehring, D. Jud, A. Lauber, C. D. Bellicoso, V. Tsounis, J. Hwangbo, K. Bodie, P. Fankhauser, M. Bloesch *et al.*, 'Anymal-a highly mobile and dynamic quadrupedal robot,' in *2016 IEEE/RSJ international conference on intelligent robots and systems (IROS)*, IEEE, 2016, pp. 38–44.

[2] "*team cerberus and team dynamo win darpa subterranean challenge final event*", `https://www.darpa.mil/news-events/2021-09-24a`, Accesed: 9-2021.

[3] R. J. Léveillé and S. Datta, 'Lava tubes and basaltic caves as astrobiological targets on earth and mars: A review,' *Planetary and Space Science*, vol. 58, no. 4, pp. 592–598, 2010.

[4] X. Huang, J. Yang, M. Storrie-Lombardi, G. Lyzenga and C. M. Clark, 'Multi-robot mapping of lava tubes,' in *Field and Service Robotics*, Springer, 2016, pp. 471–486.

[5] T. Dang, M. Tranzatto, S. Khattak, F. Mascarich, K. Alexis and M. Hutter, 'Graph-based subterranean exploration path planning using aerial and legged robots,' *Journal of Field Robotics*, vol. 37, no. 8, pp. 1363–1388, 2020.

[6] "*mit mini cheetah*", `https://www.youtube.com/watch?v=xNeZWP5Mx9s&ab_channel=MassachusettsInstituteofTechnology28MIT29`, Accessed: 11-2021.

[7] "*atlas*", `https://www.bostondynamics.com/atlas`, Accesed: 10-2021.

[8] S. Dirk and K. Frank, 'The bio-inspired scorpion robot: Design, control & lessons learned,' in *Climbing and Walking Robots: towards New Applications*, IntechOpen, 2007.

[9] "*anybotics*", `https://www.anybotics.com/`, Accessed: 11-2021.

[10] *Boston dynamics, spot*, `https://www.bostondynamics.com/products/spot`, Accessed: 10-2021.

[11] "*spot*", `https://www.youtube.com/watch?v=XnZH4izf_rI&ab_channel=BostonDynamics`, Accessed: 11-2021.

[12] S. Seok, A. Wang, M. Y. Chuah, D. Otten, J. Lang and S. Kim, 'Design principles for highly efficient quadrupeds and implementation on the mit cheetah robot,' in *2013 IEEE International Conference on Robotics and Automation*, IEEE, 2013, pp. 3307–3312.

[13] C. Semini, N. G. Tsagarakis, E. Guglielmino, M. Focchi, F. Cannella and D. G. Caldwell, 'Design of hyq–a hydraulically and electrically actuated quadruped robot,' *Proceedings of the Institution of Mechanical Engineers, Part I: Journal of Systems and Control Engineering*, vol. 225, no. 6, pp. 831–849, 2011.

[14] S. Bartsch, T. Birnschein, F. Cordes, D. Kuehn, P. Kampmann, J. Hilljegerdes, S. Planthaber, M. Roemmermann and F. Kirchner, 'Spaceclimber: Development of a six-legged climbing robot for space exploration,' in *ISR 2010 (41st International Symposium on Robotics) and ROBOTIK 2010 (6th German Conference on Robotics)*, VDE, 2010, pp. 1–8.

[15] B. H. Wilcox, T. Litwin, J. Biesiadecki, J. Matthews, M. Heverly, J. Morrison, J. Townsend, N. Ahmad, A. Sirota and B. Cooper, 'Athlete: A cargo handling and manipulation robot for the moon,' *Journal of Field Robotics*, vol. 24, no. 5, pp. 421–434, 2007.

[16] S. Kitano, S. Hirose, A. Horigome and G. Endo, 'Titan-xiii: Sprawling-type quadruped robot with ability of fast and energy-efficient walking,' *Robomech Journal*, vol. 3, no. 1, pp. 1–16, 2016.

[17] M. Ilton, M. S. Bhamla, X. Ma, S. M. Cox, L. L. Fitchett, Y. Kim, J.-s. Koh, D. Krishnamurthy, C.-Y. Kuo, F. Z. Temel *et al.*, 'The principles of cascading power limits in small, fast biological and engineered systems,' *Science*, vol. 360, no. 6387, 2018.

[18] D. W. Haldane, J. K. Yim and R. S. Fearing, 'Repetitive extreme-acceleration (14-g) spatial jumping with salto-1p,' in *2017 IEEE/RSJ International Conference on Intelligent Robots and Systems (IROS)*, IEEE, 2017, pp. 3345–3351.

[19] E. W. Hawkes, C. Xiao, R.-A. Peloquin, C. Keeley, M. R. Begley, M. T. Pope and G. Niemeyer, 'Engineered jumpers overcome biological limits via work multiplication,' *Nature*, vol. 604, no. 7907, pp. 657–661, 2022.

[20] P. Arm, R. Zenkl, P. Barton, L. Beglinger, A. Dietsche, L. Ferrazzini, E. Hampp, J. Hinder, C. Huber, D. Schaufelberger *et al.*, 'Spacebok: A dynamic legged robot for space exploration,' in *2019 international conference on robotics and automation (ICRA)*, IEEE, 2019, pp. 6288–6294.

[21] N. Rudin, H. Kolvenbach, V. Tsounis and M. Hutter, 'Cat-like jumping and landing of legged robots in low gravity using deep reinforcement learning,' *IEEE Transactions on Robotics*, 2021.

[22] "*eth zürich robotic systems lab*", `https://rsl.ethz.ch/`, Accesed: 11-2021.

[23] "*t-motor, u8*", `https://store.tmotor.com/category.php?id=38`, Accessed: 9-2021.

[24] "*gazebo robot simulation*", `http://gazebosim.org/`, Accesed: 9-2021.

[25] K. K. Landes, 'A scrutiny of the abstract,' *Bulletin of the American Association of Petroleum Geologists*, vol. 35, no. 7, p. 1660, 1951.

[26] H. Kolvenbach, D. Bellicoso, F. Jenelten, L. Wellhausen and M. Hutter, 'Efficient gait selection for quadrupedal robots on the moon and mars,' in *14th International Symposium on Artificial Intelligence, Robotics and Automation in Space (i-SAIRAS 2018)*, ESA Conference Bureau, 2018.

[27] M. Bloesch, 'State estimation for legged robots-kinematics, inertial sensing, and computer vision,' Ph.D. dissertation, ETH Zurich, 2017.

[28] G. A. Pratt and M. M. Williamson, 'Series elastic actuators,' in *Proceedings 1995 IEEE/RSJ International Conference on Intelligent Robots and Systems. Human Robot Interaction and Cooperative Robots*, IEEE, vol. 1, 1995, pp. 399–406.

[29] R. H. Cannon Jr and D. E. Rosenthal, 'Experiments in control of flexible structures with noncolocated sensors and actuators,' *Journal of Guidance, Control, and Dynamics*, vol. 7, no. 5, pp. 546–553, 1984.

[30] H. Asada and T. Kanade, 'Design of direct-drive mechanical arms,' 1983.

[31] R. Alexander *et al.*, 'Three uses for springs in legged locomotion,' *International Journal of Robotics Research*, vol. 9, no. 2, pp. 53–61, 1990.

[32] A. B. Ghansah and P. A. S. Thorseth, 'Design and control of a torque controllable quadrupedal robot-a study on the development of astro,' M.S. thesis, NTNU, 2021.

[33] "*agility robotics unveils upgraded digit walking robot*", `https://spectrum.ieee.org/agility-robotics-digit-v2-biped-robot`, Accessed: 3-2022.

[34] I.-W. Park, J.-Y. Kim, J. Lee and J.-H. Oh, 'Mechanical design of humanoid robot platform khr-3 (kaist humanoid robot 3: Hubo),' in *5th IEEE-RAS International Conference on Humanoid Robots, 2005.*, IEEE, 2005, pp. 321–326.

[35] O. Stasse, T. Flayols, R. Budhiraja, K. Giraud-Esclasse, J. Carpentier, J. Mirabel, A. Del Prete, P. Souères, N. Mansard, F. Lamiraux *et al.*, 'Talos: A new humanoid research platform targeted for industrial applications,' in *2017 IEEE-RAS 17th International Conference on Humanoid Robotics (Humanoids)*, IEEE, 2017, pp. 689–695.

[36] D. Gouaillier, V. Hugel, P. Blazevic, C. Kilner, J. Monceaux, P. Lafourcade, B. Marnier, J. Serre and B. Maisonnier, 'Mechatronic design of nao humanoid,' in *2009 IEEE international conference on robotics and automation*, IEEE, 2009, pp. 769–774.

[37] J. Englsberger, A. Werner, C. Ott, B. Henze, M. A. Roa, G. Garofalo, R. Burger, A. Beyer, O. Eiberger, K. Schmid *et al.*, 'Overview of the torque-controlled humanoid robot toro,' in *2014 IEEE-RAS International Conference on Humanoid Robots*, IEEE, 2014, pp. 916–923.

[38] F. Negrello, M. Garabini, M. G. Catalano, P. Kryczka, W. Choi, D. G. Caldwell, A. Bicchi and N. G. Tsagarakis, 'Walk-man humanoid lower body design optimization for enhanced physical performance,' in *2016 IEEE International Conference on Robotics and Automation (ICRA)*, IEEE, 2016, pp. 1817–1824.

[39] D. Kim, Y. Zhao, G. Thomas, B. R. Fernandez and L. Sentis, 'Stabilizing series-elastic point-foot bipeds using whole-body operational space control,' *IEEE Transactions on Robotics*, vol. 32, no. 6, pp. 1362–1379, 2016.

[40] M. G. Catalano, M. J. Pollayil, G. Grioli, G. Valsecchi, H. Kolvenbach, M. Hutter, A. Bicchi and M. Garabini, 'Adaptive feet for quadrupedal walkers,' *IEEE Transactions on Robotics*, 2021.

[41] J. Li, Q. Huang, W. Zhang, Z. Yu and K. Li, 'Flexible foot design for a humanoid robot,' in *2008 IEEE International Conference on Automation and Logistics*, IEEE, 2008, pp. 1414–1419.

[42] "*flex-foot*", `https://www.ossur.com/en-us/prosthetics/feet/cheetah-xceed`, Accessed: 03-2022.

[43] *Ak70 series dynamical modular ak70-10*, https://store.tmotor.com/goods.php?id=1031, Accessed: 9-2021.

[44] T. Huang, S. Liu, J. Mei and D. G. Chetwynd, 'Optimal design of a 2-dof pick-and-place parallel robot using dynamic performance indices and angular constraints,' *Mechanism and machine theory*, vol. 70, pp. 246–253, 2013.

[45] X.-J. Liu, J. Wang and G. Pritschow, 'Kinematics, singularity and workspace of planar 5r symmetrical parallel mechanisms,' *Mechanism and machine theory*, vol. 41, no. 2, pp. 145–169, 2006.

[46] R. Tedrake, *Underactuated Robotics, Algorithms for Walking, Running, Swimming, Flying, and Manipulation*. 2022. [Online]. Available: http://underactuated.mit.edu.

[47] X. Yang, Y. Dong, H. Yang *et al.*, 'D2 delta robot structural design and kinematics analysis,' in *IOP Conference Series: Materials Science and Engineering*, IOP Publishing, vol. 274, 2017, p. 012 009.

[48] M. Kamel, K. Alexis and R. Siegwart, 'Design and modeling of dexterous aerial manipulator,' in *2016 IEEE/RSJ International Conference on Intelligent Robots and Systems (IROS)*, IEEE, 2016, pp. 4870–4876.

Appendix A

Exploded view

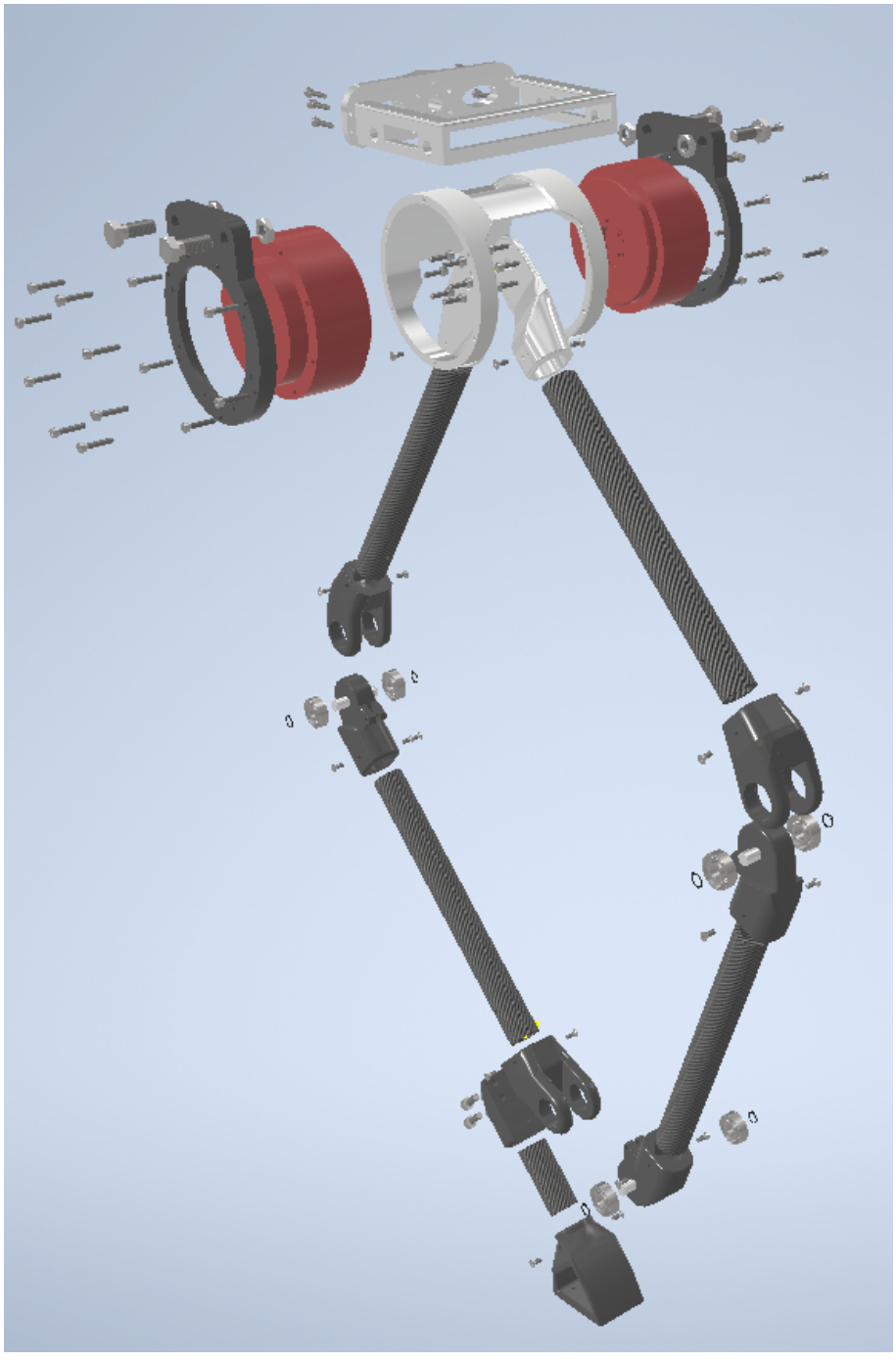

Figure A.1: Exploded view of full assembly.

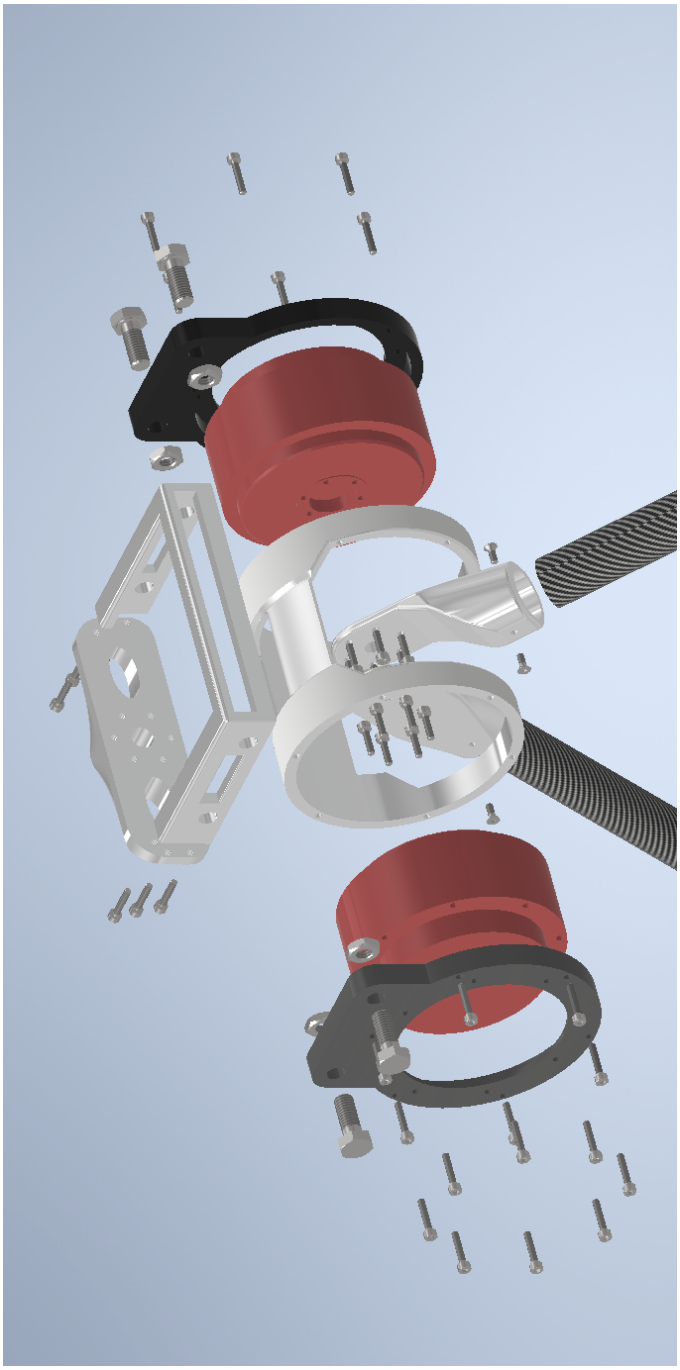

Figure A.2: Motor Housing exploded view.

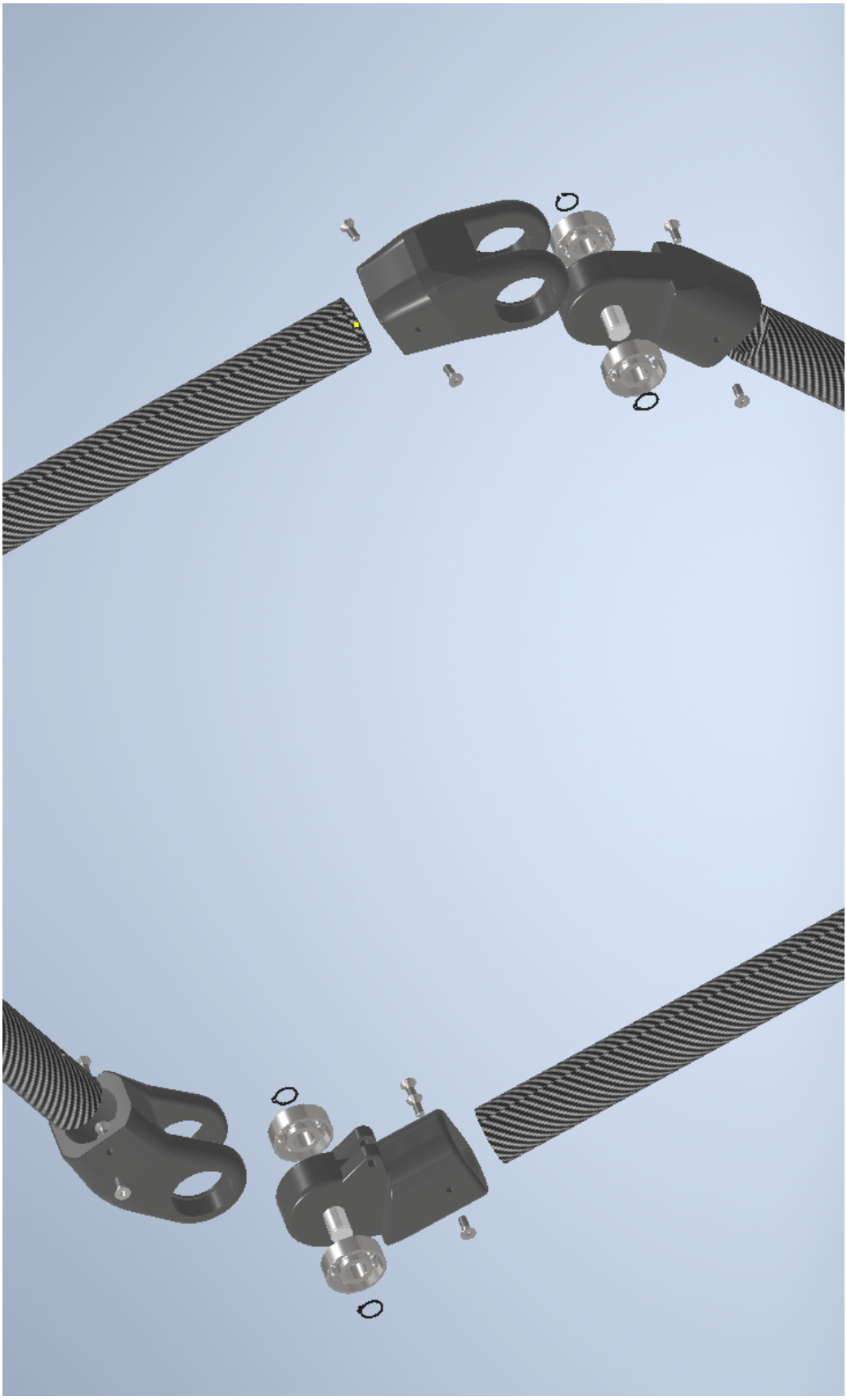

Figure A.3: Leg and joints exploded view.

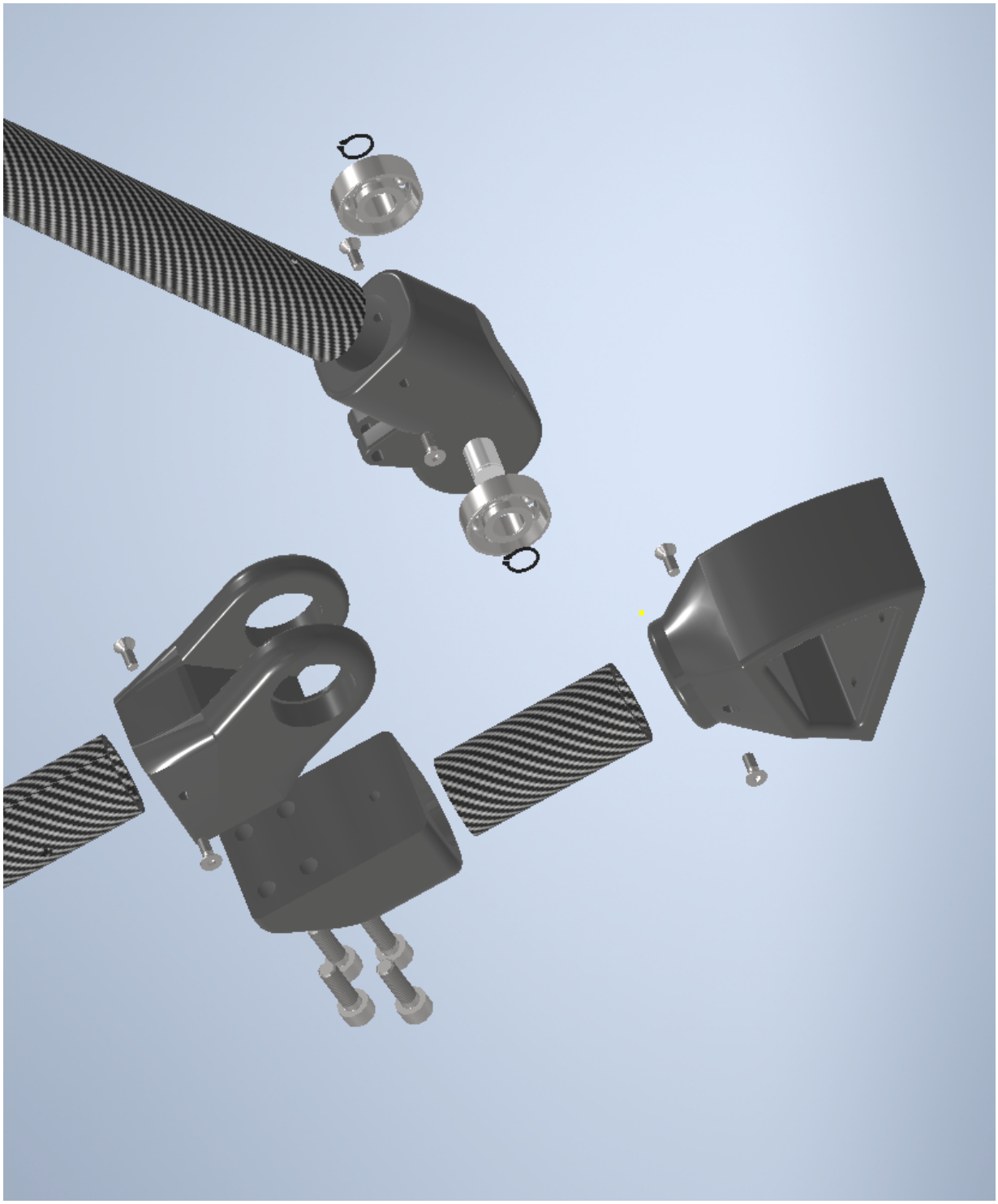

Figure A.4: Paw exploded view.

Appendix B

Full component list

Component Type	Component	Number
Manufactured part	Motor Housing	1
Manufactured part	Motor Housing Side	2
Manufactured part	Leg Connect	1
Manufactured part	Motor Connect	1
Manufactured part	Joint T	2
Manufactured part	Joint T Paw	1
Manufactured part	Joint B	3
Manufactured part	Paw Connect	1
Manufactured part	Paw Sole	1
Manufactured part	Pin	3
Purchased part	Carbon Fiber Legs	4
Purchased part	Carbon Fiber Paw Length	1
Purchased part	Motor	2

Table B.1: List over all components used in the final design.

Component Type	Component	Number
Bolt	M3x12	16
Bolt	M3x8	12
Bolt	M3x18	12
Bolt	M3x8, Countersunk	18
Bolt	M4x18	4
Bolt	M8x12	4
Nuts	M8x4	1
Bearings	22x8x7	6
Fastening rings	8	6

Table B.2: List over bolts, bearings and nuts.

Appendix C

Material information

Material information and values for all material used for components in simulations.

C.1 Carbon

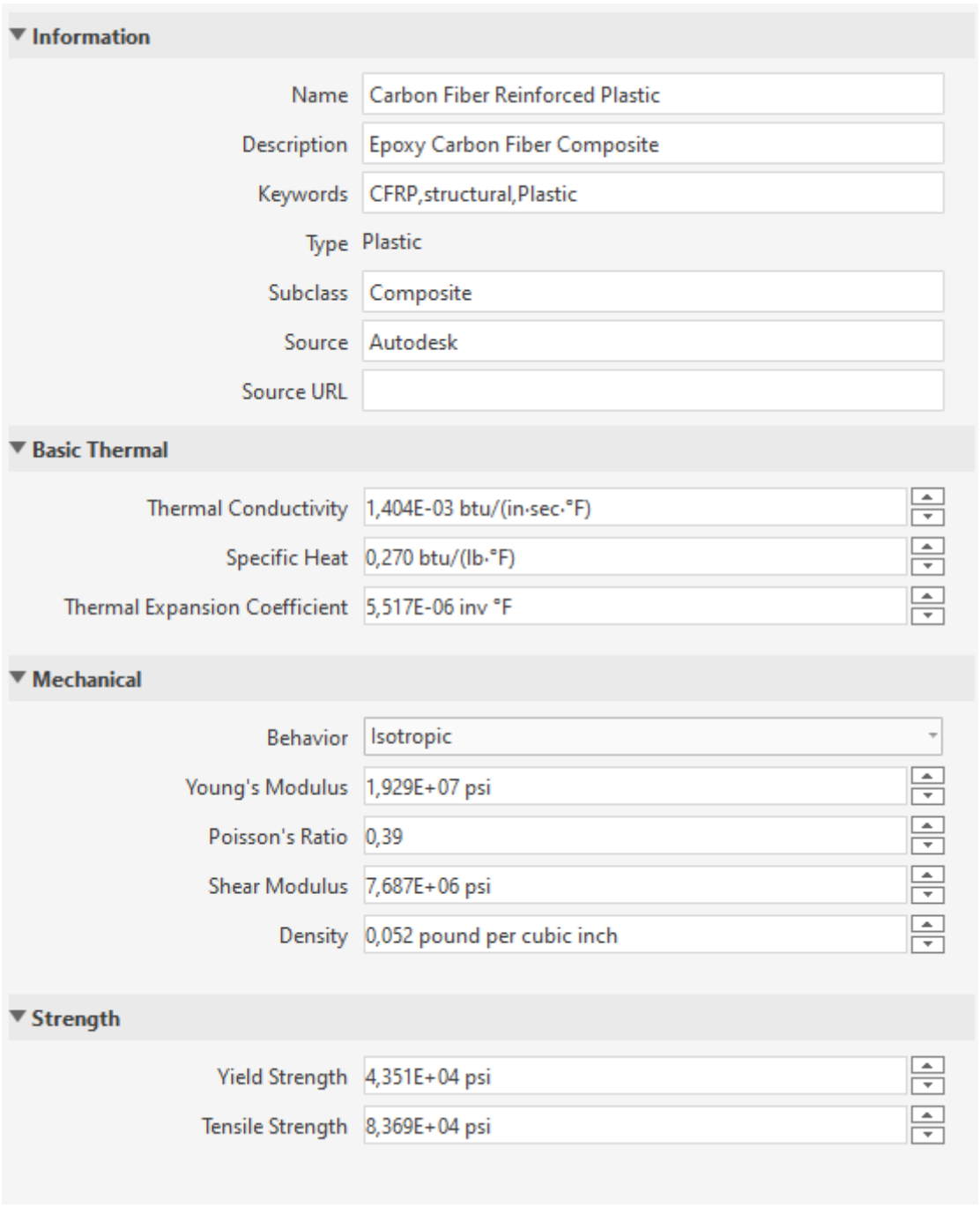

Figure C.1: Material info of carbon fiber used in Inventor FEM analysis.

C.2 POM

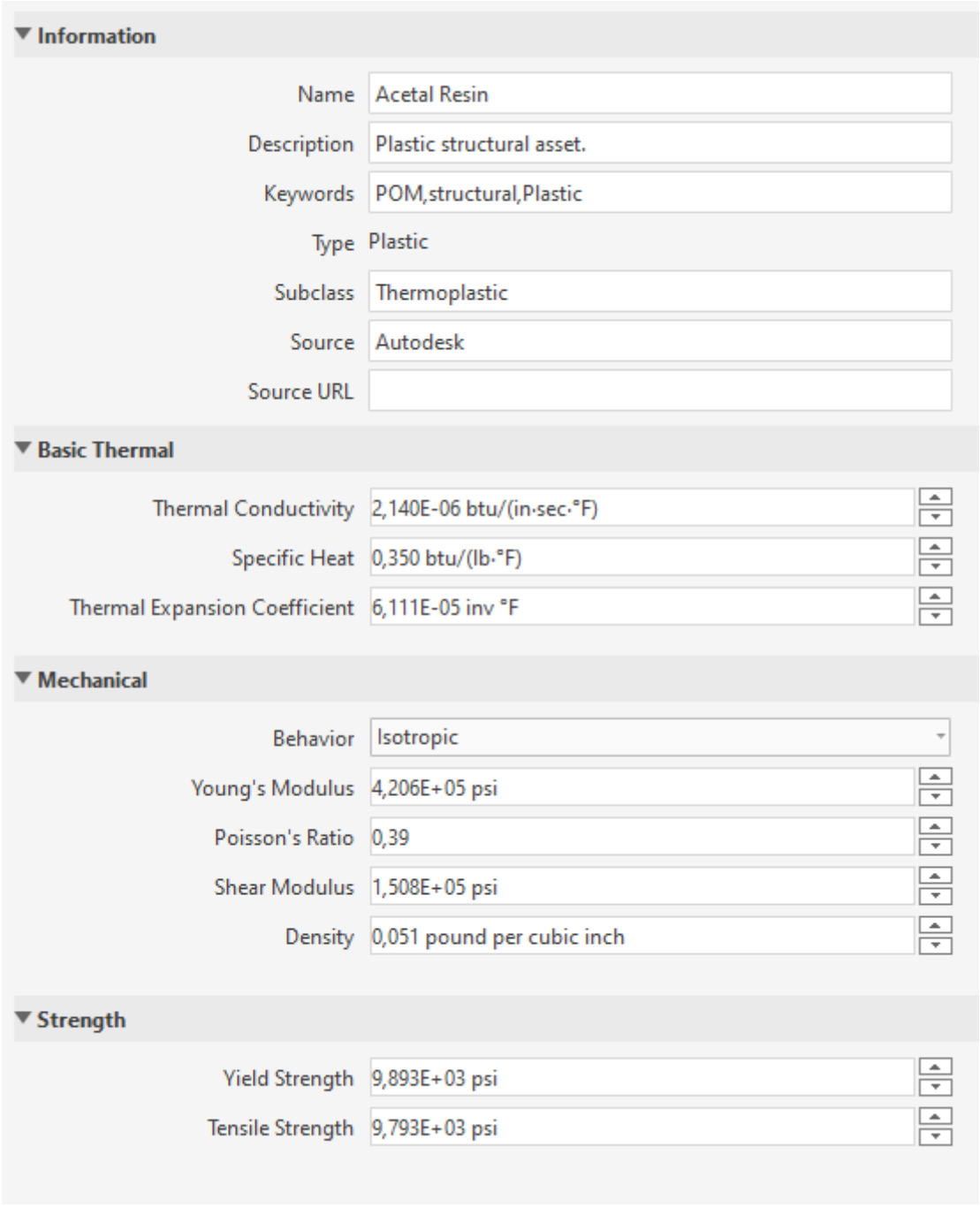

Figure C.2: Material info of POM (Acetal Resin) used in Inventor FEM analysis.

C.3 Aluminum

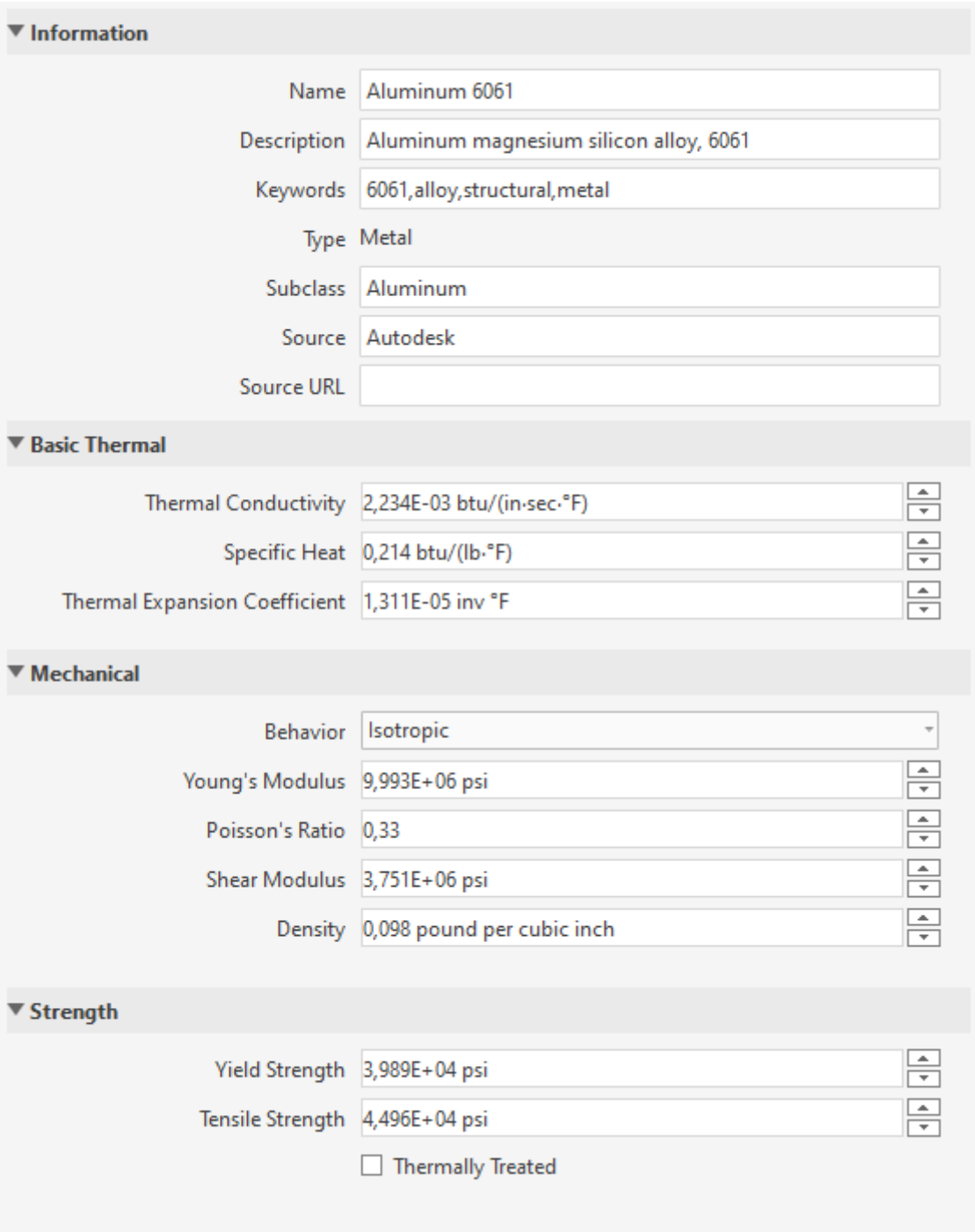

Figure C.3: Material info of aluminum used in Inventor FEM analysis.

Appendix D

Electronics

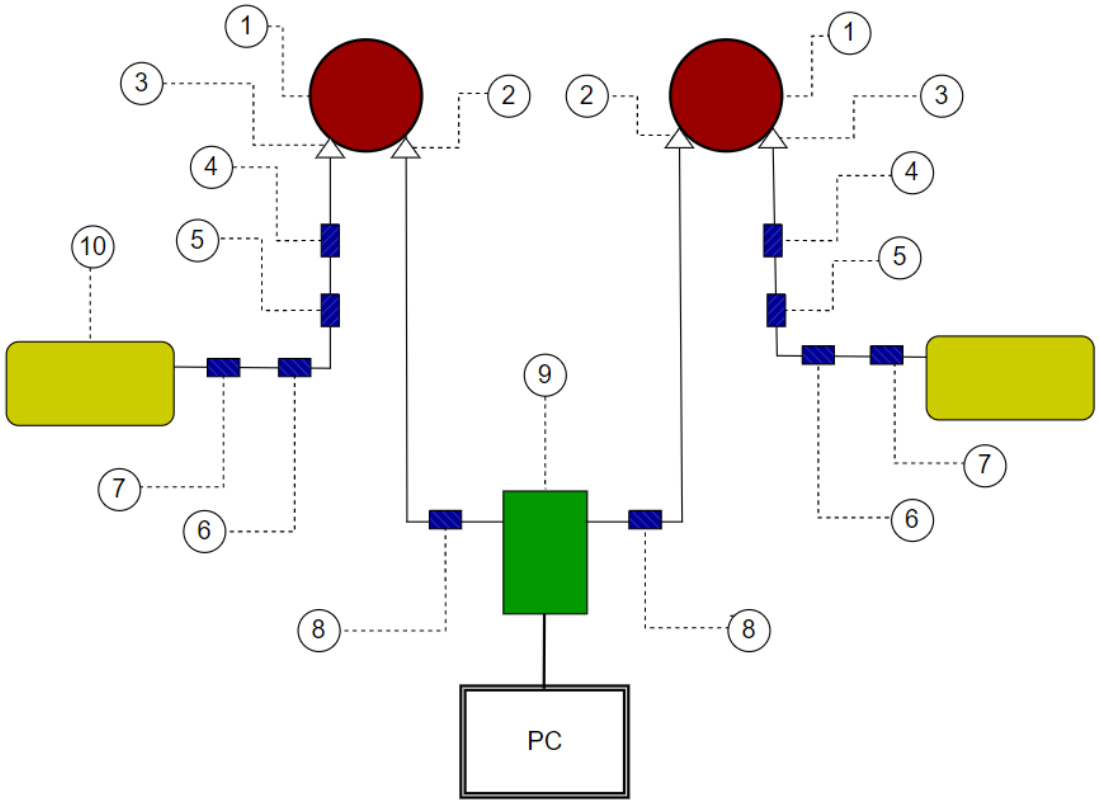

Figure D.1: Component layout for motor setup.

Component Type	Component	Number
Motor(1)	AK70-10	2
Connection(2)	CAN-Bus	2
Connection(3)	Power input	2
Coupling(4)	XT30 Regulator side	2
Coupling(5)	Female XT60 to male XT30	2
Coupling(6)	XT60 Regulator side	2
Coupling(7)	XT60 Battery side	2
Coupling(8)	Termination resistor	2
Controller(9)	Arduino Uno, CAN-Bus shield	1
Battery(10)	Gens Ace XT60, 22.2V	2

Table D.1: Electrical components list.

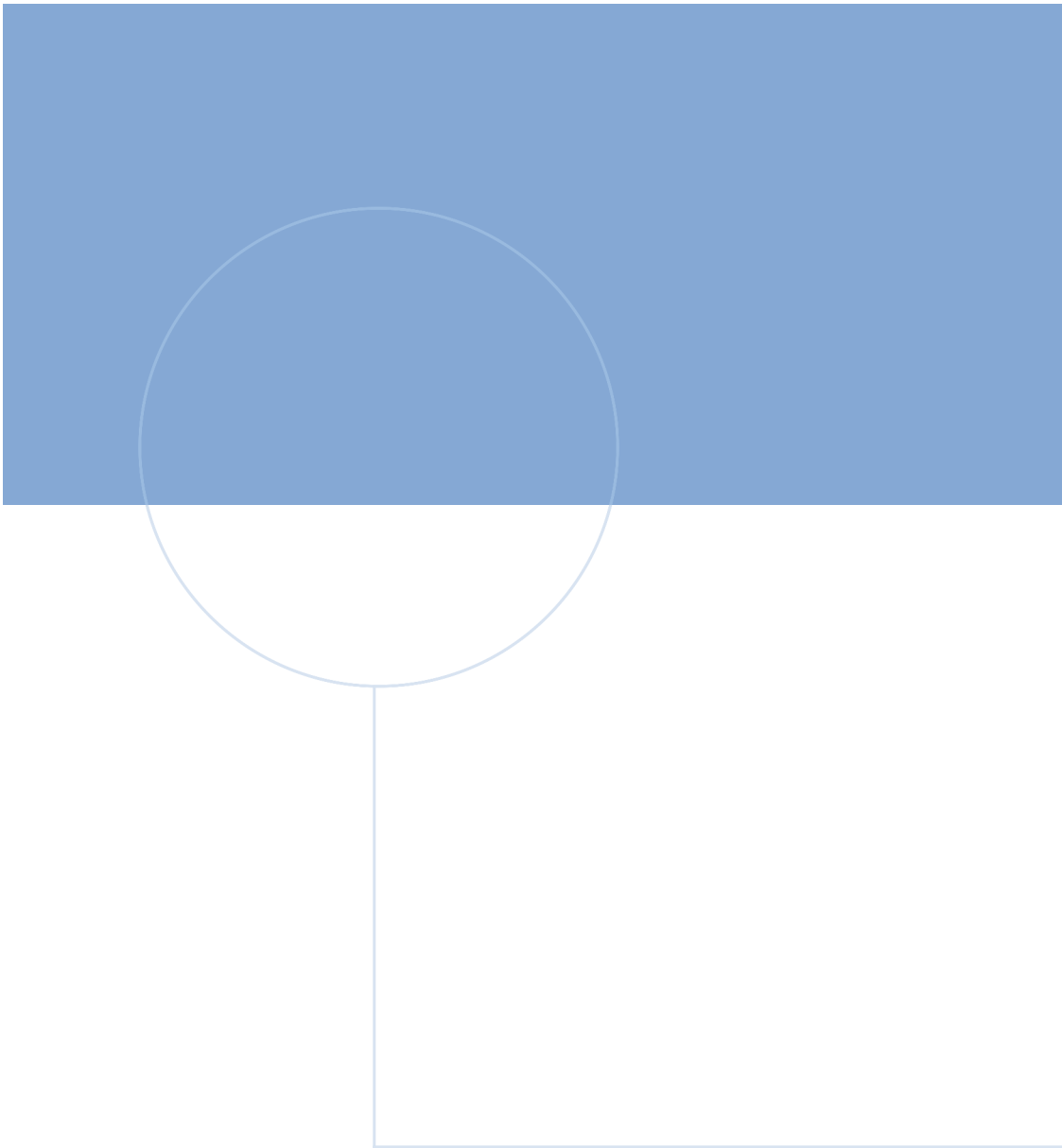

NTNU

Norwegian University of
Science and Technology